UNIVERSITY OF Hull

PROCESSING AND PATTERNING OF METAL ORGANIC FRAMEWORKS AND METAL ORGANIC GELS

Being a Thesis submitted for the Degree of Masters of Science (MSc) in Chemistry

at the University of Hull

by

Akinola Taiwo Oluwaseun

201507364

(September 2016)

ACKNOWLEDGMENT

First and foremost, I would love to express gratitude to God for the blessing, inspiration and enablement to complete this final-project.

I would like to express my sincere appreciation to my principal supervisor, Dr Jia Min Chin and co-supervisor, Dr Michael Reithofer for their constant guidance, valuable input and support without which this work would not have been possible and for opening my eyes to new possibilities.

Also my immeasurable appreciation and deepest gratitude goes to both my parents, family and friends for the financial support and moral help always being there when I need them. Also special thanks go to Emmanuel Ubuo, Zahraa Al-Mashaykhi and Jacob Balangtaa for their keen interest on me at every stage of my research work.

Table of contents

List of Figures

List of Tables

ABSTRACT

Metal Organic Frameworks (MOFs), due to their unique properties, have attracted significant research interest in diverse areas such as drug delivery, gas adsorption catalysis and bio-sensing. Although these materials have valuable attributes for future developments, the ability to control their functional properties to precise locations is important for potential applications. Also, the investigation and application of MOF structures has generally been at molecular level limiting their use for large scale industrial applications. Metal Organic Gels (MOGs) are emergent soft materials having both metal-organic framework (MOF) and gel characteristics such as flexibility, varying pore sizes and tunable porosity. These soft materials are of interest as they can easily be processed for various applications in more efficient ways than MOFs. This project aims to discuss the fabrication processing techniques employed for maximizing metal-organic composites properties and prospects for various applications.

Here, we present the use of coatings and lithographic techniques that enable MOF positioning and precise localization of NH_2-MIL-53 (Al) microcrystals on Anodised Aluminium Oxide (AAO) membrane. The advantages and limitations of each reviewed technique for the control of MOFs positioning are highlighted. X-ray and SEM measurements were used for the identification and location of the MOF crystal on the membrane. Also, the synthesis of MOGs under different conditions, factors affecting the gel properties, and how they can be photo-polymerized for processing at large scale dimensions were looked into.

Results obtained using lithographic techniques for patterning NH_2-MIL-53 (Al) microcrystals on AAO showed successful patterning but had limitations in patterning MOF crystal growth when a modulator was introduced. Mil-68 MOG was produced by using Indium metal ion salt with H_3BTC ligands. This was of primary focus due to its thixotropic properties, i.e. shearing and reforming to its original shape after applied force is removed. These thixotropic properties make the material versatile because it can potentially be processed into different shapes with the possibility of introducing polymerizable materials into the gels for crosslinking.

Acronyms

Abbreviations	
MOFs	Metal Organic Frameworks
DMF	Dimethylformamide
HMT	Hexamethylenetetramine
TCTPM	Tetra(4-cyanophenyl) methane
BDC	1, 4-benzenedicarboxylic acid
NH_2-BDC	2 amino-1,4-benzenedicarboxylic acid
BTC	1,3,5-benzenetricarboxylic acid
H_4DHBDC	2,5-dihydroxy-1,4-benzenedicarboxylic acid
ADS	2,6-anthracenedisulfonic acid
SBUs	Secondary Building Units
TEA	Triethylamine
EBL	Electron beam lithography
XRL	X-ray lithography
MW	Microwave-assisted
SURMOFs	Surface-mounted MOFs
LPE	liquid phase epitaxy
MCPs	Metal containing polymers
MOGs	Metal Organic gels
AAO	Anodised aluminium oxide,
PEGDM	Poly (ethylene glycol) dimethacrylate.
$Al(NO_3)_3{\cdot}9H_2O$	Aluminium nitrate nonahydrate
$Zn(NO_3)_2{\cdot}6H_2O$	Zinc nitrate hexahydrate
$Fe(NO_3)_3{\cdot}9H_2O$	Iron(iii) nitrate nonahydrate
$In(NO_3)_3{\cdot}XH_2O$	Indium (iii) nitrate hydrate
$Ga(NO_3)_3{\cdot}XH_2O$	Gallium (iii) nitrate hydrate
$La(NO_3)_3{\cdot}6H_2O$	Lanthanum (iii) nitrate hexahydrate
IprOH	Propan-2-ol
ZIF-8	Zeolitic Imidazolate Framework
PXRD	Powder X-ray Diffraction
SEM	Scanning electron Microscopy

Chapter 1. Processing and patterning of Metal-Organic Frameworks and Metal organic gels

1.1. Introduction

1.1.1. Outline of thesis

Porous materials have gained widespread interest in applications such as catalysis, chemical separation, biosensors and both gas storage and adsorption. A porous material is generally characterized by its surface area in m^2/g (i.e. the aggregate area available to host molecules) and the ratio between total occupied and empty space.[1] Porous substrates can be categorized into three sets based on their pore sizes, ranging from microporous materials which have pore sizes of 2 nm or below, mesoporous materials ranging with pore sizes from 2 nm and 50 nm and macroporous materials with pores size above 50 nm.[2] However, the majority of inorganic framework materials are synthesized within the microporous and mesoporous pore size range.

Metal Organic Frameworks (MOFs) are a recent addition to the class of porous frameworks comprising of metal ions and organic linkers. The ability to vary the pore size, morphology, chemical properties, functionalization and nature of MOF without altering their underlying topology, makes MOFs an emerging and important class of ultra-porous materials that has seen rapid and substantial growth holding great promises for technological applications.

Today, one way to constructing micro or nanoscale structures is the patterning and precise location of functional elements into materials for attaining specific effects or unique products. Thus far, extensive review articles on the different synthetic methods incorporated for optimizing various MOFs functionalities types[3] whereas there are sparse reviews on the topic of exploring MOFs functionalities. By integrating and positioning these multi-functional MOFs into devices, such as lab-on-a chip or microfluidic devices,[4] this could revolutionise their use for commercial applications. But the set back is the positioning of MOFs as it requires the use of support substrate such as thin films for patterning, since they are generally synthesized as single or microcrystalline powders.[5]

This study focuses on MOF crystals, whereby precise control over the positioning of MOFs is feasible by combining various new or established patterning techniques. Also, due to the presence of high surface area and uniformed size pores, these attributes make them interesting materials for applications in gas storage and absorption, gas separation, heterogeneous

catalysis,[6] drug delivery,[3] CO_2 capture,[7,8] ion exchange, biomedical imaging, sensing and optoelectronics device.[9]

The hypothesis of the study is to explore various ways for technological applications of MOFs and Metal Organic Gels (MOGs), as they are more promising when incorporated or miniaturized into devices. One of such application, is the synthesis of MOG with an acrylate functional group that would aid crosslinking upon interaction with UV-light. These gels could then be incorporated into resins used in 3-D printing for immediately curing, as well as offering functionalities within the mould to develop new types of composite materials for diverse applications.

1.1.2. Project aim and objectives

The aim of this project are in two sections; the first section focusing on nano and micro patterning of MOFs to precise locations to provide potential porous crystals with functionalities that can be tailored for numerous applications. Additionally, to achieve precise control of MOFs crystal sizes and morphology which is expected to help propel fabrication of micro-structured materials at the nanometre scale. Whilst the second section focuses on the synthesis, photo-crosslinking and processability of MOGs to achieve extensive variety of materials for diverse applications.

The objectives of this project are:

a) In order to achieve the patterning of MOFs, MOF nanoparticles will be synthesised on patterned alumina anodic with photoresist for the precise location of functional elements on to substrates
b) The adaptation of novel nano and micro-patterning protocols to aid new and help develop existing microfabrication techniques of nanoscale structures for diverse technological application[10]
c) MOGs fabrication processability will involve the synthesis and photo-crosslinking of various gels, especially indium based MOG due to its unique thixotropic properties.

1.1.3. Metal Organic Frameworks: A Brief History

MOFs are a class of highly porous materials composed of metal ions linked with organic linker molecules into a crystalline scaffold.[6] The past decade, has seen a significant growth in the study, preparation, characterization[11], functionality and topology[12] of MOF materials. This is a result of the MOFs' flexible morphology, high surface area and crystal architecture, resulting to thousands of compounds being produced.[13] The type of metal ion(s) and binding ligands used, as well as their coordination geometries determines the properties (e.g. chemical, physical, topological and architectural) of the resulting desired MOFs.[2] The nodes and linkers can self-assemble to form 1-D chains, 2-D sheets or 3-D networks (Figure 1). MOFs are promising because their properties can be tuned for various functional applications.

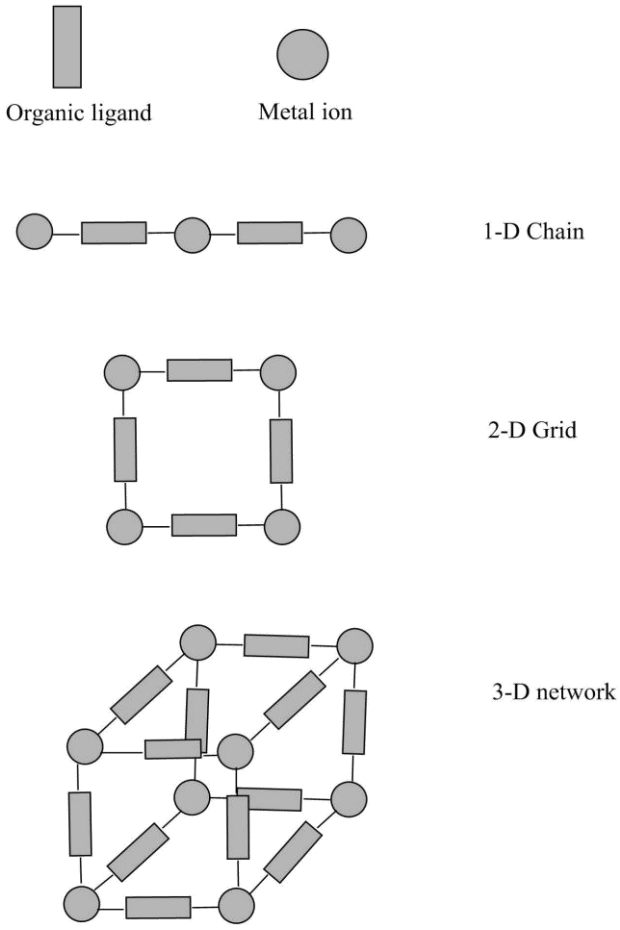

Figure 1- Self-assembly of nodes and linkers into one-, two- and three-dimensional classes of MOF architectures.

1.1.4. Building units

MOFs are built up by the assembly of an inorganic part (metal ion) and an organic part (organic ligands).[14] The two parts are termed the "primary building units" when synthesising MOFs. The metal ion is generally added in the form of salts. Organic units are typically mono-, di-,

tri- or tetravalent ligands, and the solvent used for dissolution are normally organic solvents (such as DMF, ethanol and methanol). Water can likewise be utilised instead of an organic solvent during MOF synthesis in some cases.

1.1.4.1. Metal ions

Coordination number and geometry are essential characteristics of metal ions in the construction of MOFs. They help determine the number and orientation of the binding sites in combination with divergent linkers leading to the creation of extended networks in one, two, or three dimensions.

Transition-metal ions, especially first row transition metals such as Cr^{3+}, Fe^{3+}, Cu^{2+}, Zn^{2+} are often utilized in MOFs construction. These transition metals have various metal oxidation state and coordination number, which can range from 2 to 7. Their use in MOF construction, can be attributed to their ability to coordinate with carboxylate groups.

The oxidation state and coordination numbers of the metal ion(s) are important factors (Fig 2), resulting to various geometries such as linear, square-planar, T- or Y- shaped, tetrahedral, trigonal-bipyramidal, trigonal-prismatic, octahedral, square- pyramidal etc., when governing a MOF's structure. For example, Ag and Cu ions with d^{10} configuration have been observed to produce various coordination numbers and geometries by altering the reaction conditions such as solvents, ligands and counter-anions.[15] Some metals such as group 1, group 2 and rare–metals have also been engaged in synthesis of MOFs structures.[16]

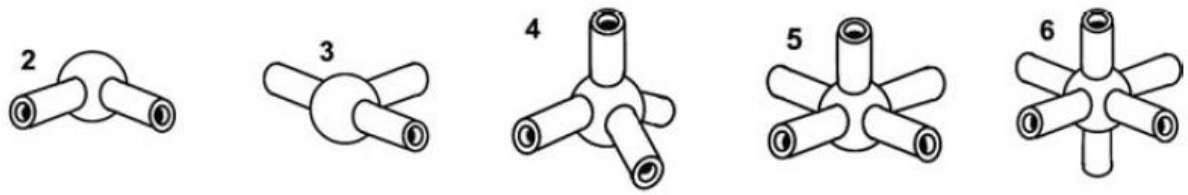

Figure 2- Example of metal ions with different coordination number. The numbers in the picture indicates the number of functional sites available for coordination. [16]

1.1.4.2. Organic linkers

Linkers are normally multidentate bridging ligands. These consist of a variety of linking sites or donor atoms, with binding strength and directionality of the ligand unique to its structures.[2] Multidentate ligands with two or more donor atoms are called di-, tri- or tetratopic depending on the number of donor atom present. Organic ligands widely used for MOF creation mostly encompass of coordinating functional groups such as carboxylate, amine, phosphate, imidazole, sulfonate, or nitrile (Fig 3).

The physical properties of MOFs are highly reliant on the organic ligand. To obtain variances in structural topologies and physical properties for various applications, one has to consider carefully the different organic linker properties such as the length of the ligand space, use of rigid ligands, its flexibility and number of binding sites during the MOF synthesis process. [2,17] Studies show that of the ligand properties, the flexibility of the bridging ligand pose some challenges. When a ligand has several probable conformations, this could lead to unexpected and unpredicted framework geometry. For example, a study of ligand flexibility, using 1,2-bis(4-pyridyl)ethane, which can assume *gauche* or *anti* conformations, shows that a variety of network geometries can indeed exist. An approach to solve this problem was the use of rigid ligands with rigid backbone such as 4,4'-bipyridine. This can be adopted to restrict the free orientation of the ligand lone pairs.[18] Though, this ligand principally has the ability to rotate about the central C-C bond, yet this rotation does not affect the mutual orientation of the two lone pairs. Examples of rigid four- connecting ligand are hexamethylenetetramine (HMT) and tetra(4-cyanophenyl)methane (TCTPM) as shown in (Fig 3).

CARBOXYLATE

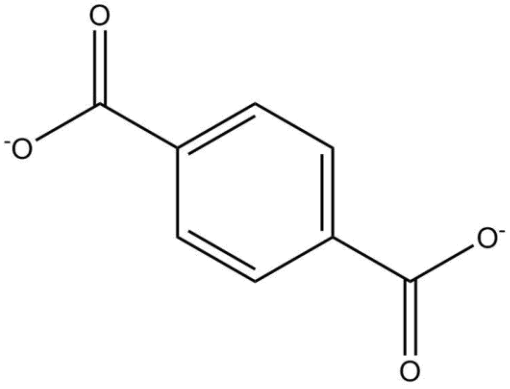

BDC

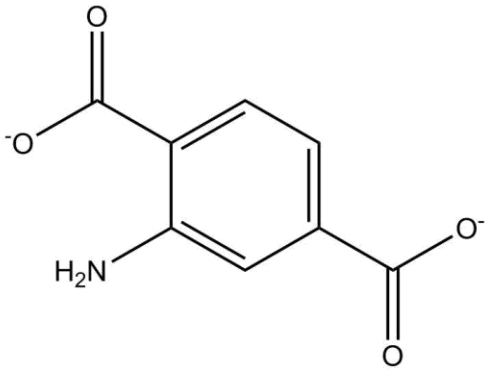

HN_2-BDC

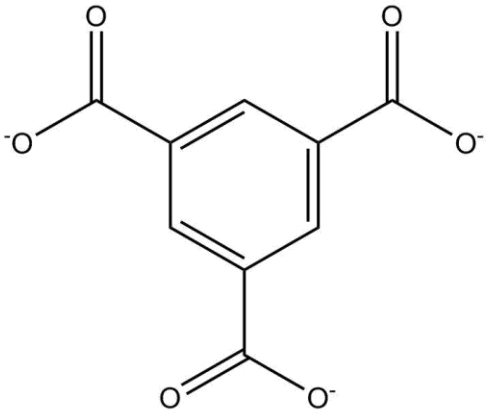

BTC

IMIDAZOLE

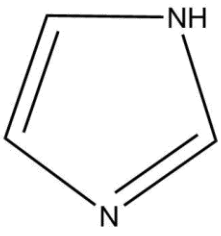

Him

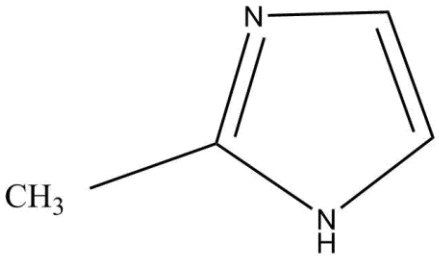

HMeIm

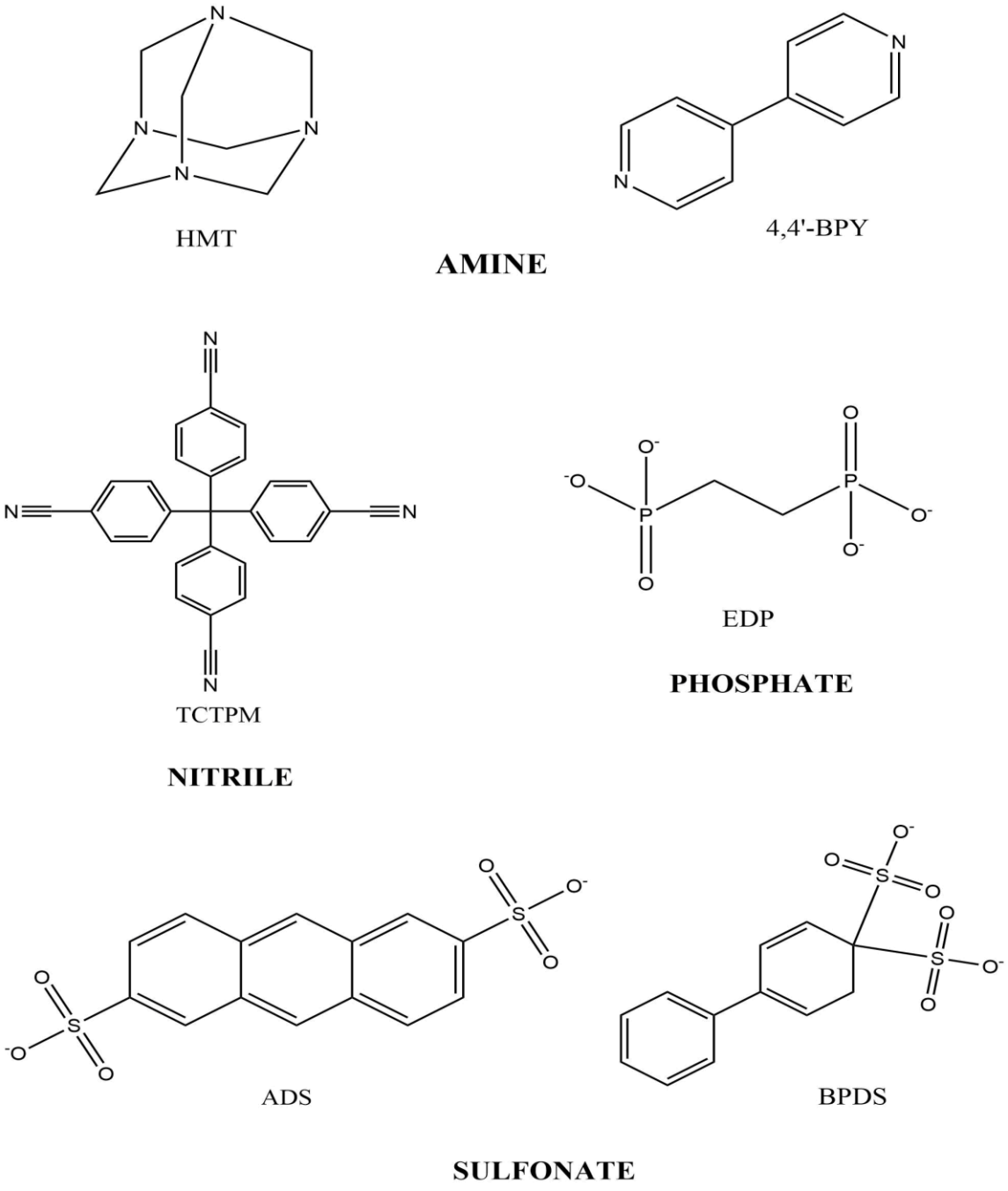

Figure 3- Examples of organic ligands used in MOFs synthesis.[2,16]

BDC= 1,4-benzenedicarboxylate, HN_2-BDC= 2 amino-1,4-benzenedicarboxylate, BTC= 1,3,5-benzenetricarboxylate, Him= imidazole, HMeIm= 2methyl imidazole, HMT= hexamethylenetetramine, 4,4' BPY= 4,4'-bipyridine, TCTPM= tetra(4-cyanophenyl)methane, EDP= 1,2-Ethylenediphosphonic acid, ADS= 2,6-anthracenedisulfonate, BPDS= 4,4'-biphenyldisulfonate.

1.1.4.3. Secondary Building Units (SBUs)

SBUs are molecular complexes and cluster entities combined alongside with organic linkers to build porous networks. SBUs are small units composed from one or more metal ions or multidentate ligands, creating rigid entities which are repeated throughout the whole network. SBUs assists with maintaining high porosity and the structural integrity of organic linkers when constructing more robust network structures. A considerable knowledge of the chemical and geometric of SBU coupled with organic ligands can help predict the final structure of the MOF crystal towards a small number of preferred topologies before commencing synthesis.[19] The steric function and rigidity helps to improve SBU impact by decreasing the possible number of network topologies arising for a specific node or linker combination.[2] Most SBUs which allow for the generation of more rigid frameworks are constructed from carboxylates (Fig 4).

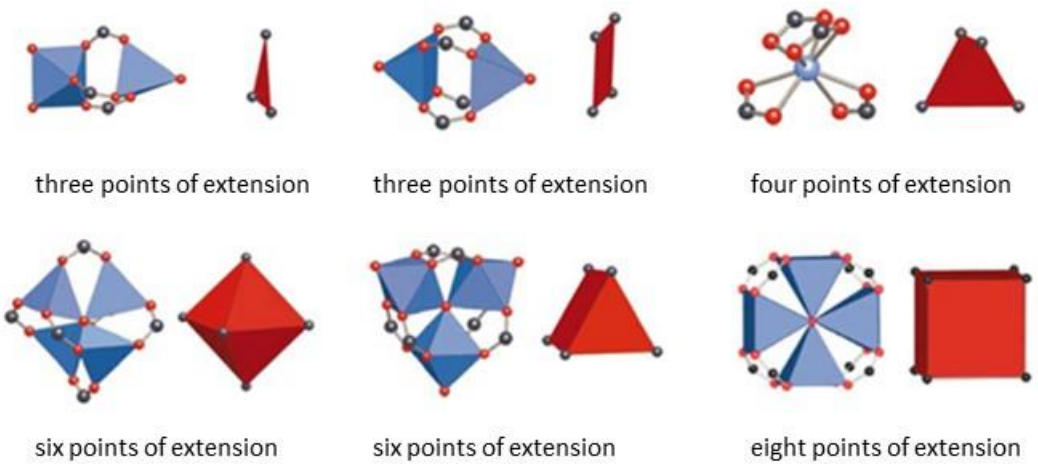

Figure 4- Examples of SBUs from carboxylate MOFs. Metal polyhedrons, blue; O, red; C, black. The polygons or polyhedrons represents by carboxylate carbon atoms (extension points) are red [16].

1.1.5. Design and Synthesis of MOFs

When designing MOFs, maintaining the functionality and structural integrity of the building blocks is paramount to obtaining high quality single crystals for structural analysis. The prediction of the MOF's structural moiety is more feasible, as synthetic modifications allows for the assembly of the building units in an intended fashion.[19] This has led to various synthetic methods (e.g. sonochemical, electrochemical, microwave etc.) being employed in MOF synthesis to yield single crystals.

MOFs are synthesized wherein metal salt and organic ligands are mixed together in a suitable solvent. This can be based on several aspects such as the reaction rate, synthesis time, stability

of synthesised MOFs, solubility, thermodynamic and activation energy of the reaction.[20] MOF synthetic reactions can either occur at room temperature or when heated to a set temperature.

There are two methods to tune the pore size, resulting in desired surface chemistries.

a) Direct self-assembly of MOFs from metal ions and organic linkers
b) Post synthesis modification of pre-constructed precursor MOFs.[21]

MOFs are synthesised by various synthetic methods such as conventional solvothermal or hydrothermal reactions via electrical heating in closed vessels which requires reaction times from several hours to days. In recent years, alternative synthesis methods (Fig 5) were adopted in an attempt to shorten synthesis time and develop smaller uniform crystals (such as the micro wave assisted process), demonstrating the benefits of producing nanoporous MOFs with the ability to tune the facile morphology, phase selectivity and narrow particle size distribution to yield high efficient results.[3,20] Sonochemical synthesis uses the application of ultrasound to chemical reactions, and creates an acoustic cavitation effect in a liquid.[22,23] In electrochemical synthesis, metal ions are produced *in situ* by anodic oxidation in the presence of the organic linker and an electrolyte, thereby producing the MOFs.[24,25] Mechanochemical synthesis involves the application of a mechanical force to break intramolecular bonds, to perform a chemical reaction.[3,9,26]

Although there have been many studies of different synthetic methods of MOFs, this report will focus on conventional solvothermal synthesis, as this was the technique employed for the research work described here. Readers interested in more detailed information of MOF synthesis are advised to view subsequent referenced journals.

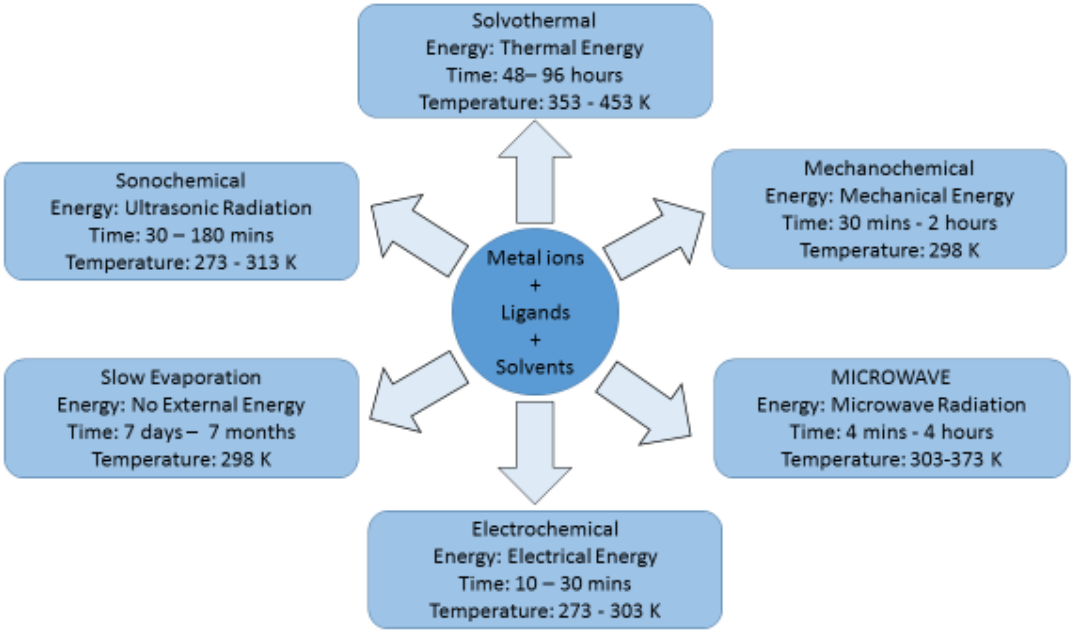

Figure 5- Synthesis conditions commonly used for MOF preparation [27]

Table 1- Representative of some MOFs using various synthetic approach.[3]

Synthesis Method[a]	Sample	Metal	Ligand[b]	Synthesis conditions	
				Solvent[c]	Conditions
CS	MOF-5	$Zn(NO_3)_2{\cdot}4H_2O$	H_2BDC	DMF/chlorobenzene	120°C, 24 h
	UiO-66	$ZrCl_4$	H_2BDC	DMF	120°C, 24 h
	Cr-MIL-101	$Cr(NO_3)_3{\cdot}9H_2O$	H_2BDC	H_2O (add 1 M HF aq)	220°C, 8 h
	IRMOF-3	$Zn(NO_3)_2{\cdot}4H_2O$	$H_2BDC\text{-}NH_2$	DEF	85°C, 96 h
	AL-MIL-53-NH_2	$Al(NO_3)_3{\cdot}9H_2O$	$H_2BDC\text{-}NH_2$	DMF	130°C, 5 days
	ZIF-8	$Zn(NO_3)_2.4H_2O$	HMeIm	DMF	85°C, 72 h
MW	MOF-5	$Zn(NO_3)_2{\cdot}4H_2O$	H_2BDC	NMP	800 W, 105 °C, 30 mins
	Fe-MIL-53	$FeCl_3{\cdot}6H_2O$	H_2BDC	DMF	300 W, 150 °C, 10 mins
	IRMOF-3	$Zn(NO_3)_2{\cdot}6H_2O$	$H_2BDC\text{-}NH_2$	DEF/EtOH	150 W, 35 s
	HKUST-1	$Cu(NO_3)_2{\cdot}3H_20$	H_3BTC	EtOH	300 W, 140 °C, 1 h
	Cr-MIL-100	$C_3H_9CrO_9S_3$	H_3BTC	H_2O (HF aq. addition)	220 °C, 4 h
	ZIF-8	$Zn(NO_3)_2{\cdot}6H_2O$	HMeIm	DMF	140 °C, 3 h
SC	MOF-5	$Zn(NO_3)_2{\cdot}6H_2O$	H_2BDC	NMP	60 W, 30 mins
	HKUST-1	$Cu(OAc)_2{\cdot}2H_20$	H_3BTC	DMF : EtOH : H_2O= 3:1:2	150 W, 1 h
	PCN-6, PCN-6’	$Zn(NO_3)_2{\cdot}4H_2O$	H_3BPDC	DEF	PCN-6; 300 W, 1 h; PCN-6’; 150 W, 1 h
	ZIF-8	$Zn(NO_3)_2{\cdot}6H_2O$	HMeIm	DMF (add TEA + NaOH aq.)	300 W, 1 h
EC	Al-MIL-53	$Al(NO_3)_3{\cdot}9H_2O$	H_2BDC	H_2O : DMF= 90:10	Electrolyte: KCI, 90 °C, 10 mA

	Al-MIL-53-NH_2 Al-MIL-100 ZIF-8	$Al(NO_3)_3 \cdot 9H_2O$ $Al(NO_3)_3 \cdot 9H_2O$ $Zn(NO_3)_2 \cdot 6H_2O$	$H_2BDC\text{-}NH_2$ H_3BTC HMeIm	H_2O : DMF= 90:10 H_2O/EtOH= 25:75 DMF	Electrolyte: KCI, 90 °C, 10 mA Electrolyte: KCI, 60 °C, 50 mA Electrolyte: MTBS,[d] 25 °C, 50 mA
MC	HKUST-1 ZIF-8 ZIF-4	$Cu(OAc)_2 \cdot 2H_2O$ ZnO ZnO	H_3BTC HMeIm HIm	No solvent/MeOH DMF DMF	25 Hz, 15 mins 5-60 mins, 30 Hz 5-60 mins, 30 Hz

[a]CS= conventional solvothermal heating, MW= microwave-assisted, SC= sonochemical, EC= electrochemical, MC=mechanochemical synthesis

[b]H_2BDC= 1,4-benzenedicarboxylic acid, $H_2BDC\text{-}NH_2$= 2-amino-1,4-benzenedicarboxylica acid, H_3BTC= 1,3,5-benzenetricarboxylica acid, HMeIm= 2methyl imidazole, H_4DHBDC=2,5-dihydroxy-1,4-benzenedicarboxylic acid, H_3BPDC= 4,4'-biphenyldicarboxylica acid, Him=imidazole

[c]DMF =*N*,*N*-dimethylformamide, DEF= *N*,*N*-diethylformamide, NMP= *N*-methyl-2-pyrrolidone, HF= hydrofluoric acid, MeOH=methanol, EtOH= ethanol, TEA= triethylamine

[d]MTBS= tributylmethylammonium methyl sulfate

eBr-BODIPY= 1,3,5,7-tetramethyl-4,4-difluoro-8-bromomethyl-4-bora-3a,4a-diaza-s-indacene (optical imaging contrast agent)

[f]THt= tetrahydrothiophene (sulfur odorant components)

1.2. Nano-imprint Lithography and Micro Patterning of MOFs

The ability to create new structures or downsize existing structures at micro and nanometre dimension is essential in today's modern science and technology. When developing new or existing microstructures, improving or retaining the material's peculiar characteristics such as high performance, low energy consumption, low cost and portability is of primary importance.[28] In recent years, the increased capacity to limit functional properties of a material to a controlled position allowed for easy construction and fabrication of efficient nano-functional devices for a wide variety of tasks and applications. The ability to construct various functional devices at nanoscale dimension was as a result of engaging microfabrication and micro patterning techniques. Additionally, this allowed for features to be controlled and manipulated to nanometre scale dimension. This further allowed for miniaturization of functional elements into devices for various mass production and application.[29]

Microelectronics is an outstanding instance of the nano- and micro- patterning techniques employed to precisely control the position, size and location of a functional material for a specific use or for an intended purpose.[30] The potential to keep developing at the nanometre scale ensures a continuation in the scaling down of utilitarian devices. The practice of either combining both improved nano fabrication or existing micro patterning techniques with materials having excellent properties into devices could be termed 'miniaturization'.

MOFs have several significant characteristics based on their unique composition and structure such as high porosity, flexible pore surface, diverse structures, thermal stability and high surface area.[31] The aforementioned attribute makes MOFs interesting and promising materials applicable both for research and industrial applications, such as gas adsorption, storage and catalysis, sensing, drug delivery, bio medics etc. However, the majority of MOFs synthesised are µm-nm crystals in powder form, which do not fulfil all specific needs for direct application and are quite tasking for integration into miniaturized devices.[32] To explore the full benefits of the MOFs' functional properties, the ability to incorporate and control the position of the functional properties, with patterning techniques such as nano-imprint and micro patterning, would make them relevant functional materials in technological application. The basic principles involved when controlling the position and location of functional materials in components or devices roughly follow.[30]

- Process optimizations: the system of fabricating or adjusting the process to obtain desired functional materials.
- Engineering: control of the geometry of the material and tuning the properties for specific application.
- Integration into a useful platform: efficiently connecting the functional material with other components

Over the years, while attempts proceeded on the synthesis and functionalization of MOFs, there has been a substantial amount of research effort committed into incorporating and positioning of MOF functional properties (e.g. porosity, surface area) into devices for various commercial application. This resulted to designing advance new effective path for the precise control of MOFs location on substrates. [10] This report states a number of diverse nano and micro patterning techniques available for patterning MOFs, but due to a large number of strategies developed within recent years for very specific applications, this report's analysis is by no means exhaustive.

The patterning method used in fabricating of nanostructured materials and the study of size-dependent properties can be classified either a bottom-up or a top-down approach.[10,33] This synthetic approach is being applied to MOF formation.

Bottom-up processes uses techniques which depend completely on supramolecular science, (especially self-assembly) as an effective path for the fabrication of complex materials.[34] It can be viewed as a synthetic approach where building blocks are added onto a substrate to form nanostructures. The bottom-up approach allows for the spatial control of MOFs via the growth of the porous crystals in pre-identified locations.[30] However, using self-assembly as the bottom-up fabrication technique poses a challenge as it can be difficult to govern the location and integration of such materials into miniaturised systems.[30] By the use of "bottom-up" approaches, much has been acquired about the role of cluster structure, number of surface vs interior atoms, and quantum confinement effects in controlling the size dependent properties.[33] Due to the difficulty arising from self-assembly, a wide variety of bottom-up patterning techniques have been directed towards MOFs for precise control. These include: electrochemical deposition, surface functionalisation, contact printing, nucleating agents, microfluidics, conversion from ceramics and ink-jet printing. These various strategies are still being optimized, so the advantages and limitation are presently not fully known.

Advantages of the bottom-up approach over top down approach are that: the bottom-up approach has a better chance of creating nanostructures with less defects, more homogenous chemical composition, and better short- and long-range ordering.[35] Also, they are less expensive and faster on a larger scale compared to the top-down approach. The fabrication methods of complex system allows for the combination of both the bottom-up and top-down approached for a desired result.

Top-down approaches use larger (macroscopic) initial structures, which can be externally-controlled in the processing of nanostructures. Top-down techniques entail the creation of "nanostructures" from a large parent entity. A top-down approach can in this manner be viewed as an approach by the progressive removal of building blocks from the substrate to form a nanostructure. Top-down approaches uses advanced lithographic technologies to reduce the scale of bulk matter from the μm to the 10 nm regime.[33]

The technique was broadly created for the scaling down of structures and moreover allows for the preparation of solid-state features approaching the molecular length scale.[34] Advanced lithography techniques are being explored for regulating the size, shape, spacing and location of functional groups to establish the miniaturization of nanostructured devices. Lithography techniques includes photolithography, electron beam lithography (EBL), X-ray lithography (XRL), optical lithography, soft lithography and ion beam lithography.[33,36] Depending on the various lithography techniques, they can be further classified based on the high throughput resolution as either micro or nano fabrication techniques.[29] As the name suggests, for micro fabrication, the resolution obtained during the fabrication process is at the micro metre scale range, while for nano fabrication, the resolution and pattern generated is obtained in the nano metre scale regime (e.g. sizes of 100 nm or less).[37]

1.2.1. Microfabrication techniques

Micro fabrication techniques are known to have their establishment in the field of microelectronics and semiconductors. They are techniques developed for the fabrication of desired structures or devices at micro-metre scale. The desired structure can be achieved from two techniques known as "bulk micromachining," where the structure may be constructed within the bulk of a substrate material; or "surface micromachining" which employs the structure being constructed on the surface of the substrate. In some cases, to successfully attain the fabrication of a desired structure, both bulk and surface micromachining might be combined.[29] The diverse microfabrication techniques employed are photolithography (most

widely used), soft lithography (uses an elastomeric stamp or mould to transfer pattern to a substrate), film deposition, etching and bonding.

1.2.2. Nano-fabrication

The nano fabrication technique uses principles similar to microfabrication to obtain a resolution and generate patterns in the nano metre scale regime (e.g. sizes from 1-100nm). Some still refer sizes up to 1000 nm as nanoscale structures. Techniques developed were a result of the limitation associated to microfabrication techniques in implementing much smaller nanostrcutures which tend to be very complex and expensive when achieving miniaturization smaller than 100 nm scale. Examples of various nanofabrication techniques include electron beam lithography (EBL), focused ion beam lithography, colloid monolayer lithography and molecular self-assembly. Photolithography and electron beam lithography will be discussed in details. More informations on the other fabrication techniques can be viewed in the referenced journals.[28,29,36]

1.3. Lithography

Lithography is a process of transferring a pattern from one medium to another.[38] The quality of a lithographic exposure is determined by three parameters: resolution, registration and throughput value. Resolution refers to the minimum feature measurement that can be transferred with high fidelity to a resist film on a wafer. Registration measures how accurately pattern styles on successive mask are aligned or overlaid with respect to previously defined patterns on the same wafer (Fig 6). Throughput takes to account the amount of wafers that can be exposed per hour for a given mask level and accordingly measure of the effective performance of the lithographic process. Lithography involves transfer of an image from a template to a substrate. This transfer process can be based on 3 steps:

i. Coating of a substrate (Si wafer or glass) with a sensitive polymer layer called resist
ii. Exposing the resist to light, electrons or ion beams
iii. Developing the resist image with an appropriate chemical (developer), unveiling a positive or negative image on the substrate depending on the type of resist used.

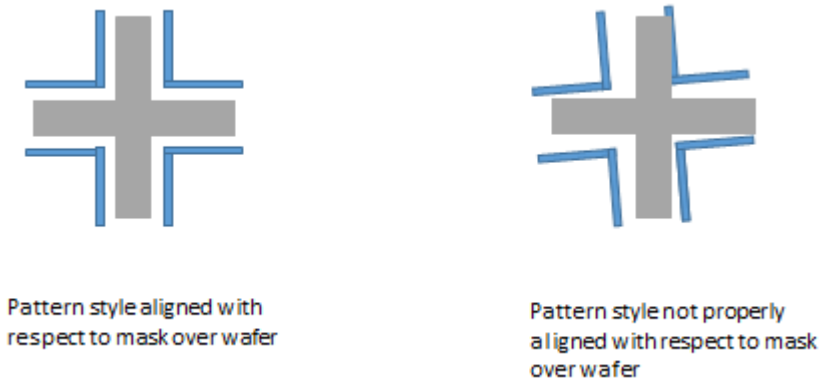

Figure 6-Schematic diagram illustrating successful and non-successful registration of pattern style with respect to mask over wafer

1.3.1. Nanoimprint lithography

In 1995, Stephen *et al.*, revealed the term "nanoimprint" or "imprint lithography" to be derived from "nanolithograhy" by the illustration of a mechanical method staging high 10 nm resolution patterning with high throughput.[39] Nanoimprint lithography is a patterning technique employed in the manufacturing process and has shown the ability to successfully pattern sub-25 nm structures with high throughput and less cost.[39,40] The lithography operates by chemically deforming the material to suit the shape of the mould.

1.3.1.1. Principles of nanoimprint lithography

Nanoimprint lithography includes two essential steps as shown in Fig (7). The first step is the imprint step, in which a mould with a nanostructure on its surface is pressed into a thin thermoplastic polymer film on a substrate that is heated above its glass transition temperature (i.e the region where a polymer transit from a hard glassy material to as soft, rubbery material). Above the transition temperature, the polymer which is thermoplastic behaves as a viscous liquid and can flow under pressure, easily conforming to the shape of the mould. The mould is then removed. This step leads to the replication of the mould nanostructure in the resist films pressed against. As such the imprint design makes a thickness contrast in the resist. The second step is the pattern transfer, in which an anisotropic etching process (e.g. reactive ion etching (RIE) is utilized in uprooting the residual resist in the compacted region. This stage transfers the thickness contrast pattern into the entire resist.[39,40]

Nanoimprint lithography has an advantage over other lithography techniques in producing high resolution, because it does not use any energetic beams which limit resolution by the effects of wave diffraction, scattering and interference in a resist, and backscattering from a substrate.

Imprint lithography is moreover a physical process rather than a chemical process and is fundamentally quite different from stamping, using a monolayer of self-assembled molecules.[40]

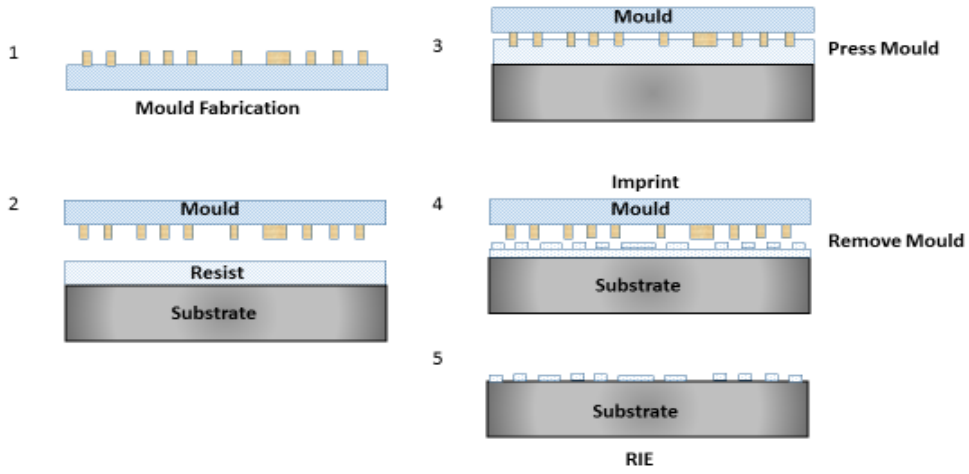

Figure 7- Schematic diagram of nanoimprint lithography process. (1) fabrication of mould of any design, (2) pressing of mould onto resist film, (3) using of mould to create an imprint through resist, (4) mould removal, (5) removal of residual resist in the compressed areas to obtain genuine pattern transfer.

1.3.2. Electron beam lithography (EBL)

EBL or E-beam lithography uses beam of electrons to scan pattern across the surface covered with a sensitive film called a resist to electrons by applying a voltage, thus depositing energy in the desired pattern on the resist film. Magnetic lenses are used in focusing the beam.[29] Electron beam lithography has gained a wide application in nanofabrication techniques due to its excellent high resolution (e.g. sizes as small as 50 nm) and its flexibility. The high resolution can be attributed to improvement in emission filaments, reduction of beam diameter and the use of electronic radiation.[38,41] Despite the great resolution achieved, E-beam lithography has some drawbacks. (a) Working with high vacuum level, EBL is both slow and expensive for an industrial scale. So this is limited to electron optics. (b) The maximal area of the writing field, numerical aperture and the resolution are restricted from the diameter and shape of the beam in the focus point.[38]

An EBL system consists of the following parts: (i) an electron gun or electron source that supplies; (ii) an electron column that "shapes" and focuses the electron beam; (iii) a mechanical stage that position the wafer under the electron beam; (iv) a wafer handling system that automatically feeds wafers to the system and unloads them after processing; and (v) a computer system that controls the equipment. [36]

There are two distinct schemes an EBL system utilizes when patterning as seen in Fig (8):

- Projection printing: makes use of a mask to pattern, wherein a particularly large-sized electron beam pattern projected in parallel passes through the mask using a high precision lens system onto a resist coated substrate.
- Direct writing: directly makes use of an electron beam to pattern onto a resist coated substrate. The resist is chemically and physically transformed due to the energy radiated from the electron beam. This system thus eliminates the expenses and time consumed in the production of masks.

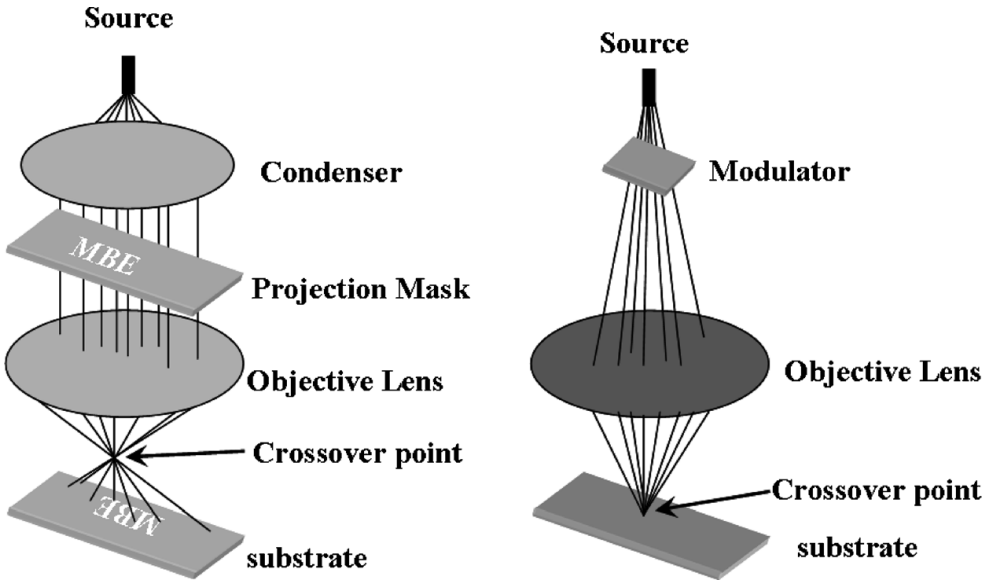

Figure 8- diagram illustrating the distinct scheme of project printing and direct writing [36]

1.3.3. Photolithography

Photolithography is one of the most extensively used microfabrication techniques in microelectronic and semiconductor device fabrication. It involves transferring a pattern using a radiation source with wavelength(s) from a photomask to the surface of the substrate.[36] This lithography process uses light source (e.g. UV, deep-UV, extreme-UV or X-ray) to expose a layer of light sensitive polymer (photoresist) through a mask. The mask is made up of a nearly optical glass plate containing the desired pattern in the form of a thin (100 nm) Chromium layer.[41,42] Note that the pattern is defined by a transparent and opaque region (opaque area made of an absorber metal) on a UV- transparent background.[41] The image replicated by the mask is defined by the type of photoresist used in patterning the process. A positive resist under exposure, breaks down and becomes more soluble when washed in a developer. While a negative photoresist gives you the inverse of the mask by crosslinking an under exposed region

to photon irradiation, hence, becoming insoluble in a developer solution. The unexposed regions from the mask are easily washed away using a suitable solvent.[30]

The basic steps involved in photolithography can be classified into three distinct process (Fig 9): [29,36]

a. The substrate material is coated with a thin film of photoresist or light sensitive polymer.
b. The substrate and photoresist are then exposed to UV light through a mask encompassing of the desired pattern and used to selectively illuminate the photoresist.
c. The exposed substrate is then submerged into a developing solution.

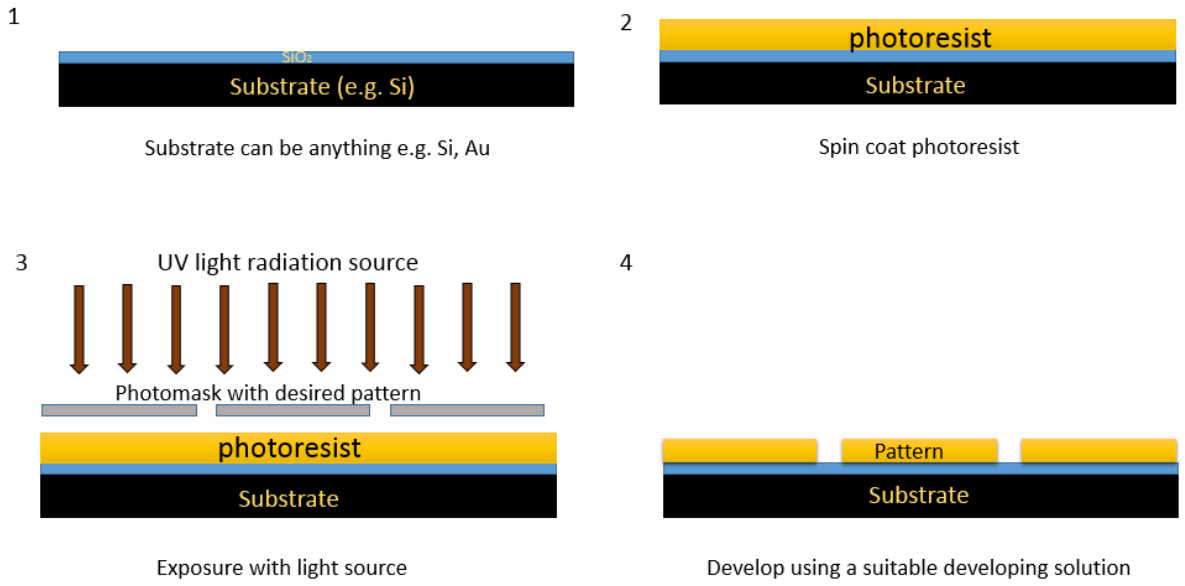

Figure 9- Schematic representation of a photolithographic process sequence

1.3.3.1. Drawbacks associated with photolithography

Although the principles of photolithography are simple, the actual implementation to fabricating nanostructures are quite difficult and expensive. This is as a result of:

i. The continued shrinking of feature size to obtain high resolution nanostructures significantly lesser than 100nm scale is quite laborious due to diffraction effects present. Generally, it has been observed that when using UV light (360-460 nm), the resolution of contact mode lithography is typically 0.5-0.8 µm. Which is not a high resolution for nanofabrication. This is due to the inability to minimize the gap between the mask and the flat substrate below ~ 1µm, even after the use of a vacuum system to hold the two parts together. In a bid to acquire a higher resolution, "next generation lithographic" techniques have been employed. These techniques however uses very expensive

equipment (capital and operating cost), and are therefore limiting to selected applications.[41]

ii. The masks and photoresists need to be properly aligned to obtain a good patterning on the substrate.

iii. The need to carefully control the density of defects during the process.

iv. It is not that effective in introducing specific or unique chemical functionalities into a substrate.[28]

v. It is constrained to mostly materials using photoresists and semiconductors, and not fundamentally with glass, plastics ceramics.[28]

Printing, stamping, and moulding are other developed lithography process using mechanical process instead of photons and electrons.

1.3.3.2. Photoresist

The photoresist can be classified into two types based on the chemical nature (i.e. possible transformation upon exposure to light), as illustrated in Fig 10. They are chemically modified upon exposure to photon light. The two resists are a positive and negative photoresist. A positive resist breaks and becomes more soluble in a developing solution due to exposure upon UV light. This changes the chemical and physical structure of the resist so it becomes more soluble in the developer. A positive resist prints a pattern that is similar to the pattern on the mask. Since positive resists do not crosslink, a positive resist develops where they have been exposed while the unexposed areas remain on the substrate. Examples include the PMMA Series (e-beam), Gluon gL2000 (e-beam) and S1800 Series (g-line).

A negative becomes crosslinked on exposure to UV light resulting in the resist becoming insoluble in the developing solution. A negative photoresist operates by printing a pattern or image that is the inverse pattern on the mask. A negative resist resides on the surface which is exposed to light, thus the developer solution removes only the unexposed regions. Negative resists are more widely used in integrated circuit processing because they allow for precise control for small geometry features. Examples of negative photoresist are the AZ nLOF 2000 series, AZ 15nXT, SU-8 series (i-line) and KMPR Series (i-line) from Microchemicals companies.[29,30,36]

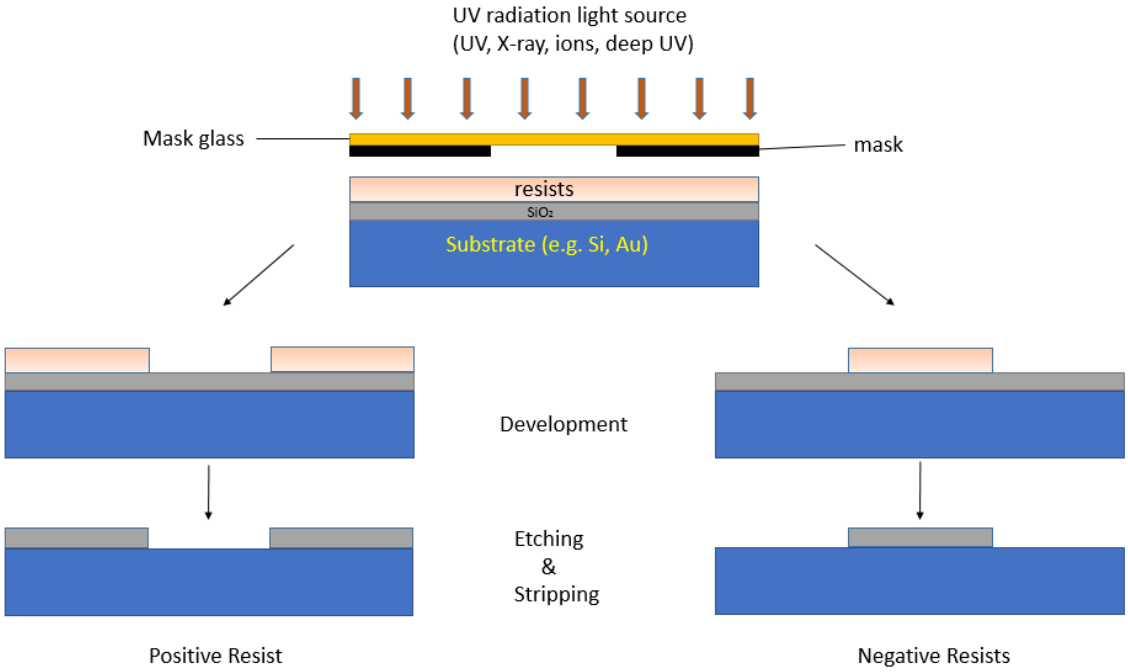

Figure 10- Schematic diagram illustrating the concept of both positive and negative photoresist

1.3.3.3. Photomasks

Photomasks proffer a platform for replicating a pattern transfer to a substrate material by acting as a transfer artefact (Fig 11 a). The photomask is a nearly optically flat glass (transparent to near UV light) or quartz plate (transparent to deep UV light) with an absorber pattern metal (e.g. an 800 Å -thick Chromium layer). The mask-patterned surface is transferred to form an image pattern on a receiving substrate (Fig 11 b). This can be further fabricated into manufacturing microelectronic, mechanical or micro devices.[43]

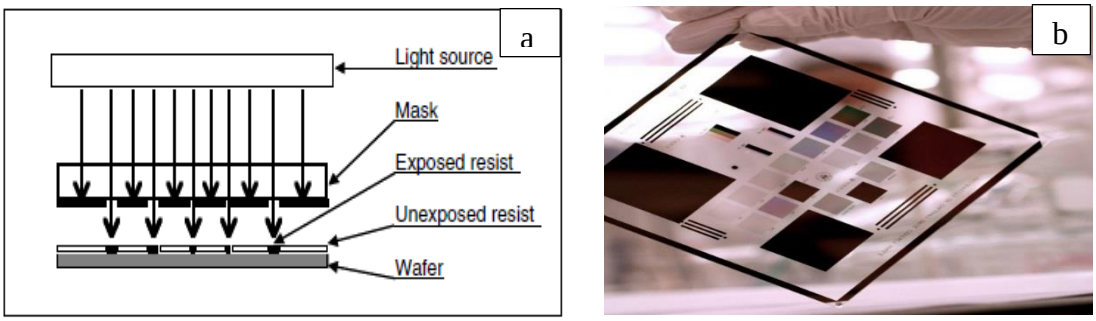

Figure 11- (a) Schematic diagram illustrating the concept behind a photomask application,[43](b) picture of a patterned photomask which is transferrable onto a substrate.

1.3.4. MOF Thin films

Thin films serve as a base platform where various functionalities are built upon the substrates, for the establishment of a unique purpose or application. Films can act as a structural or functional role in design. Extra functions like superconducting, conducting, insulating, semi conducting, transparent, catalytic, piezoelectric and other layers are constructed at the substrates by deposition, where further processing of the thin film for rendering functionalization can prevail.[44] Generally, most crystalline MOF powders are obtained by the accustomed solvothermal synthesis which is not suitable for direct application. For this reason, MOF films do help to provide a stable support to which MOFs can rigidly be anchored, not accessible by ordinary MOF powder. [1,45] Examples illustrating the application of MOF thin films include catalysis, gas separation, optical and chemical sensors. One step in achieving a MOF based device is the development of a MOF film, which could offer enormous advantages for technological applications. Creation and growth of MOF thin films on different substrates can be based on 3 different major concepts that are: [46]

a) The direct growth or deposition from solvothermal mother solutions (this method broadly utilizes a functional substrate in preparing a MOF thin film).
b) The assembly of preformed, ideally-sized and shaped selected nanocrystals.
c) Stepwise layer-by-layer growth onto the substrate.

Two other techniques that have been developed were also added in this report[45]

d) The electrochemical deposition of thin MOF- films on metal substrates
e) The deposition of MOF thin films using a gel-layer approach

A standard approach when preparing MOF thin films is to first select an existing MOF of interest (e.g. by the scale of its pores) and a method to process it as a film on top of a given substrate. This may cause a difference in the film processing method which might be more or less specific to the desired MOF, resulting in a large number of methods that lack generic applicability.[1]

1.3.4.1. Classes of MOF thin films

There are two distinct classes of MOF thin films recognised generally: Polycrystalline films and SURMOFs (surface-mounted MOFs), as seen in (Fig 12). Polycrystallines can be associated to more or less random oriented MOF crystals or particles that lie on a surface. The crystals can be both properly inter-grown to entirely cover the surface or scattered (presence of

holes). In some cases, there might be an exception in which the interaction with the surface allows for the preferred attachment of the crystals in a single direction with respect to the substrate and each other, resulting in preferentially oriented films or crystallites. The size of the MOF particles obtained often resides in the micrometre range, and is used to determine the thickness of the thin film. Evaluating the properties of such films might be challenging and are expected to be identical to the properties of the bulk powder material. SURMOFs are the second class of MOF thin films. They consist of ultrathin MOF multilayers (in the nano metre range) that are perfectly oriented (at least in the direction of the growth). They are prepared by stepwise liquid phase epitaxy (LPE) on a functionalized substrate.[47,48] SURMOFs are exceptionally smooth. The roughness of their surface is within the order of a few elementary cells, and they may be often quasi-epitaxially grown on the substrate so that the thickness of the film and the crystallite domain size can be precisely controlled.[1] It has been found that the use of self-assembled monolayers with a specific end-group such as –COOH or –OH can be used to regulate the crystallographic orientation of the film.[49] The ideal SURMOF could be additionally characterized by means of large crystalline domain in the plane of the growth. Also note it is quite hard to have a genuine control of the thickness of a SURMOF.

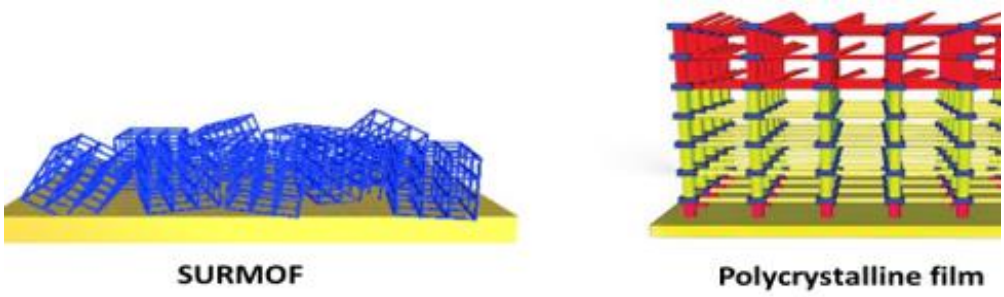

Figure 12- The difference in orientation between SURMOF and polycrystalline[1]

1.3.4.2. Thin film synthesis method

Generally, the fabrication of MOF thin films of crystalline frameworks follows one of the two methodologies: Direct synthesis and seeded growth methods, associated to zeolite films approach; and Langmuir-Blodgett and layer-by-layer thin film deposition techniques associated to coordination polymer films. These two famous techniques in preparing thin films are now translated to preparing MOF thin films. Note SURMOFs can only be produced using the Langmuir-Blodgett or layer-by-layer technique.[1] The synthesis methodology will be briefly explained; those interested in the detailed synthesis and application of MOF thin films are encouraged to read various excellent review articles.

1.3.4.2.1. Direct synthesis

Direct synthesis is a form of system where a substrate is used bare (or modified by organic molecules, i.e. SAMs) together with an appropriate growth solution. Growth occurs at the surface and sometime also in solution simultaneously, leading to crystals attached to the substrate surface in a more or less intergrown and continuous fashion.[48]

1.3.4.2.2. Seeded or secondary growth

Seeded growth is a common approach used especially in the fabrication of zeolite thin films. This technique involves film growth from pre-attached seed crystals.[50] This method has caused great popularity in MOF thin film fabrication because many MOFs tend to have low heterogeneous nucleation on density on porous ceramics. The technique entails two steps: *preparation and deposition of seed*. They are often executed under solvothermal conditions.[48] Seeded growth has been claimed to permit a better overall microstructure as well as a lower dependency on the nature of supports in a polycrystalline.[50]

1.3.4.2.3. Langmuir-Blodgett Layer-by-Layer deposition technique

MOF layers are produced in a Langmuir-Blodgett (LB) apparatus where they are conveyed one after another onto a silicon substrate with intermediate rinsing steps. The layers are conceived by weak interactions, such as π stacking between pendant groups in a manner identical to interdigitated MOFs. NAFS-1 AND NAFS-2 are example of MOFs developed through this technique.[51] NAFS-1 is composed of cobalt–containing porphyrin units (CoTCCP) connected together by binuclear copper paddle-wheel units in a 2D array of CoTCCP-Py-Cu, which can be transferred to a silicon substrate in a layer-by-layer style.[47] To ensure right π stacking, pyridine molecules are bonded to the axial position of the copper ions perpendicularly to the 2D layer. The overall thickness of the film relates to the number of deposited layers. NAFS-2, a layer-structured MOF was constructed similarly to NAFS-1. The main contrast is the nonappearance of the pyridine ligand in the axial position and the porphyrine cage being empty, resulting in less efficient stacking with an average tilt angle of 3° between layers.[51]

1.3.4.3. Deposition on substrate.

The solvothermal mother solution approach has been known to effortlessly deposit MOF thin films onto a functionalized solid substrate. Just as with any other crystalline materials, the formation of MOF has two steps: nucleation and subsequent growth. The filtered solvothermal mother solution could contain nuclei for MOF development, as with SBUs as mentioned above. These nucleation sites will be deposited onto the substrate, and crystal growth will take place

at the surface. Also, even for a bare substrate (without any functional groups such as silica), there is an increase in crystal size as the deposition process progresses. However, no crystal is generated when the filtered mother solution is kept where it is. In other cases, crystallization may exist through methods such as heating and supersaturating by directly immersing the substrate into a reactant solution. Substrates particularly having functional groups favour MOF growth by serving as heterogeneous nucleation sites. The whole idea is to utilize a substrate for inducing nucleation and subsequent MOF growth in a 2D scale, thus fabricating MOF thin films.[47]

Table 2 Representative preparation methods for MOF thin films [47]

Methods	Typical MOF	Substrate used
Growth/ deposition from solvothermal mother solutions	MOF-5, ZIF-8	COOH-terminated SAM
The direct oriented growth/ deposition from solvothermal solution	HKUST-1	COOH, OH and CH_3-terminated SAMs
Microwave-induced thermal deposition	MOF-5	nanoporous anodized alumina discs coated with various conductive thin films
Colloidal deposition method	MIL-89	Side-polished silicon wafers
Layer-by-layer or liquid phase epitaxy (LPE) of SURMOFs	HKUST-1 and $[M_2(L)_2(P)]^{a0}$	COOH, OH and pyridyl-terminated SAMs
Electrochemical synthesis	HKUST-1	Copper substrates
Evaporation induced crystallization	HKUST-1	Silanol, vinyl or COOH functionalized surface
Gel-layer synthesis	HKUST-1 and Fe-MIL-88B-NH_2	COOH, OH-terminated SAM on gold wafer
Liquid phase interface growth	ZIF8, HKUST-1	Substrate free

a) M: Cu^{2+} , Zn^{2+} ; L: dicarboxylate linker; P: dinitrogen pillar ligand.

1.4. Gels

Gels are ubiquitous semi solid materials found in everyday life applications. Example of gels adopted in the commercial world are hair gels, lithium grease, soaps, toothpaste, contact lenses and cosmetic products etc. Gels can be recognized by a simple "inversion test," if the material is able to support its own weight without flowing when turned upside down. Gels are characterized by elastic cross-linked systems comprising of fluid filling up the interstitial space of the network. Outwardly, gels are generally fluid in any case, but carry on like viscoelastic solids due to a three dimensional cross-linked system in the liquid, which can aid sustaining the gel from deforming when an external force applied is removed. In this manner, gels could be referred to as strong, weak or pseudo gels[52] depending on the network crosslinking within the fluid, as well as the flow behaviour when in an unfaltering state. Both strong and weak gels behaves as a solid in a small deformation regime. A weak gel acts as a liquid order when subjected to a large deformation, as the network crosslinks can be broken and reformed, such as colloidal gels and biopolymers gels.[52] Whereas, strong gels retains solid state even under a large deformation, as a swollen elastic body. Psuedo gels on the other hand, are entangled polymer systems which over a range of time scales, physical entanglements within polymers chains emulates chemical crosslinks giving these materials gel–like properties.[52]

Gels can be categorized based on colloidal phases (a single-phase system and two phase system), nature of solvent (hydrogels, organogels and xerogels), physical nature (elastic gels and rigid gels) and rheological properties (plastic gels, pseudo-plastic gels and thixotropic gels).[53]

1.4.1. Mechanism of gelation

Gelation refers to the process of arbitrary connecting macromolecular subunits chains together to larger branched polymer by arrangement of an infinite network (Fig 13).[54] Regardless of what kind of polymers are linked, the transition point at which the gel acts as neither a liquid nor as a solid is known as "gelation" and the critical point where gel first occurs is known as the "gel point".[52] At the critical gel point, the liquid viscosity becomes infinite so neither is the system a liquid nor a solid, as the equilibrium elastic modulus is zero.[52] Beyond the gel point, evolution of elastic modulus takes place with the progression of the cross-links.[55] In 1987, Chamber and Winter defined how the critical gel point could be determined. The critical gel point is the point at which two moduli show a power law dependence on the applied frequency

over an extensive range of frequencies, or rather the ratio of shear moduli, tan (δ), is independent of frequency.[52]

$$G', G'' \alpha\ \omega'' \quad \frac{G''}{G'} = \tan(\delta) = \tan(\frac{n\pi}{2})$$

Where G' and G'' are the elastic and viscous shear moduli, ω =1Hz, stress=5 Pa. The phase angle δ depicts the relative importance of the G' and G''.

A gel is considered ideal if the shear moduli at the critical gel points are equal and n = 0.5. Gels containing defects, do have the phase angle δ= $n\pi/2$ independent of frequency with n in the range of 0.5 to 1. Non-ideal gels have a larger value of n.

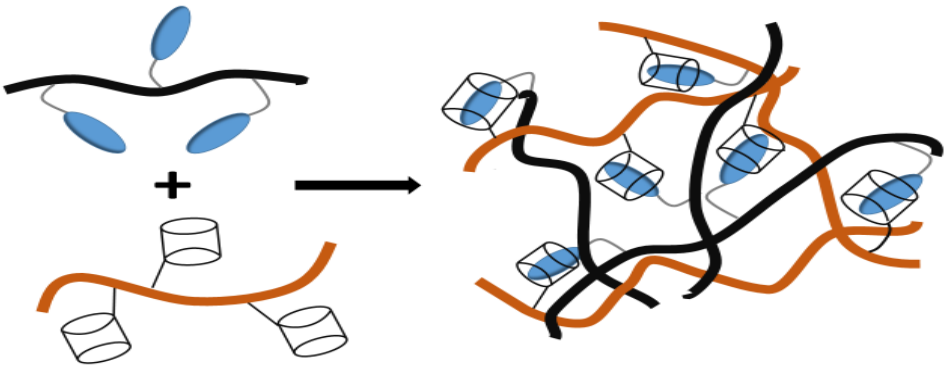

Figure 13-Gelation mechanism, physical or chemical crosslinking of smaller macromolecules into larger clusters.

From reviews of past research works, two distinctive gelation mechanism have been distinguished: physical and chemical gelation as seen in (Fig 14). Physical gelation is the noncovalent crosslinking of polymeric chains into macroscopic network called physical gels or thermoreversible gels. The crosslink physical bonds result from forces such as van der Waals interactions, π-π interactions or Hydrogen bonding, and are very sensitive to variations of pH, temperature and ionic content. Physical gels can be further sub divided into strong gels and weak gels.[57,58] Chemical gelation on the other hands involves covalent bonding of molecules into three-dimensional networks thus always resulting in a strong gel.[56] The three relevant chemical gelation processes can be subcategorized as condensation, vulcanisation and addition polymerization.[54]

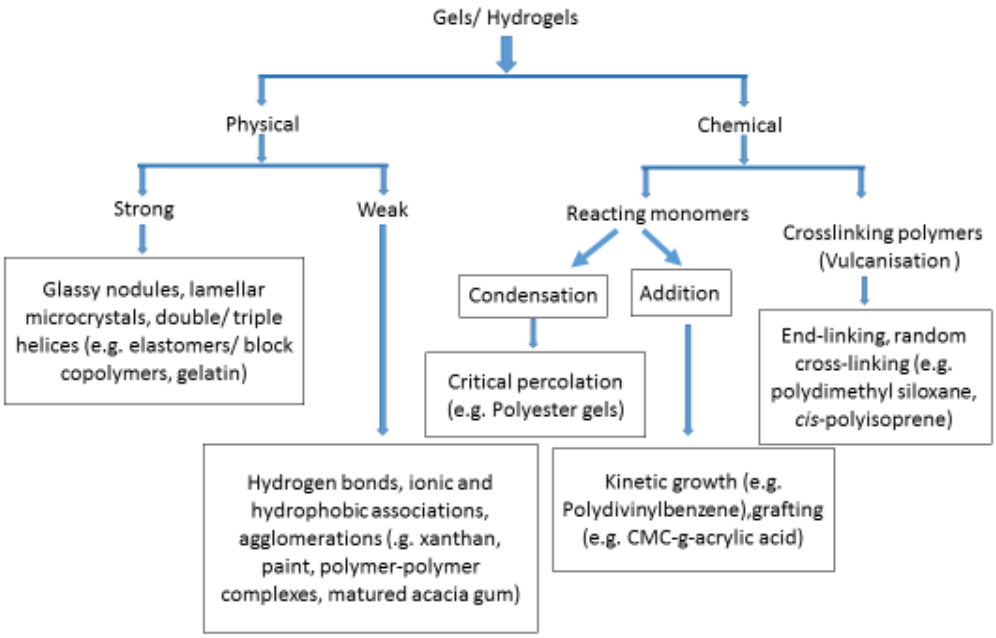

Figure 14-Classification of gelation mechanism with relevant examples.[54]

1.4.2. Thixotropic gels

Thixotropy is a time-dependent shear thinning property,[59] and is the ability of certain gels to decrease in viscosity (i.e. becoming thinner) as stress over time increases and re-establish its viscosity again when at rest (Fig 15). This unique property offers these gels wide applications such as thickening agents for foods and cosmetics, paint additives and inks, ceramics, resins, pharmaceutical fillers and medical devices.[60] A common drawback associated with thixotropic materials is that when handling these materials, they could progressively breakdown on shearing and not regain their viscoelastic properties or slowly rebuild at rest. The time of recovery varies from minutes to hours after the breakdown time.

Key components used when defining thixotropic properties are:[61]

i. It is dependent on viscosity
ii. It indicates a time-dependent decrease in the viscosity instilled by flow or agitation
iii. It is reversible and recovers when the flow is reduced or stopped.

The word thixotropy was coined from the Greek words “thixis” (stirring shaking) and “trepo” (turning changing).[62] Thixotropic is therefore defined as a phenomenon which depicts a reversible change from a flowable fluid to a solid-like elastic gel as a result of time-dependent changes in the viscosity impelled by temperature, pH and other factors with no adjustment in the volume of the system. Thixotropy in an isothermal system is the reversible decrease of

viscosity with increase in shear rate. A thixotropic material turns to fluid when applied forces is acting upon is increased, such as stirring, shaking or pumping and returns to its viscous state if left at rest. When trying to obtain an ideal thixotropy gel, important factors such as pH, temperature, polymer concentrations, polymer modification or combinations, addition of cations or anions, play a vital role in the thixotropic properties of the fluid.

Thixotropic systems are characterized to follow non-Newtonian systems, as the viscosity is dependent on the shear rate, therefore having no constant viscosity.[59] A pseudo plastic system is an example which observes non–Newtonian systems, following a time-dependent change in the viscosity. Thixotropic properties are observed when reducing the viscosity with time under constant shear. A progressive breakdown to further reconstruction of the liquid structure results to an increase of shear, which is a consequence of in-flow collision and Brownian motion. The Brownian motion causes random thermal agitation of atoms and molecules which displays the particles to move to their most favourable positions where they can, from a structure–entropy perspective.[59,63]

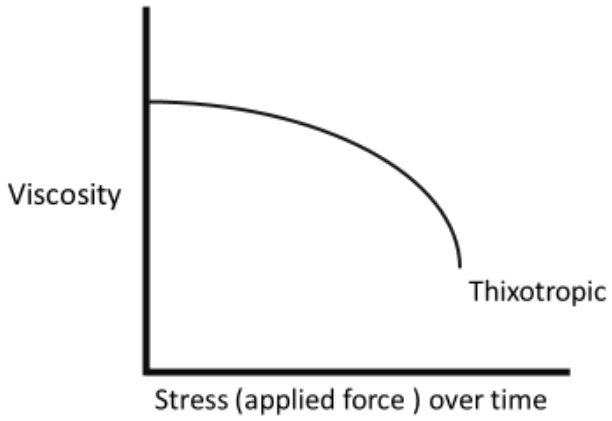

Figure 15-schematic diagram illustrating thixotropy profile (viscosity vs time).

1.4.3. Metal organic gels

In recent times, the incorporation of metallic units into polymer chains for functional metal-containing materials has gained much research interest due to their diverse potential applications. Metal-containing polymers (MCPs) are polymeric materials characterized by metal-ligands coordination units[64] possessing large surface areas and tuneable chemical properties that make them excellent candidates for applications such as gas separation, hydrogen storage, catalysis, sensing and drugs delivery etc.[65] MCPs can be categorized into three groups:[64]

i. MOFs having a three- dimensional network structure which are insoluble.
ii. Long chain one dimensional macromolecules often processed and can further aggregate into various higher dimensional nanostructures.
iii. Three dimensional networks which possess the ability to solidify liquids, i.e. MOGs.

Over the past few decades, there has been a remarkable growth in studies on MOGs as a result of their inherent potential as soft materials possessing both MOF and gel characteristics.[66] in comparison to MOFs, MOGs are extension based on coordination complexes. Although various organic ligands with metal ions have been employed to manufacture an extensive number of MOFs, relatively few studies abound on the concept of MOGs. A study conducted by Liu *et al*. (2009) showed that MOG can be obtained using coordinative binding between multipodal ligands and metal ions.[67] Consequent to the close similarities between MOFs and MOGs, there is need to distinguish both polymers in a bid to understand each of them extensively. Various reviews establish MOFs as metal-ligand compounds that display "long range ordered" one-, two-, or three- (1D, 2D, or 3D) dimensional structures whereas MOGs depends on metal-ligand coordination that display "short range ordered" 1D, 2D, 3D structure either by coordination or other supramolecular interactions.[67] Another distinguishing factor is in the exhibition of infinite long-ranged order with periodic arrangement of asymmetric in MOFs whereas MOGs show finite short ranged order with periodically disordered arrangement of the building units.[67]

1.4.4. Synthesis of MOGs

The synthesis of MOGs include the supramolecular self-assembly of coordination complexes through non-covalent interactions such as hydrogen bonding, π-π stacking, hydrophobic interactions and van der Waals forces.[68] The synthesis of a coordination complex (i.e. hydrogen-bond acceptor /donor motifs) between organic ligands and coordination compound results in the formation of MOGs in the presence of excessive ligands. Gel formation and growth of coordination complex is controlled by the amount of ligands close to the metal atoms. The gels are produced by weak non–covalent bonding between the ligand and solvents molecules or coordination complexes.

When constructing MOGs a crucial factor to note is that, it is not only the building units that are of importance, but the approach in which they are connected. An understanding of how the building units reticulate (form a network structure) has assisted material designers in establishing principles required for predictive capability.[19] Additionally, specific functional

groups can also be incorporated when synthesising MOGs, thus offering a possible choice for designing, reconstructing and controlling the structure and supramolecular interactions of gel.[66] Taking into account the vast number of metal ions and organic ligands, studies on MOGs are awaiting immense investigation.

1.4.5. Interest in MOGs

Great development and different synthetic methods have been adopted for the synthesis of MOFs. This is a result of their high surface area, pores sizes and flexible network systems, as they are promising materials in applications such as gas storage, separation, optoelectronics and catalysis.[69] However, the low solution processability of the crystalline MOF significantly restrain its application in device fabrication and biological sciences.[69] The significant reason in the restriction of the MOFs fabrication processability is by reason of its physical fragility.[70] Examples of such, is the functional group present in the ligand of the MOFs immensely limiting the progress and applications of functional MOFs. Applications such as sensing and catalysis, requires the use of robust MOFs because they are highly thermally or chemically stable. This is due to their synthesis at elevated temperature, solvothermal reactions or microwave irradiation often used to enact the coordination reactions. Nevertheless, the drawback to these approach is that, it degrades the active functional groups on the ligands, therefore restricting the functionality of the synthesized MOFs unlike MOFs produced using room temperature synthetic approach. Whereas they are not highly thermally or chemically stable.[70]

Another challenge is the fabrication of thin film coating as solid support to which MOFs are rigidly attached, providing access to various applications.[45] Some other applications uses patterning techniques which require thin films materials for processability, which can be quite challenging when positioning MOFs since they are generally synthesized as microcrystalline powders. Fabrication of different MOF thin film may be required for compatibility with the MOF compound, which might not be cost effective.

To circumvent this issue, new platforms were adopted by incorporating the use of metal-ligand coordination chemistry to coordinate the self-assembly of polymeric gels such as MOGs in supramolecular and coordination chemistry. The incentive for the application of metal-ligand interactions, is to build higher dimensional structures which permit the formation of controllable and extended structures by virtue of their dynamic nature. Also the easy proccessability and dynamic nature of MOGs are explored for applications in various fields due to their reversible sol-gel behaviour.[69]

1.4.5.1. Problems encountered with MOGs

The synthesis of MOG is an active new area of research, which hold much promise for the future. But a major difficulty to afford new MOGs is to genuinely comprehend the key factors governing the gelation process to envisage robust enough gels with low syneresis.[71] Furthermore, the investigation and exploitation of MOG structures generally has been at the molecular level and practically little is known about how their large scale structure may be controlled or modified for use.[72]

Chapter 2. Experimental design and methodology

2.1. Chemicals and reagents

2.1.1. Solvents

Water: used throughout this work was deionised water with a pH value of 6.7 with conductivity of 18.2 MΩ cm^{-1}. The water was used for hydrothermal synthesis, cleaning and rinsing of laboratory glassware and other appropriate equipment.

Absolute Ethanol: obtained from VWR Chemicals (99.7 %) was used as a major solvent in the preparation of MOFs and gels. Also used for rinsing and removing excess ligands after solvothermal synthesis.

Methanol: purchased from VWR Chemicals (AnalaR) was used as a major solvent in the preparation of MOGs and refluxing.

Dichloromethane: purchased from VWR Chemicals, France (100 %) was used for the synthesis of PEGDM. It was also utilized when confirming hydro/organic gel dissolution in organic solvents.

Ethyl ether: purchased from VWR Chemicals (100 %) was used as an extracting organic solvent during synthesis

2.1.2. Reagents

Methacrylic anhydride: obtained from Sigma Aldrich was used for preparation and functionalization of Polyethylene glycol to Poly (ethylene glycol) dimethacrylate.

Acetic acid: purchased from VWR Chemicals was used as a modulator for MOF growth.

Acrylic acid: purchased from Sigma Aldrich was used as a monomer for reacting with photoinitiator required for photo-crosslinking.

Metal salts: $Al(NO_3)_3{\cdot}9H_2O$, $In(NO_3)_3{\cdot}XH_2O$ and $Cr(NO_3)_3.9H_2O$ were purchased from Sigma Aldrich. $La(NO_3)_3{\cdot}6H_2O$ and $Ga(NO_3)_3{\cdot}XH_2O$ were purchased from Alfa Aesar. The metal salts were used to provide metal ions needed for metal-ligand bond coordination of MOFs or MOGs

Organic linkers: Terephthalic acid, 2-aminoterephthalic acid and 1,3,5-benzenetricarboxylic acid, purchased from Sigma Aldrich were used as bridging organic linkers required for the synthesis of MOFs and gels.

Alumina membranes: purchased from Whatman (Whatman Anodisc inorganic filter membrane, pore size 0.02 µm, 13mm diameter). The alumina membrane functioned as both Al^{3+} source as well as a support for MOF growth.

Glass cover slips: were purchased from Thermo Scientific (10-12 mm thickness) and used supporting glass slip during solvothermal MOFs synthesis.

Photoinitiators: Irgacure 184 and 2959 from Ciba were used as agent for inducing free radical polymerisation of various materials.

Table 3-summary of chemicals and reagents used.

Chemicals and Products	Supplier	Purity/Grade
Terephthalic acid	Sigma Aldrich	98 %
2-aminoterephtalic acid	Sigma Aldrich	99 %
1,3,5-benzenetricarboxylic acid	Sigma Aldrich	95 %
Aluminium nitrate nonahydrate	Sigma Aldrich	≥98.0 %
Indium (iii) nitrate hydrate	Sigma Aldrich	99.9 %
Chromium (iii) nitrate nonahydrate	Sigma Aldrich	99 %
Iron(iii) nitrate nonahydrate		
Lanthanum (iii) nitrate hexahydrate	Alfa Aesar	99.9 %
Zinc nitrate hexahydrate	Sigma Aldrich	98%
Gallium (iii) nitrate hydrate	Alfa Aesar	99.9 %
Sodium hydroxide	Fisher Scientific, UK	99.07 %
Alumina membranes	Whatman Anodisc inorganic filter membrane	Diam. 13 mm, pore size 0.02 µm
2-methyl imidazole		
Acetic acid	VWR Chemicals	
Glass cover slips	Thermo Scientific	
Ethanol Absolute	VWR Chemicals	99.7 %
Methanol	VWR Chemicals	AnalaR
Acetone	VWR Chemicals	100.0 %

Propan-1-ol	BDH AnalaR	99.5 %
2-propanol	VWR Chemicals	99.7 %
Butan-1-ol	Fisher Chemicals	99.3 %
Butan-2-ol	Avocado Research Chemicals, Ltd	99 %
1-pentanol	Sigma Aldrich	99+ %
2-heptanol	Sigma Aldrich	96 %
1-nonanol	Avocado Research Chemicals, Ltd	98 %
1-undecanol	Avocado Research Chemicals, Ltd	99 %
Poly(ethylene glycol)	Alfa Aesar, Uk	
Triethylamine (TEA)	Fisher Chemicals	> 99 %
Methacrylic anhydride (MA)	Sigma Aldrich	94 %
Dichloromethane	VWR Chemicals	100.0 %
Ethyl ether	VWR Chemicals	100 %
Chloroform	VWR Chemicals	99.8 %
Hydroxyl Propyl Cellulose	Sigma Aldrich	99 % through
N,N–dicyclohexylcardodiimide (DCC)	Alfa Aesar	99 %
4-dimethylamino-pyridine (DMAP)	Alfa Aesar	99 %
Activated molecular sieve		
Toluene	VWR Chemicals	100 %
Photoinitiator Irgacure 2959	Ciba Specialty Chemicals	
Photoinitiator Irgacure 184	Ciba Specialty Chemicals	
Polyvinylpyrrolidone K 90	Fluka	
Acrylic acid	Sigma Aldrich	99 %
Allyl alcohol	Avocado Research Chemicals, Ltd	99 %
AZ nLOF 2070 dil 1:0, 40 2.0 µm	MicroChemicals	
AZ 726 MIF developer	MicroChemicals	

2.2. Instrumentation

2.2.1. Scanning Electron Microscopy (SEM)

Scanning Electron Microscopy (SEM) analysis was performed with a HITACHI TM 1000 microscope with an accelerating voltage of 15 kV. Samples were mounted on glass slide with a conductive carbon tape and placed into the SEM. The stubs (15 X 10mm) for holding samples was screwed to the microscope and measurement taken with magnification ranging from 20-10,000 x as seen in (Fig 16).

Figure 16-Hitachi TM 1000 microscope

2.2.2. Powder X-ray Diffraction (Powder XRD)

Powder X-Ray Diffraction (PXRD) measurements were performed on a PANalytical Empyrean Series 2 Diffractometer operating Cu $K_{\alpha 1}$ (λ = 1.54056 Å) radiation (Fig 17). All samples were scanned with a power setting of 40 kV and 30 mA using automatic slits with an irradiated sample length of 10 mm at a step size of 0.0262° and a net time per step of 73.4s. The results obtained were compared to a database of diffraction patterns.

Figure 17-PANalytical, Empyrean X-ray diffractometer

2.2.3. White light interferometer

The white light interferometry was carried out with a Vecco WYKO NT1100 and used for measuring the depth and topography of the ablated alumina membrane surface (Fig 18). Alumina membranes were loaded onto the instrument and by using objective lens, the interference of white light was captured to determine the topography and surface depth our fabricated lithography techniques.

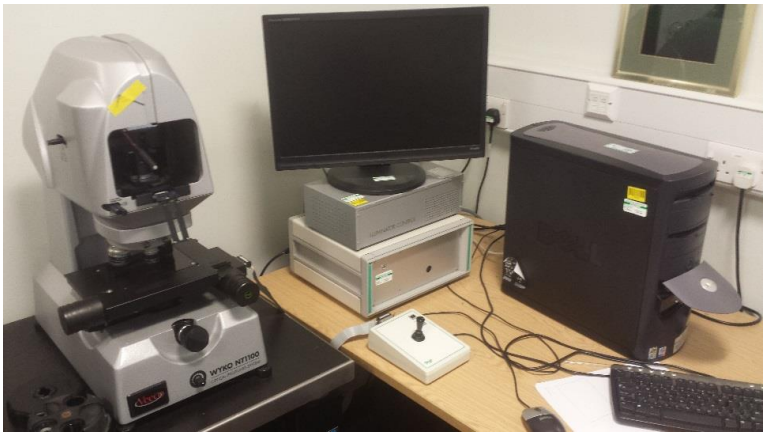

Figure 18- Vecco WYKO NT1100 white light interferometer

2.2.4. UV light source

The UV-light source used in this project were LV 204 with an output [60 w (4-5 mw/cm^2)] as seen in (Fig 19 a) and Spectroline EN-160L / FBE (6 W) in (Fig 19 b) both providing long radiation wavelength of 365 nm.

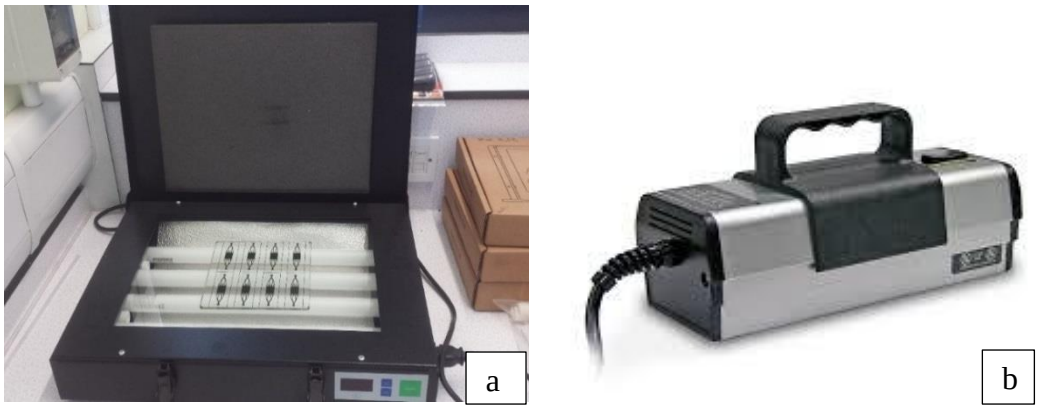

Figure 19- images of UV-light sources (365nm) and photomask with a pre-design used to transfer patterns on alumina membrane via photolithography.

2.2.5. Spincoater:

Spincoater was used in this project for coating anodisc membrane with photoresist needed for patterning techniques for MOFs growth (Fig 20). Variable speeds were used for achieving uniformity and different resist thickness.

Figure 20-Spincoater machine used for coating thin film substrate on alumina discs.

2.2.6. NMR Spectrometry

NMR were recorded on a Jeol JNM ECP400 spectrometer with TMS $\delta_H = 0$ as the internal standard or residual protic solvent. [$CDCl_3$, $\delta_H = 7.26$]. Chemical shifts are given in ppm (δ) and coupling constants (J) are given in Hertz (Hz). ^{1}H NMR were recorded at 400 MHz with the central peak of $CDCl_3$.

2.2.7. Hydro/Solvothermal method of MOFs synthesis

Hydrothermal synthesis refers to any heterogeneous reaction in the presence of a solvent (aqueous or non-aqueous) at high temperature and pressure greater than 1 atm in a close system.[73] The crystal growth is performed in an apparatus consisting of a steel pressure vessel called Teflon lined autoclave (Fig 21). These vessels are made of thick–walled steel materials with an internal cup and lid made of Teflon able to withstand high temperature and pressure for a long period of time. Teflon lines were used to prevent corrosion of the internal cavity of the autoclave during synthesis.

Figure 21-Autoclaves used for MOF synthesis process.

2.3. Experimental Procedure

Experimental part A: Synthesis of MOFs nanoparticles

2.3.1. MOF General Synthesis:

All hydrothermal or solvothermal reactions were run in an autoclave with a Teflon liner filled not more than 50 % of the vessels volume and placed in an oven at a set temperature.

2.3.2. Synthesis of the NH_2-MIL-53(Al) nanoparticles

Nanoparticles were synthesised as precursor material required for synthesis of NH_2-MIL-53(Al) microrods on anodisc. NH_2-MIL-53(Al) nanoparticles were synthesized according to reported literatures.[12] 2-aminoterephthalic acid (380.4 mg, 2.1 mmol) was added to a 50 mL centrifuge tube. Then, 2.1 mL of 2.0 M aq. NaOH solution was introduced to yield a pale yellow solution. In a separate 50 mL centrifuge tube, Al $(NO_3)_3 \cdot 9H_2O$ (787 mg, 2.1 mmol) was added. The volume in each tube was increased to a total of 15 mL by the addition of H_2O. Sonicating both tubes for 10 minutes will ensure even dispersion of the particles. Then, content from both bottles were combined in a 100 mL Teflon lined stainless steel autoclave, sealed and left to react in an oven at 120 °C for 72 h. The resulting mixture was collected by centrifugation at 5000 rpm for 30 mins. The supernatant was decanted leaving the yellow solid. The solid was washed with ethanol and collected by centrifugation at 5000 rpm to remove excess ligand. The resulting solid was further purified by refluxing in methanol at 90 °C for 6 h in a round bottom flask to remove unreacted ligand. After refluxing, the solid was collected by centrifugation and washed with ethanol twice. Supernatant was decanted leaving beige coloured solid. The resulting solid was dried overnight in an oven at 80 °C (Fig 22).

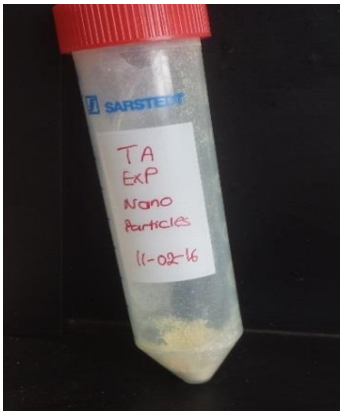

Figure 22-synthesized NH_2-MIL-53(Al) nanoparticles.

2.3.3. Synthesis of MIL-53(Al)

MIL-53(Al) was hydrothermally synthesized according to previously reported methods.[74] $Al(NO_3)_3 \cdot 9H_2O$ (13 g, 34.6 mmol) and terephthalic acid (2.88 g, 17.3 mmol) were mixed with DI water (50 mL) with mole ratio Al: BDC: H_2O (1:0.5:80). The mixture was then placed into a Teflon-lined steel autoclave in an oven set at 150 °C for 72 h. After completion the reaction was allowed to cool to room temperature. The resulting white product was centrifuged at 5000 rpm for 30 mins, the supernatant decanted and washed with DI water before centrifuging again. The washing procedure was repeated 3 times. The resulting product was dried in a vacuum at room temperature.

2.3.4. Synthesis of ZIF-8 nanoparticles in an aqueous system

ZIF-8 frameworks were synthesized based on previously reported methods.[75] It started with mixing aqueous solution of $Zn(NO_3)_2 \cdot 6H_2O$ into an aqueous solution of 2-methylimidazole and stirring the mixture at room temperature for 5 mins. Besides the two solution were all filtered by filter paper before mixing. An example of the ZIF-8 synthesis is as follows. $Zn(NO_3)_2 \cdot 6H_2O$ (0.59 g, 1.96 mmol) in 4 mL DI water was added into a solution of 2-methylimidazole (11. 4 g, 138.86 mmol) in 40 mL DI water, with molar ratio of zinc to 2-methylimidazole 1:70. Precipitation occurs immediately and the product was collected by repeated centrifugation at 5500 rpm for 45 mins and washed with DI water three times. The obtained product was dried in an oven at 65 °C overnight.

2.3.5. Synthesis and growth of NH_2-MIL 53(Al) microcrystals on patterned Anodisc membrane

Synthesis of NH_2-MIL 53(Al) microcrystals was performed according to previously reported procedure.[12] 2-amino terephthalic acid (280 mg, 1.55 mmol) was suspended in 10 mL of deionised water placed in a vial for ultra-sonication for 15 mins. The suspension was then transferred to a 100 mL Teflon lined stainless steel autoclaves, rinsing the vial with 5 mL of water (adding up a total of 15 mL of deionised water). A piece of Whatman alumina membrane (13 mm diameter patterned by spin coating of photoresist) was supported on a wet glass for adherence. The glass slide with the alumina disc was placed into the solution. The autoclave was sealed and heated in an oven at 120 °C for 48 h, after which it was allowed to cool to room temperature. The alumina disc on the glass substrate was then rinsed thoroughly with ethanol to remove any excess ligand, after which the disc was dried at room temperature.

2.3.6. Synthesis and of NH_2-MIL 53(Al) microrods on Anodisc membrane

10 mg of pre-synthesized NH_2-MIL-53(Al) nanoparticles were suspended in 10 ml of deionised water. A single piece of Whatman alumina membranes (plain and patterned) were submerged separately into the nanoparticles suspensions and shaken for about 3 mins, then removed from the nanoparticle suspension and placed onto a glass cover slip while wet. The cover slip was placed into a 100ml Teflon lined stainless steel autoclave, carefully ensuring that the disc was stuck firmly to the slip from the water surface tension. 2-Aminoterephthalic acid (280 mg, 1.55 mmol) was suspended in a 7.5 ml of deionised water and the suspension was added gently to the autoclave, taking care not to move the alumina discs from the glass slip surface. 7.5 ml of acetic acid was added to the mixture gently. The autoclave was sealed and heated in an oven at 120 °C for 48 h, after which it was allowed to cool to room temperature. The alumina disc was retrieved and rinsed thoroughly with ethanol to remove any excess ligand. After rising with ethanol, the disc was dried at room temperature.

NOTE**:** The patterned resist was coated only on one side of the alumina membrane, leaving the back uncoated. During the synthetic growth of microrods, the membrane surface consisting the patterned resist was positioned upwards on the glass slide in the autoclave. Likewise, in another autoclave, the side containing the patterned resist was positioned in contact with the glass slide, to observe both outcomes after hydrothermal synthesis (Fig 24). Results of earlier experimental procedures confirmed spatial control of NH_2-MIL-53(Al) MOF microcrystal was possible with photoresists. Therefore, a modulator (acetic acid) was introduced to observe the growth and patterning of the MOF crystals under a patterned photoresists condition.

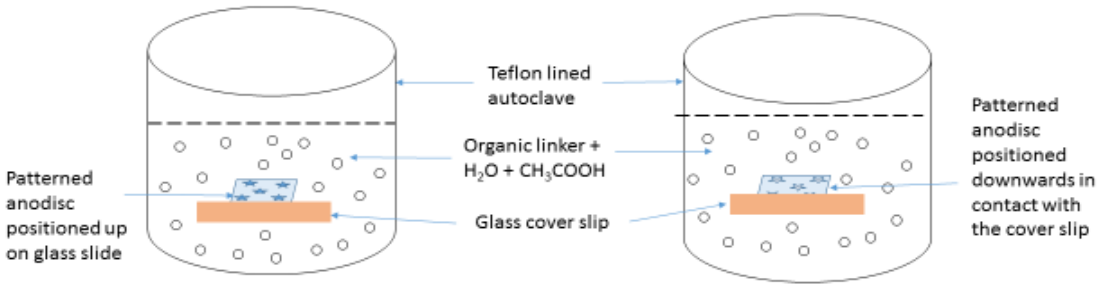

Figure 23-Schematic diagram of the positioning of anodisc on cover slips during solvothermal synthesis

2.3.7. Coating of negative photoresist on Anodisc

The coating of photoresist on alumina disc was attained by spin-coating of negative resist (AZ nLOF 2070) at an initial 700 rpm of for 1 sec before attaining the second speed of 4000 rpm

for 30 seconds on a spin coater, to yield a resist thin film. After the spin coating, the resist film on the alumina membrane was soft baked at 100 °C in an oven for approximately 12 mins. This helps complete crosslinking making the resist profile thermally stable. The coated alumina was aligned with a mask and then exposed to UV-light source (i-line sensitive 365 nm, 60 W) for 60 seconds. Post Exposure Bake (PEB) was performed for about 6 mins using an oven at 110 °C after exposure to UV-light. After post baking was complete, a developer (AZ 726 MIF) was used for approximately 4 mins to develop the patterned resist.

2.3.8. Dispersion of MOF nanoparticles in water and Dichloromethane using PVP polymer

To disperse MOF nanoparticles, 30 mg PVP (MW= 40,000 Aldrich) was dissolved in 6 ml water by ultrasonic dispersion for 30 mins. 30 mg of MOF nanoparticles (MIL-53(Al), NH_2-MIL-53(Al) and ZIF-8) to be dispersed were added separately into the PVP solution. The solutions were then ultra-sonicated at 45 °C for 1 h. The resulting product was collected by repeated washing and centrifugation at 3500 rpm for 30 mins. The yield product was vacuum dried at room temperature overnight. To further disperse the PVP coated MOF nanoparticles in DCM, the dried MOF nanoparticles were dissolved in 3 mL of DCM and put in a sonicator for approximately 1 h. Characterization of the particle size was obtained by SEM analysis (as seen in Fig 36).

Experimental part B: Synthesis of Metal Organic gels

2.3.9. Synthesis and characterization of photo-crosslinkable Poly (ethylene glycol) dimethacrylate

PEGDM was prepared according to previously reported process.[76] 5 g of PEG ($M_n \approx 10{,}000$ g/mol), 2.2 equiv of MA (0.34 g, 2.2 mmol) and TEA (0.2 mL, 0.002 mmol) were reacted in 15 mL of DCM over freshly activated molecular sieve (3 g) for 4 days at room temp. The solution was filtered over alumina and precipitated into ethyl ether. The filtered product was later dissolved in DCM and precipitated with diethyl ether to remove traces of unreacted MA. The product obtained was filtered and dried in a vacuum overnight at room temperature.

2.3.9.1. Preparation of PEGDM Hydrogels.

Photo-polymerized hydrogels were prepared accordingly to a previously repeated procedure.[76] PEGDM (10 % by mass fraction) and aqueous Irgacure 2959 solution (0.1% by mass fraction)

were mixed in deionized water and shaken until dissolved. The PEGDM solution was cured with a long wavelength UV light source (365 nm, 6 W) for 3 h to obtain hydrogels.

2.3.9.2. Preparation of PEGDM Organogels using various solvents

A general reaction for PEGDM organogels is as follows: PEGDM (10 % by mass fraction) and Irgacure 2959 (0.1 %) were mixed in EtOH, MeOH or DMF separately. The solution was heated in an oven at 80 ^{o}C for approx 30 secs to dissolve the PEGDM in the solvents. The solution was then cured with UV- light source (365 nm, 6 W) for 3 h to obtain the photo-crosslinked gels. Ethanol was replaced with methanol and DMF solvent. Photo-crosslinked gels were obatained after 3 h with solvent ethanol and methanol while DMF resulted in no gel as a results of its absorption in the UV spectrum.

2.3.10.Synthesis of Indium based Metal Organic gels (MIL-68)

Synthetic procedure using various solvents

The preparation of MIL-68 MOGs using a variety of organic solvents was performed. All of the solvents are listed table below. Typically, MIL-68 MOGs were prepared through simple mixing of metal salts and organic linker in a solvent. An example of the synthesis is as follows. $In(NO_3)_3{\cdot}XH_2O$ (0.12 g, 0.4 mmol) and 1,3,5-benzenetricarboxylic acid (0.084 g, 0.4 mmol) were each dissolved in 2 ml solvent (EtOH, MeOH, iPrOH and Acetone) separately. The resulting solution was left to stand at 80 °C for gelation in a closed vial for 1 h. MIL-68 gels were obtained with solvents EtOH, MeOH and iPrOH. Acetone evaporated thus no gel was produced, as only yellow dried precipitate was obtained after solvothermal synthesis as seen in Table 4. The formation of gel was determined by test-tube inversion method with the gel recovery time, the time taken for the gel to set back to original state upon removal of the applied stress, obtained by using a stopwatch.

M: Metal salt L: ligands S: Solvent

Table 4- Synthesis of In-BTC gel using various solvents.

MIL-68		Mass (g)	Mw (g/mol)	mmol	Vol (ml)	GEL	Gel recovery time
M	$In(NO_3)_3{\cdot}XH_2O$	0.12	300.83	0.4			
L	BTC	0.084	210.14	0.4			
S	EtOH	-	-	-	2	YES	20 mins
S	MeOH	-	-	-	2	YES	1 h
S	IPrOH	-	-	-	2	YES	1 h

S	Acetone	-	-	-	2	NO	-

2.3.11.Synthesis of MIL-68 MOGs using ethanol water mixture

Synthesis was as follows: $In(NO_3)_3 \cdot XH_2O$ (0.12 g, 0.4 mmol) was dissolved in a solvent mixture (% v/v EtOH + H_2O). After the complete dissolution of the metal slats, H_3BTC (0.084 g, 0.084 mmol) was introduced into the solution as seen in Table 5. The solution was kept in an oven at 80 °C for gelation in a closed vial at different times (1, 4, 6, 12, 24, and 48 h).

Table 5-synthesis of MIL-68 using various solvent mixture ratio

$In(NO_3)_3 \cdot XH_2O$ (g)	H_3BTC	mmol $In(NO_3)_3 \cdot XH_2O$	mmol BTC	Total solvent mixture (ml)	% ratio of solvent (EtOH %+ H_2O %)	Gel
0.12	0.084	0.4	0.4	2	50 (1 ml) : 50 (1 ml)	NO
0.12	0.084	0.4	0.4	2	60 (1.2 ml) : 40 (0.8 ml)	NO
0.12	0.084	0.4	0.4	2	70 (1.4 ml) : 30 (0.6 ml)	NO
0.12	0.084	0.4	0.4	2	80 (1.6 ml) : 20 (0.4 ml)	NO
0.12	0.084	0.4	0.4	2	90 (1.8 ml) : 10 (0.2 ml)	NO
0.12	0.084	0.4	0.4	2	95 (1.9 ml) : 5 (0.1 ml)	NO

2.3.12.Synthesis of MIL-68 MOGs using alcohol solvents with increasing alkyl chain length

$In(NO_3)_3 \cdot XH_2O$ was dissolved in 2 mL solvent (1-propanol, 1-Butanol, 2-Butanol, 1-pentanol and 2-heptanol) separately, followed by the addition of 1,3,5-benzenetricarboxylic acid/ terephthalic acid. The solution was vortexed until the resulting mixture was clear. The resulting solution was left to stand at room temperature for gelation in a closed vial. The gels viscosity were not determined, as rheological measurement were not performed on the gels due to limited time during the project. In this project, an appropriate amount of good gel concentration is a moderate viscous gel (not too viscous or less viscous), which was attained by visually looking and ease of shaking of the gel, simply by experimenting with different mmol concentration during synthesis.

2.3.12.1. Using alcohol solvent 1-propanol

$In(NO_3)_3 \cdot XH_2O$ was dissolved in 2 ml solvent of 1-propanol and 1,3,5-benzenetricarboxylic acid added into the solution (Table 6). A gel was obtained at room temperature.

Table 6-Synthesis of MIL-68 gel using solvent (1-propanol)

MIL-68	**$In(N0_3)_3 \cdot XH_2O$ (g)**	**H_3BTC (g)**	**Solvent (2 ml)**	**mmol $In(N0_3)_3 \cdot XH_2O$**	**mmol BTC**	**Gels**	**Reset time (mins)**	**result**
IN BTC	0.12	0.084	1-propanol	0.4	0.4	YES	1 min	Highly viscous gel
IN BTC	0.06	0.042	1-propanol	0.2	0.2	YES	3-4 mins	Appropriate amount for a good gel concentration

2.3.12.2. Using alcohol solvent 1-propanol with BDC ligand

$In(NO_3)_3 \cdot XH_2O$ was dissolved in 2 ml solvent of 1-propanol and 1,4-benzenedicarboxylic acid added into the solution (Table 7). The resulting solution was left to stand at 80 °C for gelation in a closed vial for 24 h.

Table 7-Synthesis of MIL-68 gel using solvent (1-propanol)

MIL-68	**$In(N0_3)_3 \cdot XH_2O$ (g)**	**H_2BDC (g)**	**Solvent (2 ml)**	**mmol $In(N0_3)_3 \cdot XH_2O$**	**mmol H_2BDC**	**Gels**	**Reset time (mins)**	**result**
IN BTC	0.12	0.084	1-propanol	0.4	0.4	NO	Does not gel	White precipitates of metal and ligands flocculating below the solevnt

2.3.12.3. Using alcohol solvent 1-Butanol

$In(NO_3)_3.XH_2O$ was dissolved in 2 ml solvent of 1-Butanol and 1,3,5-benzenetricarboxylic acid added into the solution (Table 8). A gel was obtained at room temperature.

Table 8-Synthesis of MIL-68 gel using solvent (1-butanol)

MIL -68	$In(N0_3)_3 .XH_2O$ (g)	H_3BTC (g)	Solvent (2 ml)	mmol $In(N0_3)_3 \cdot XH_2O$	mmol BTC	Gels	Reset time (mins)	result
IN BTC	0.06	0.042	1-Butanol	0.2	0.2	YES	Less than a minute	High viscous gel formed at room temperature

2.3.12.4. Using alcohol solvent 1-pentanol

$In(NO_3)_3.XH_2O$ was dissolved in 2 ml solvent of 1-pentanol and 1,3,5-benzenetricarboxylic acid added into the solution (Table 9). A gel was obtained at room temperature.

Table 9-Synthesis of MIL-68 gel using solvent (1-pentanol)

MIL -68	$In(N0_3)_3 .XH_2O$ (g)	H_3BTC (g)	Solvent (2 ml)	mmol $In(N0_3)_3 \cdot XH_2O$	mmol BTC	Gels	Reset time (mins)	result
IN BTC	0.0630	0.042	1-pentanol	0.2	0.2	YES	6-10 mins	Weak gel
IN BTC	0.0902	0.0630	1-pentanol	0.3	0.3	YES	1-2 mins	Suitable amount for a good gel concentration

2.3.12.5. Using alcohol solvent 2-heptanol

$In(NO_3)_3 \cdot XH_2O$ was dissolved in 2 ml solvent of 2-heptanol and 1,3,5-benzenetricarboxylic acid introduced into the solution (Table 10). The resulting solution was left to stand at room temperature and also left to stand at 80 °C for gelation in a closed vial at various time: 1, 3 and 4 h.

Table 10-Synthesis of MIL-68 gel using solvent (2-heptanol)

MIL -68	$In(N0_3)_3$ .XH_2O (g)	H_3BT C (g)	Solvent (2 ml)	mmol $In(N0_3)_3$ ·XH_2O	mmol BTC	Gels	Reset time (mins)	result
IN BTC	0.0630	0.042	2-heptanol	0.2	0.2	NO	Does not gel	White precipitates of metal salt with ligand

2.3.13.Synthesis of Metal Organic gels using Gallium and lanthanum metal ions with H_3BTC or H_2BDC ligands

Gallium belong to group (iii) on the periodic table with aluminium and indium which have been proven to successfully produce gels. The aim is to see if a gel was obtainable using gallium salt, comparing and contrasting the different properties of the gels.

2.3.13.1. Gallium Metal Organic Gels using H_3BTC

$Ga(NO_3)_3·XH_2O$ was dissolved in 2 ml solvent EtOH by vortexing. 1,3,5-benzenetricarboxylic acid was added into the solution afterwards. The resulting solution was left to stand at room temperature for gelation in a closed vial. The experimental procedure was repeated replacing EtOH with solvents 1-propanol or 2-propanol as seen in Table 11.

Table 11- Synthesis of Gallium BTC MOG

		Mass(g)	Mw (g/mol)	mmol	ml	GEL	properties
M	$Ga(NO_3)_3.XH_2O$	0.1022	255.74	0.4			
L	H_3BTC	0.084	210.14	0.4			
S	EtOH	-	-	-	2	YES	Non – thixotropic
S	1-propanol					YES	
S	2-propanol					YES	

2.3.13.2. Gallium Metal Organic Gels using H_2BDC

$Ga(NO_3)_3·XH_2O$) was dissolved in 2 ml solvent EtOH by vortexing. 1,4-benzenedicarboxylic acid was later introduced into the solution. The resulting solution was left to stand at 80 °C for gelation in a closed vial for 1 h. The experimental procedure was repeated replacing EtOH with solvents 1-propanol or 2-propanol as seen in as seen in Table 12.

Table 12-Synthesis of Gallium BDC MOG

		Mass(g)	Mw (g/mol)	mmol	ml	GEL	properties
M	$Ga(NO_3)_3 \cdot XH_2O$	0.1022	255.74	0.4		Very Weak gel	Weak gel which degrades in few hours (losing its properties from a gel to a fluid)
L	H_2BDC	0.0664	166.13	0.4			
S	EtOH/	-	-	-	2		
S	1-propanol	-	-	-	2		
S	2-propanol	-	-	-	2		

2.3.13.3. Lanthanum Metal Organic Gels

$La(NO_3)_3 \cdot 6H_2O$ was dissolved in 2 ml solvent (EtOH and 1-propanol) separately. 1,3,5-benzenetricarboxylic or 1,4-benzenedicarboxylic acid was introduced into the solution afterwards. The resulting solution was left to stand at 80 °C for gelation in a closed vial for 1h and later increased at various time of 4, 6, and 12 h (Table 13 and 14).

Table 13-Synthesis of Lanthanum BTC MOG with different solvents

		Mass(g)	Mw (g/mol)	mmol	ml	GEL
M	$La(NO_3)_3 \cdot 6H_2O$	0.1732	433.01	0.4		NO
L	H_3BTC	0.084	210.14	0.4		
S	EtOH/	-	-	-	2	
S	1-propanol	-	-	-		

Table 14-Synthesis of Lanthanum BDC MOG with different solvents

		Mass(g)	Mw (g/mol)	mmol	ml	GEL
M	$La(NO_3)_3 \cdot 6H_2O$	0.1732	433.01	0.4		
L	H_2BDC	0.0664	166.13	0.4		
S	EtOH	-	-	-	2	NO
S	1-propanol	-	-	-	2	

Experimental Part C: Synthesis and photo-crosslinking of MOG gels

2.3.14.Synthesis and photo-crosslinking of Metal Organic gels with various solvents

Various research reviews explored using EtOH and MeOH as common solvents for synthesising different MOGs with distinctive morphological, physical and chemical characteristics. Synthesis and photo-polymerization of MOGs with both solvents were as follows: PEGDM (0.0792 g, 0.4 mmol) with I2959 (0.1% by mass fraction) was dissolved separately in a 2 ml ethanol. The solvent was heated in an oven for approximately 30 secs to dissolve the PEGDM. Afterwards, metal salts and organic ligands were introduced into the mixture and heated to 80 ^{o}C in an oven for 1 hour. The reaction procedure was repeated using methanol solvent in place of ethanol.

Crosslinking the organogels: The resulting gels obtained after synthesis were photo-polymerized with UV-light (365 nm, 6 W) for 3 h. Table 15 -18 shows the different experimental setup used during MOG synthesis.

M: Metal salt L: ligands S: Solvent photoinitiator= 0.002079 g

Table 15-Synthesis of photo-crosslinkable Al-BTC gels

MIL 100 (Al)		Mass (g)	Mw (g/mol)	mmol	Vol (ml)	Gel
M	$Al(NO_3)_3{\cdot}9H_2O$	0.1500	375.15	0.4		
L	BTC	0.0840	210.14	0.4		
S	EtOH	-	-	-	2	YES
S	MeOH	-	-	-	2	YES
	PEGDM	0.0792	198.21	0.4		

Table 16-Synthesis of photo-crosslinkable Al-BDC gels.

MIL 100 (Al)		Mass (g)	Mw (g/mol)	mmol	Vol (ml)	Gel
M	$Al(NO_3)_3{\cdot}9H_2O$	0.1826	375.15	0.5		
L	BDC	0.0664	166.13	0.4		
S	EtOH	-	-	-	2	NO
S	MeOH	-	-	-	2	NO
	PEGDM	0.0792	198.21	0.4		

Table 17-Synthesis of photo-crosslinkable Fe-BTC gels.

MIL-100 (Fe)		Mass (g)	Mw (g/mol)	mmol	Vol (ml)	Gel
M	$Fe(NO_3)_3 \cdot 9H_2O$	0.1616	404.60	0.4		
L	BTC	0.084	210.14	0.4		
S	EtOH	-	-	-	2	YES
S	MeOH	-	-	-	2	YES
	PEGDM	0.0792	198.21	0.4		

Table 18-Synthesis of photo-crosslinkable Cr-BTC gels.

MIL-101 (Cr)		Mass (g)	Mw (g/mol)	mmol	Vol (ml)	Gel
M	$Cr(NO_3)_3 \cdot 9H_2O$	0.1601	400.15	0.4		
L	NH_2BDC	0.0724	181.15	0.4		
S	EtOH	-	-	-	2	YES
S	MeOH	-	-	-	2	YES
	PEGDM	0.0792	198.21	0.4		

2.3.15.Synthesis and crosslinking of Indium Metal Organic Gels (MIL-68)

Synthesized PEGDM (0.0792 g, 0.4 mmol) with I2959 (0.1 % by mass fraction) were dissolved separately in 2 ml solvent of Ethanol. The solvent was heated in an oven for approximately 30 secs to dissolve the PEGDM, before introducing the metal salt ($In(NO_3)_3 \cdot XH_2O$, 0.4 mmol) and organic ligand (H_3BTC, 0.4 mmol) into the solution. The mixture was heated in an oven at 80 ^oC for 1 hour. Ethanol was replaced with methanol or Isopropanol with the same synthesis conditions. Table 19-21 shows the different experimental setup during MOG synthesis with various experimented PEGDM, photoinitiator and M- L molar ratio to finding the ideal concentration needed for gelation.

M: Metal salt L: ligands S: Solvent photoinitiator= 0.002079 g

Table 19-synthesis of MIL-68 MOGs using different solvents with molar ratio M:L:PEGDM (1:1:1, 1:1:0.5, 1:1:0.25)

MIL-68		Mass (g)	Mw (g/mol)	mmol	Vol (ml)	Gel
M	$In(NO_3)_3 \cdot XH_2O$	0.12	300.83	0.4		
L	BTC	0.084	210.14	0.4		
S	EtOH	-	-	-	2	
S	MeOH	-	-	-	2	
S	IPrOH	-	-	-	2	
monomer	PEGDM	0.0792	198.21	0.4		NO
	PEGDM	0.0396	198.21	0.2		NO
	PEGDM	0.0198	198.21	0.1		NO

Table 20-synthesis of MIL-68 with increasing ligand concentration

MIL-68		Mass (g)	Mw (g/mol)	mmol	Vol (ml)	Gel
M	$In(NO_3)_3 \cdot XH_2O$	0.12	300.83	0.4		
L	BTC	0.336	210.14	1.5		
S	EtOH	-	-	-	2	NO
S	MeOH	-	-	-	2	NO
S	IPrOH	-	-	-	2	NO
	PEGDM	0.0792	198.21	0.4		

Table 21-reducing the mole ratio concentration of the PEGDM and increasing the metal ion concentration

MIL-68		Mass (g)	Mw (g/mol)	mmol	Vol (ml)	Gel
M	$In(NO_3)_3 \cdot XH_2O$	0.24	300.83	0.8		NO
M	$In(NO_3)_3 \cdot XH_2O$	0.1804	300.83	0.6		NO
L	BTC	0.084	210.14	0.4		
S	EtOH	-	-	-	2	
S	MeOH	-	-	-	2	
S	IPrOH	-	-	-	2	
	PEGDM	0.0396	198.21	0.2		

2.3.16.Synthesis of MIL-68 MOGs using a % ratio of monomer (allyl alcohol or acrylic acid) with alcohol solvent

$In(NO_3)_3 \cdot XH_2O$ was dissolved in 2 ml solvent [1-propanol/1-butanol 95 % (v/v) + allyl alcohol/acrylic acid 5 % (v/v) and 1,3,5-benzenetricarboxylic acid introduced into the solution. For acrylic acid reagent mixture, the resulting solution was left to stand in an oven for gelation at 80 °C in a closed vial for 5 mins. While solvent mixture with allyl alcohol produce a gel at room temperature as seen in table 22 and 23.

Table 22-Synthesis of Indium MOG using mixed solvents ratio of 1-propanol + allyl alcohol/acrylic acid

		Mass(g)	Mw (g/mol)	mmol	ml	GEL	Reset time (mins)
M	$In(NO_3)_3 \cdot XH_2O$	0.0902	300.83	0.3			
L	H_3BTC	0.063	210.14	0.3			
S	1-propanol + allyl alcohol (5 %)	-	-	-	2	YES	3-5 mins
S	1-propanol (95 %, 90 %) + acrylic acid (5 %, 10 %)	-	-	-	2		3-5 mins

Table 23-Synthesis of Indium MOG using mixed solvents ratio of 1-butanol + allyl alcohol/acrylic acid

		Mass(g)	Mw (g/mol)	mmol	ml	GEL	Reset time (mins)
M	$In(NO_3)_3 \cdot XH_2O$	0.0902	300.83	0.3			
L	H_3BTC	0.063	210.14	0.3			
S	1-butanol + allyl alcohol (5 %)	-	-	-	2	YES (yellow gel)	2-4 mins
S	1-butanol (95 %, 90 %) + acrylic acid (5 %, 10 %)	-	-	-	2	YES	2-4 mins

2.3.17.Photopolymerization of acrylic acid

Synthetic procedure: synthesized according to previous reported method.[77] For efficient polymerization, the inhibitor (hydroquinone) present in acrylic acid was removed by passing the liquid monomer through an alumina oxide column. A mixture containing acrylic acid (99 vol %) + I 184 (1 % w/v) solution was irradiated with UV-light source (365 nm, 6 W) for 30 mins or strong UV light (60 W) for 1 min. The gel was immersed and its swelling observed in water.

2.3.18.Photo-crosslinking of Metal organic gels using acrylic acid with photo-initiator

Acrylic acid has been proven for fast photo-crosslinking within the shortest time frame. A vol % ratio of the reactant monomer consisting of the photoinitiator was mixed alongside the solvent used in coordination synthesis to crosslink the gels when irradiated with UV-light.

Experimental procedure:

$In(NO_3)_3 \cdot XH_2O$ was separately dissolved in ethanol/ 1-propanol (90 % v/v) of a 2 ml solvent. After the dissolution of the metal salt, 10 % (v/v) acrylic acid containing photoinitiator Irgacure 184, was added into the solution and mixed thoroughly by vortexing. 1,3,5-benzenetricarboxylic acid was also introduced into the solution afterwards. The solution was left to stand at 80 °C for gelation in a closed vial for 10 mins in an oven. The gel obtained was then irradiated with UV-light (365 nm 60 W) for crosslink for 2 mins.

Chapter 3. Results and Discussion

3.1. Interest in NH_2-MIL-53(Al) MOF nanocrystals

Experimental methods of NH_2-MIL-53(Al) were constructed for the functional patterning of the MOF to precise locations. As this will provide an almost infinite array of potential porous crystals with functionalities that can be tailored for numerous applications. Interest in NH_2-MIL-53(Al) MOF nanocrystals, is that it allows tuning of the nanocrystals for various applications by designing the structure of organic linker at pre-synthesized stage.[78] Additionally, a series of NH_2-MIL-53(Al) crystals with different sizes and shaped can be derived by altering the composition of the mixed solvents while retaining all other conditions unchanged. The presence of an amino group on the ligand allows for easy post-synthetic modifications (PSM), thus resulting in different physical and chemical properties. The NH_2-MIL-53(Al) has a 1D diamond-shaped channel with free standing amino groups having a pore diameter close to 7.5 Å as shown in Fig 24.[79] Also, NH_2-MIL-53(Al) MOFs show high thermal (~410 ^oC) and chemical stability (useful for electrochemical test), when compared with other MOF compounds which decompose in a few hours to days.

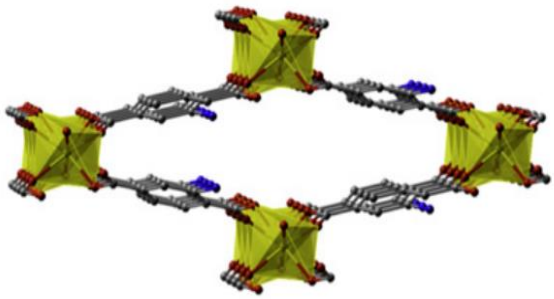

Figure 24-Crytsal structure of NH_2-MIL-53(Al) ions linked by µ2-OH bridges which yield 1D chains.[79]

3.2. Interest in Anodised aluminium oxide membrane

Previous experimental methods according to Tristan *et al.*, 2013 showed the size and shape of MOF crystal formation is possible via coordination modulation on anodisc.[12] Porous alumina membrane also called Anodised Aluminium Oxide (AAO), was employed in this project for MOF crystal growth due to its multi-functional properties as a metal source (Al^{3+}) and substrate for the patterning of MOF crystals.

AAO, a nanoporous membrane has received revitalized interest in photonics, fuel cells, microfluidics, and tissue engineering and drug delivery applications.[80] The porous alumina membrane comprises of an ordered hexagonal arrangement of cells with a central pore per cell that elongates from top to bottom of the layer.[81] A unique potential of this porous membrane, is the possibility to modify or functionalize the characteristics and performance of the materials by various surface coatings. Also, different pore sizes, aspect ratios and shapes can be obtained depending on the application and purpose of the membrane. The idea is to coat alumina membrane with a patterned resist which allows crystal growth of MOFs on uncoated regions and impedes crystal growth on coated regions, during hydro/solvothermal synthesis.

Application of coatings on the membranes was based on two different coating techniques:

a) Alumina membrane coated with negative photoresists by spin coating. UV lithography was performed on the coated membrane with a photomask (Fig 25 a)
b) Alumina membrane was gold sputtered (Gold was used because is chemically inert, as seen in Fig 25 b)

Micro-patterning of alumina membrane with a photoresist was achieved through UV-lithography, whilst patterning of alumina membranes with gold coating was obtained by ablating the gold surface membrane with a laser beam (laser ablation), as seen in (Fig 25 c). The concept behind the nano and micro patterning is to allow crystal growth only on the uncoated regions of the membrane.

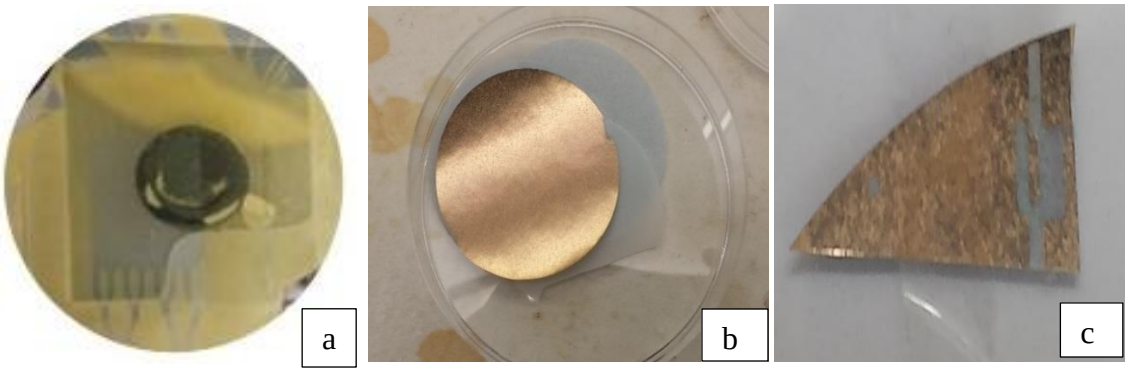

Figure 25-. Images showing alumina membranes coated with different resist (a) Result of a developed patterned photoresist using UV-lithography, (b) alumina membrane sputtered by gold coating, (c) a pattern created by ablating gold away from the surface of the membrane

Result of Part A Experiments

3.3. Characterization of MOF nanocrystals (MIL-53(Al), NH_2-MIL-53(Al) and ZIF-8)

3.3.1. MIL-53(Al):

Scanning electron microscopy imaging of MIL-53(Al), showed that crystal sizes ranged from 3-10 µm and the shape to be rod- like (Fig 26 a). The crystallinity of the powder was determined by PXRD measurement pattern which was not similar to that of the published pattern data (Fig 26 b), showing that the MIL-53 (Al) sample has not been synthesized. The difference between the spectra of the theoretical and synthesized MIL-53(Al) might be as a result of impurity in the sample over a period of time.

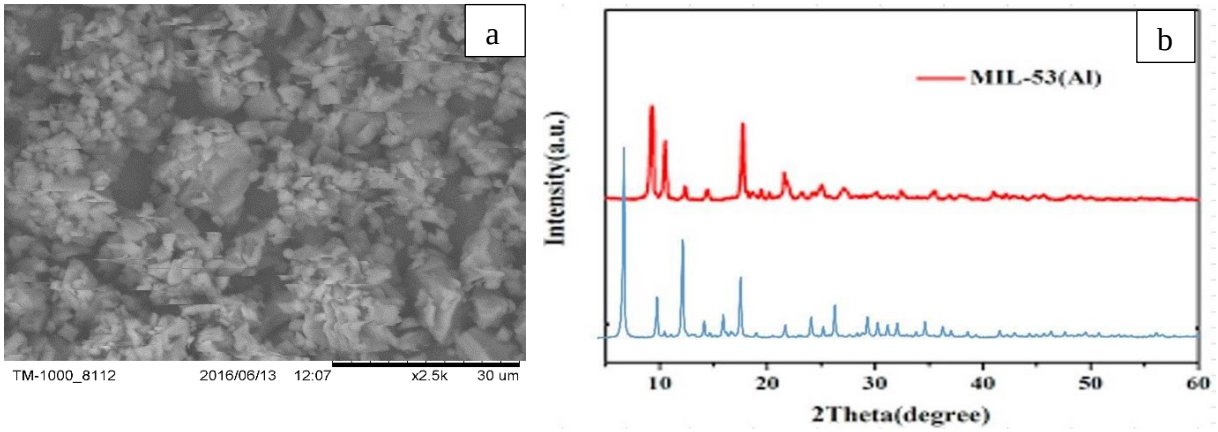

Figure 26 (a) SEM image of synthesized MIL-53(Al), (b) XRD patterns of published (red) and synthesized MIL-53(Al) (blue).

3.3.2. ZIF-8:

Fig 26 shows the powder X-ray diffraction patterns and SEM images of the synthesized aqueous ZIF-8 nanoparticles. SEM images reveal the nanoparticles were hexagonal shaped crystals with particles size 1-5 µm (as see in Fig 27 a). Comparing the synthesized sample XRD pattern to pattern simulated from the published structure data,[82] shows that the crystal synthesized is a ZIF-8 material with peaks broadening at $2\theta \approx 7°$ and $2\theta \approx 13.5°$ (Fig 27 b).

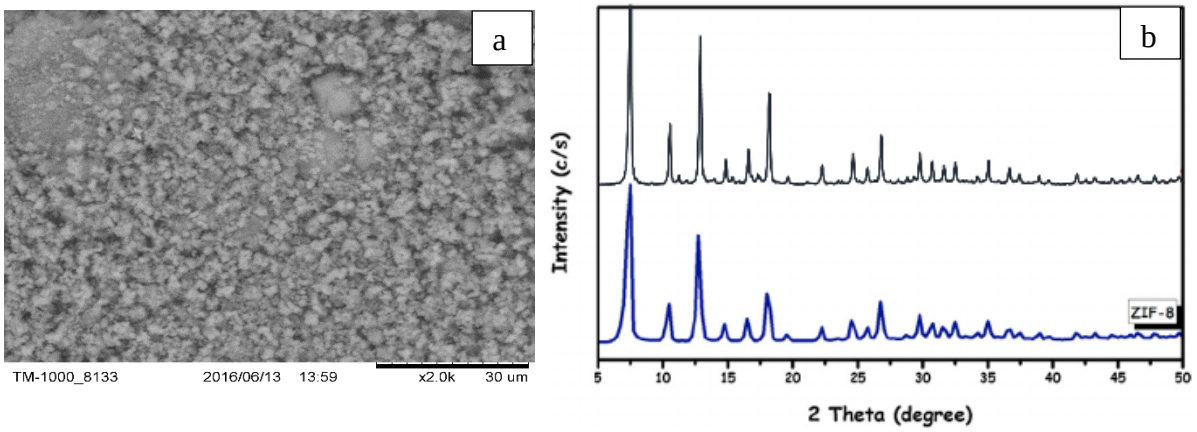

Figure 27- (a) SEM image of synthesized of ZIF-8 crystal, (b) XRD patterns of published (blue) and synthesized ZIF-8 crystal (black).

3.3.3. NH_2-MIL-53(Al):

Scanning electron microscopy (SEM) images show that the crystallites of NH_2-MIL-53(Al) are micro square rods with size ranging from 10-40 µm (Fig 28 a). The XRD patterns of the NH_2-MIL 53(Al) exhibits peaks similar to MIL-53(Al) single crystals. The amino functional group shows a peak at $2\theta \approx 7.5°$ which similar to the published NH_2MIL-53(Al) crystal patterns (Fig 28 b).

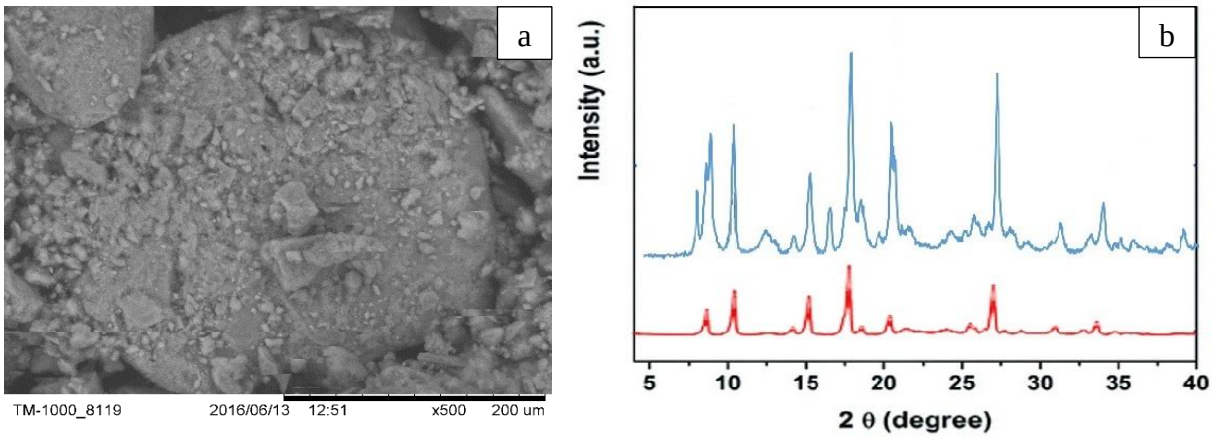

Figure 28-(a) SEM image of synthesized of NH_2MIL-53(Al), (b) XRD patterns of published MIL-53(Al) (red) and synthesized NH_2MIL-53(Al) crystal (blue).

3.4. Analysis of NH_2-MIL 53(Al) microcrystals on Anodisc

Following the growth of MOF crystals on patterned anodisc under hydro/solvothermal conditions, images and characterization of the crystals were obtained using a scanning electron microscope (SEM) and Powder X-ray Diffraction (PXRD) analysis. Images obtained from the

SEM made it possible to determine the size, structure, aspect ratio, length and width of the crystals, while PXRD helped identified the crystallinity and components present in the crystal structures.

3.4.1. SEM analysis of microcrystals of photoresist Alumina membrane

Reaction of Al^{3+} present in alumina with 2-aminoterephthalic acid results in NH_2-MIL 53(Al) crystal growth. Scanning electron microscopy (SEM) images revealed surface regions where such growth occurred due to absence of resists, and regions where growth was ceased as a result of resist present (Fig 29 a). In addition, it was observed that crystals produced with photoresist anodisc, had smaller size ratios (approximately 3-10 µm, as seen in Fig 29 c) when compared to NH_2-MIL 53(Al) nanoparticles synthesized using metal salts. This could be a result of insufficient Al^{3+} for M-L coordination, shielded by the resist. SEM images were poor as a result of the low resolution SEM Tablet (TM 1000) used and the charging effect created.

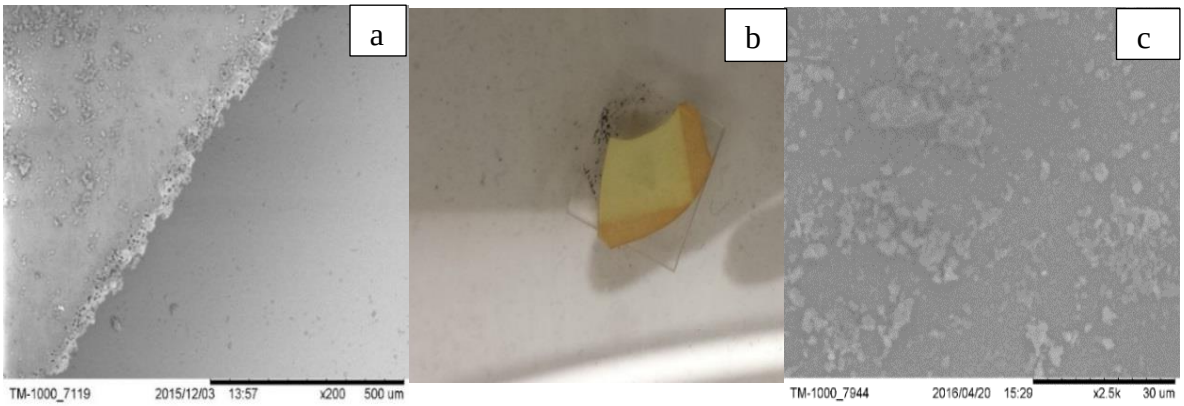

Figure 29- a) SEM image showing distinct areas between MOF growths on patterned resist at x200 magnification (dotted regions indicates areas with MOF microcrystal growth while smooth regions indicates area without MOF growth), (b) Picture of a patterned alumina membrane with photoresists (darker yellow region represent area with coated photoresist preventing MOF microcrystal growth. While light yellow region represent area where MOF microcrystal growths were observed due to absence of photoresist), (c) SEM image of the NH_2-MIL 53(Al) microcrystals at 2.5k magnification.

3.4.2. Powder X-ray diffraction analysis of photoresist alumina membrane

Further characterization was done on to show that the crystal growth on patterned photoresist was NH_2-MIL 53(Al) microcrystals. The XRD patterns of the NH_2-MIL 53(Al) microcrystals synthesized on anodiscs (Fig 30 c) is identical and in good agreement with the as-synthesized and simulated single crystal sample (Figs 30 a&b).[79] Peaks were observed at $2\theta \approx 10$ °, 15 ° and 17 °, indicating MIL 53, and at $2\theta \approx 7$ °, confirming the presence of the amino functional group. This shows the product is NH_2-MIL 53(Al) microcrystal. The NH_2-MIL 53(Al) pattern (Fig 30 c) has a good crystallinity level with the peaks clearly positioned and separated from

the noise peaks. The increase in the amount of noise peaks was attributed to the presence of pores present in the anodisc during XRD measurement.

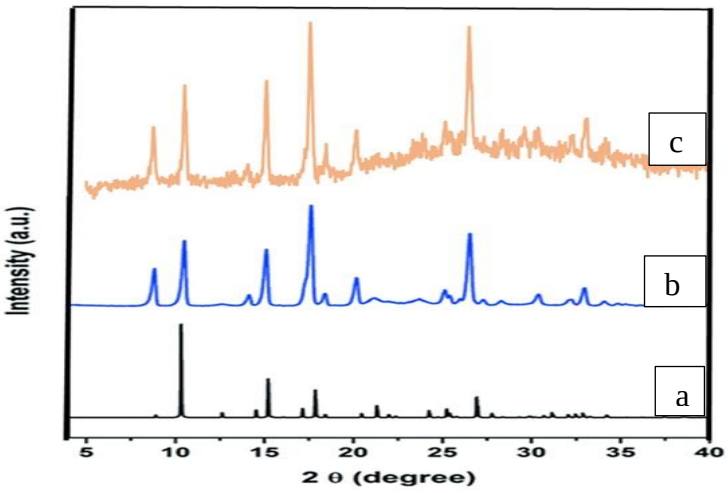

Figure 30-PXRD pattern of (a) MIL 53(Al), (b) published NH_2-MIL-53 (Al) sample (blue), (c) synthesized NH_2-MIL 53(Al) crystal on porous AAO membrane (orange).

Discussion: SEM and PXRD showed patterning of MOFs was successful. XRD patterns reveals growths were NH_2-MIL 53(Al) crystal, and with SEM showing the controlled growth of microcrystals on coated and uncoated regions of the alumina membrane. Additionally, XRD patterns also confirm the resist not altering the structure morphology of the MOFs as it was similar to NH_2-MIL 53(Al) nanoparticles. Attempts using Raman spectroscopy to characterize the NH_2-MIL 53(Al) crystal was unsuccessful. Factors limiting Raman spectroscopy measurement are: published database for NH_2-MIL 53(Al) are rare, as well as significant peaks could not be identified clearly from the noise peaks when measured. This is attributed to the porous interstices within the membrane, as the noise peaks could still be seen from the measured PXRD.

UV-lithography proved a good patterning technique for the growth of MOF crystals on alumina membrane. This technique allowed for regions of the photoresist exposed to UV-light to be cross-linked while regions unexposed are washed off by developers. The crosslinked photoresist act as a coating to impede M-L interaction which results in MOF crystal growth, whilst the resists washed off from the membrane create a pathway of interaction for metal to ligand bond coordination to occur.

3.4.3. Growth of microcrystals on gold sputtered alumina membrane

Scanning electron microscopy imaging of NH_2-MIL 53(Al) revealed no MOF crystals growth on gold sputtered alumina membrane. This was evident as the uncoated lines with no gold

coatings, showed no MOF microcrystals growth when examined under SEM microscopy as seen in (Fig 31 a).

Different depths of line were ablated on the gold coated membrane to control the amount of Al^{3+} accessible for Metal–ligand coordination. The depths ablated via laser ablation technique were attempted to be measured using a White light interferometry. This characterization technique was unsuccessful as the white light from the interferometer, interfered with the pores of the membrane thus making it impossible to determine the depths of the patterned lines as see in Fig 32.

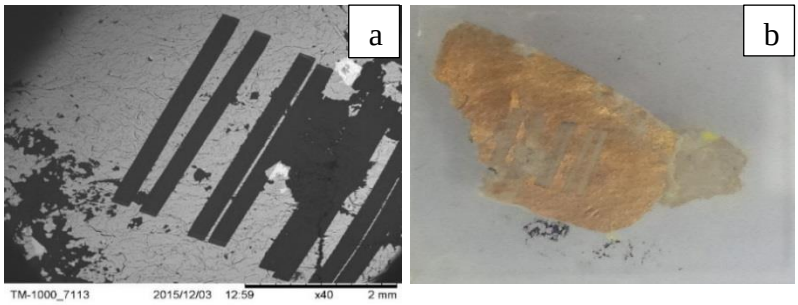

Figure 31- (a) SEM image showing the absence of MOF crystals growth on micro patterned lines (black lines), (b) picture illustrating the micro patterned line fabricated by the ablation of a laser beam.

The different depth lines ablated were tried for synthesis of NH_2-MIL 53(Al) microcrystals. SEM images still revealed the absence of MOF crystal growth on the uncoated regions on alumina membrane despite the different depths ablated. From the above result, gold sputtered coating on alumina membrane was not a viable coating technique like the photoresist coating used for the controlling of MOF microcrystals growth at certain locations.

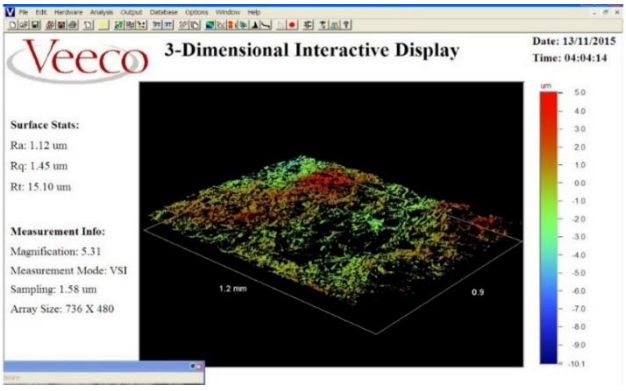

Figure 32-white light interferometer showing the topography and surface depth of alumina membrane sputtered with gold

Discussion: Possible reasons for the failed patterning of MOFs crystals with gold sputtered resist could be that, the laser beam diameter was not small enough to penetrate and lift off completely the gold layers within the interstices of the alumina membrane. Thus impeding the

presence of Al^{3+} required for M-L coordination. To overcome this hurdle, in 2008, Grigoras *et al*., suggested that alumina membrane could be cleaned with force flow of ethanol before use.[80] This will aid open certain pores which could still be closed, especially close to the surface area. Alumina membranes also when sputtered with gold layers should be fixed in a vertical position inside the chamber. This way the pores are situated perpendicularly to the flow of gold atoms, minimising the gold entering inside the pores (Fig 33).[80]

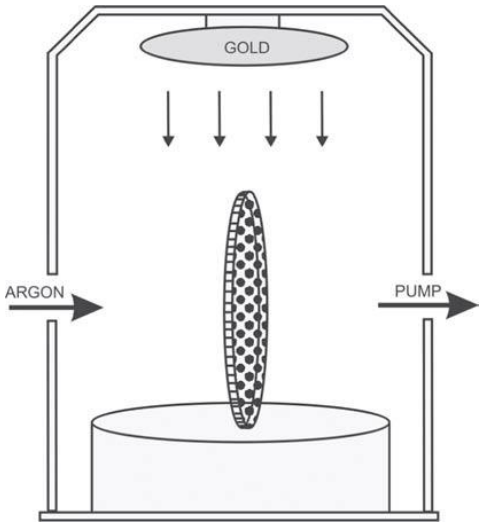

Figure 33-Ideal positioning when setting up for gold sputtering on membrane.[80]

3.5. Analysis of NH_2-MIL 53(Al) microrods on patterned photoresist Anodisc

Following the successful patterning of NH_2-MIL 53(Al) microcrystal on alumina with photoresists using UV-lithography, the technique was further employed for the patterning of NH_2-MIL 53(Al) microrods on anodiscs. MOF microrods were synthesized by incorporating a modulator (acetic acid) for oriented growth, perpendicularly aligned to the support. The only difference when synthesizing MOF microcrystal and microrods is the modulator introduced.

Results of patterned microrods synthesized were compared to plain alumina (without resists and patterning) used as a standard. SEM imaging of NH_2-MIL 53(Al) microrods revealed that membrane side containing the patterned resist, when positioned upward produced patches of microneedles with a spiny 'microflower' growth that were similar to the standard membrane (Fig 34a). While the backside without coating produced sparsely dense microneedles not properly aligned (Fig 34 b). The results showed, the microflowers produced were not restricted by the patterned photoresist as crystal growth dominates the entire surface of the patterned membrane as seen in (Fig 34 a, smaller picture).

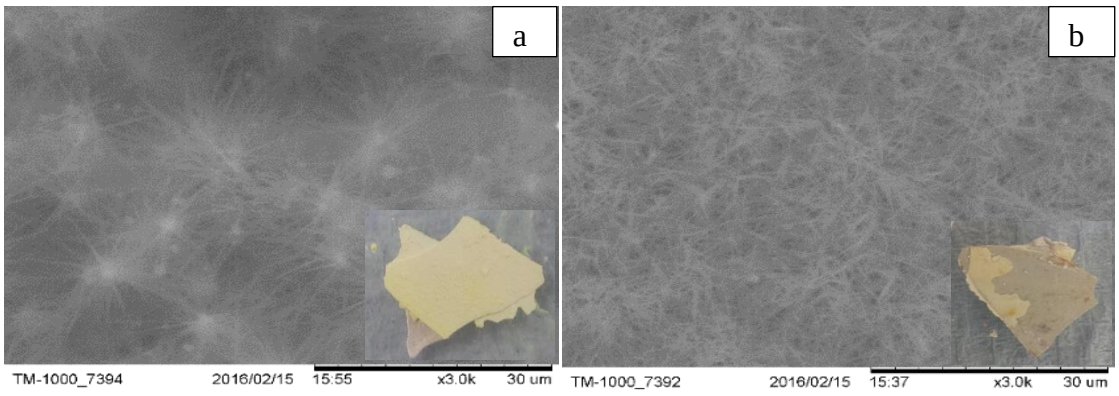

Figure 34-SEM images and pictures of NH_2-MIL 53(Al) microrods patterned resist positioned upwards on glass slides. (a) SEM image showing growth of microflowers covering the entire surface of the resists including the micro patterned lines. Smaller image represent picture of the microflowers anodisc, (b) SEM image showing anodisc back view of dense micro needles not properly aligned. Smaller image represent picture of microneedles growth on membrane.

To reduce the microrods growth from dominating the entire surface of the membrane coating, the side consisting of the patterned resist was positioned in contact with glass slip as opposed to former positioned upward. The concept is that the glass substrate should decrease nucleation growth of MOF crystals, thus eliminating the 'microflower' effect produced. This approach was unsuccessful, although the crystal growth of the microflowers were drastically reduced but did not adhere to the patterned lines created for control, as seen in the SEM (Fig 35 a). Additionally, the patterned lines were much visible (Fig 35 a, smaller pics) compared to the full microflower growth as seen in (Fig 34 a, smaller pics). The backside of the alumina membrane without a photoresist coating showed similar results of sparsely dense microneedles not properly aligned (Fig 35 b).

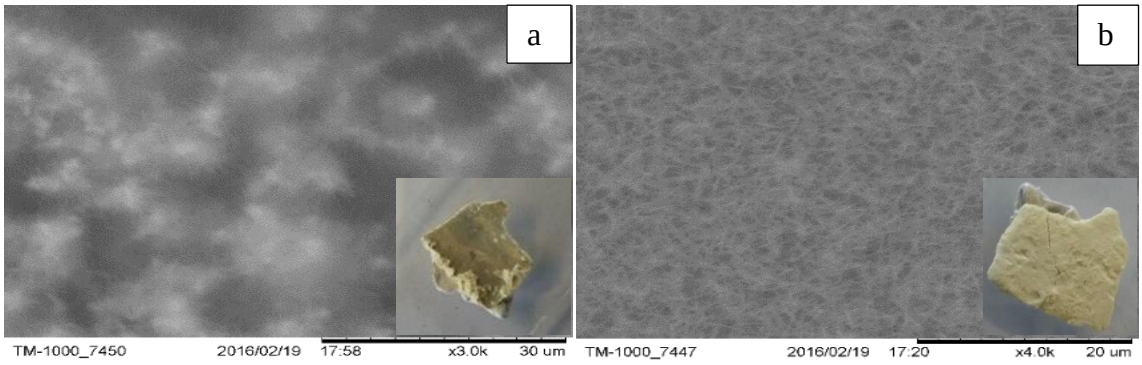

Figure 35-SEM images and pictures of NH_2-MIL 53(Al) microrods patterned resist when positioned in contact with glass slip. (a) SEM image showing reduced growth of microflowers overshadowing the entire surface of the patterned resists including the micro patterned lines. Smaller picture show microflowers growth on anodiscs, (b) SEM image of reduced dense micro needles growth not properly aligned. Smaller picture show backview of microneedles growth on membrane.

Discussion: From the results obtained above, the microneedle growths with microflowers surpassed the lithographed technique designed for MOF control on the anodisc. This is because the growth seen was not inhibited on both side of the membrane when positioned either upward or in contact with the glass slide. Reasons might be the patterned lines generated by lithography technique were not deep enough to constrain the growth of perpendicularly aligned microneedles. Therefore, microneedle growth starts at regions uncoated with resist and extends over coated regions by generating a substrate over the coated regions for continued growth of microflowers on the membrane. (Fig 34 & 35).

The result of the successful patterning of microcrystals on photoresist anodisc compared to the unsuccessful patterning of microrods on anodisc is due to the modulator (acetic acid) used. The approach proved a good patterning technique for microcrystals, as micro square rods were produced whereas microrods produced microneedles which were few microns higher than depth of patterned lines created for control. The technique shows patterning was unsuccessful in controlling MOF crystal growth in the presence of a modulator when introduced.

3.6. Dipersion of nanoparicles in water using PVP

A simple dispersion test was done to analyse by dissolving of PVP-coated nanoparticles into water and DCM separately. The nanoparticles disperse with ease in both solvents when vortexed for few mins (Fig 36). SEM characterization was done to analyse if there was a change in the crystal structure of the nanoparticles after coating with PVP (Fig 37). SEM showed a similar aspect ratio, morphology and crystal size range obtained for MIL-53(Al) and NH_2-MIL-53(Al) crystals before and after coating the nanoparticles. While SEM images of ZIF-8 shows flowery crystal growth obtained after coating with PVP compared to the hexagonal shaped crystals of ZIF-8 nanoparticles.

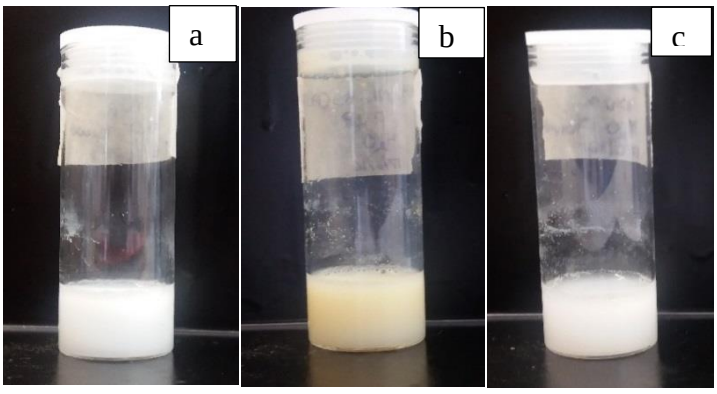

Figure 36-Dispersion of MOF nanoparticles in water. (a) MIL-53(Al), (b) NH2-MIL-53(Al), (c) ZIF-8 nanoparticles

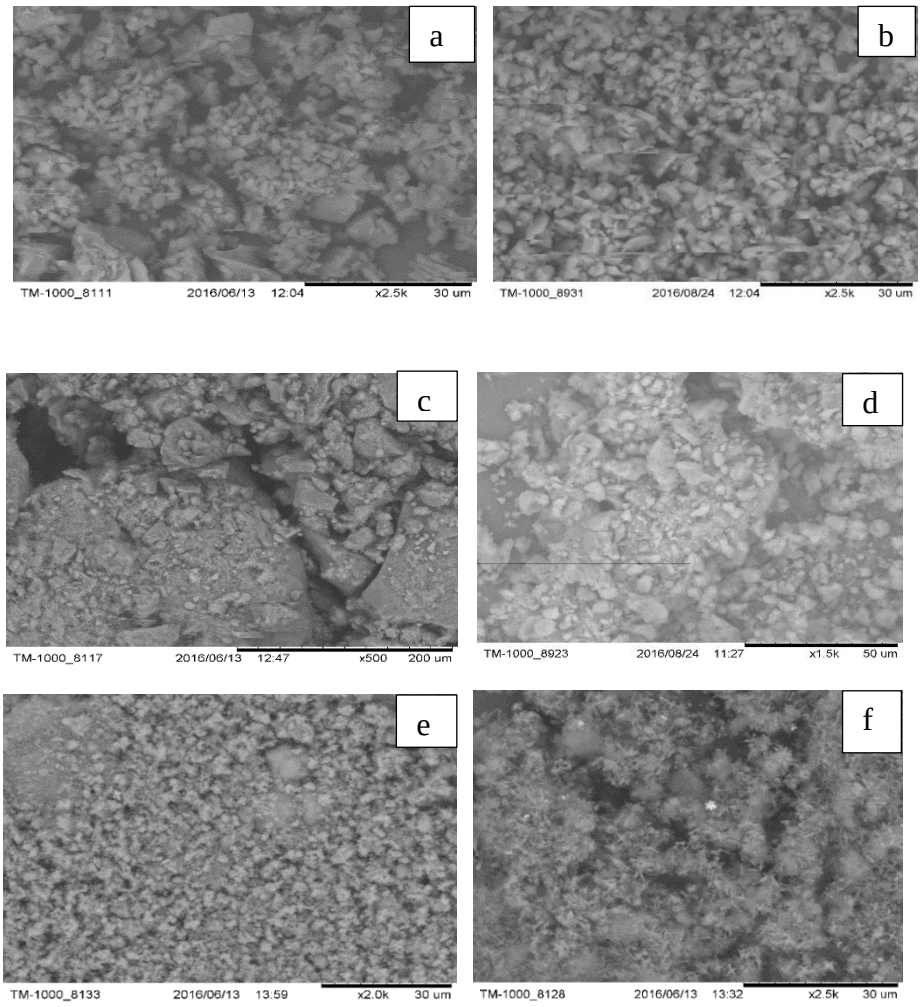

Figure 37-SEM image of MIL-53 (Al,) NH_2-MIL-53(Al) and ZIF-8 before and after coating with PVP. (a) SEM image of MIL-53 (Al) before coating with PVP, (b) SEM image of MIL-53 (Al) after coating with PVP, (c) SEM image of NH_2-MIL-53(Al) before coating with PVP, (d) SEM image of NH_2-MIL-53(Al) after coating with PVP, (e) SEM image of ZIF-8 before coating with PVP, (f) SEM image of ZIF-8 after coating with PVP.

Discussion: Dispersion of the nanoparticles as seen in (Fig 36 a-c) was achieved by incorporating a water soluble polymer (PVP) which is amphilic, non-ionic and used as a surfactant to stabilize nanoparticles in polar solvents. The good affinity for polar solvent as well as the good affinity to various polymer is due to having both the hydrophilic head and hydrophobic tail. It was observed that nanoparticles coated with PVP were easily dispersed in organic solvents like dichloromethane when vortexed. PVP was used instead of other common polyelectrolyte because it is water soluble, non- charged and can be used in various medical applications.[83 84]

Result of Part B Experiments

3.7. Characterization of Poly (ethylene glycol) dimethacrylate

The polymer synthesized was characterized by Proton NMR using deuterated chloroform as solvent. The PEG hydroxyl group reacts with methacrylic anhydride to form PEGDM. PEG has a chemical shift at $\delta \approx 3.64$. Methylene protons of MA observed chemical shift at $\delta \approx 5.54$ and 6.12 with 2 ^{1}H NMR respectively when reacted with PEG as seen in (Fig 38). The integral value for characteristic PEG peaks ($\delta \approx 3.64$) was about 2.17k. the integral value for each of the characteristics MA peak (($\delta \approx$ 5.54 and 6.12) was 2. The conjugation efficiency was determined to be 41. 8%; the calculation for this can be seen in appendix 1.

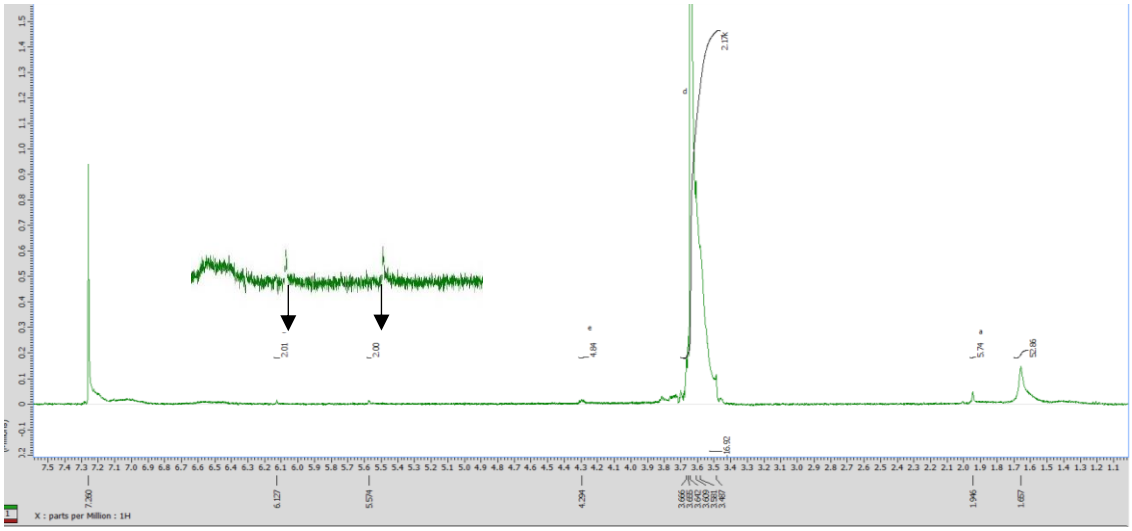

Figure 38- NMR spectra analysis of PEGDM.

3.8. Result of crosslinked hydrogel

The hydrogels were formed by the mechanism of free radical polymerization, whereby UV-light interact with a photoinitiator (I2959). A UV-light (365 nm, 6W) was irradiated on the solution. The PEGDM hydrogel crosslinks after 30 mins of UV exposure and was dissolved in water to confirm its crosslinking by its swelling in water (Fig 39).

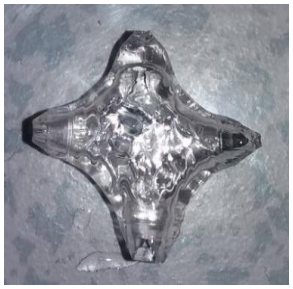

Figure 39- Photo-polymerized PEGDM hydrogel after immersion in water.

3.9. Result of PEGDM Organogels using various solvents

Hard and soft organogels were obtained by the photo-crosslinking of PEGDM with solvents ethanol and methanol, as seen in Fig 40 a&b. while photo-crosslinking of PEGDM with DMF solvent result in no gel produced, as the solvent absorbs in the UV region (365 nm) when irradiated. All solutions were irradiated with a long wave length UV-light source (365 nm 6W). It was observed that gels in methanol crosslinks faster than ethanol with an exposure time of 1 h, but yield a soft thin film gel (Fig 40 b). Gels in EtOH produce hard whitish gel after UV-light exposure for 3 h (Fig 40 a). The reason is that the methanol solvent evaporates much rapidly than ethanol, thereby resulting to a less thin gel produce when photo-irradiated as there is less solvent available for conversion. Both gels obtained were immersed in water to confirm the crosslinked gels by their swelling properties (Fig 40). Solubility test were performed on the gels by dissolving in various organic solvents such as DCM, EtOH, and acetone which remained insoluble afterwards. Since it's possible to crosslinks solvents by introducing a photo-polymerizable monomer, this would be employed for the crosslinking of MIL-68 gels.

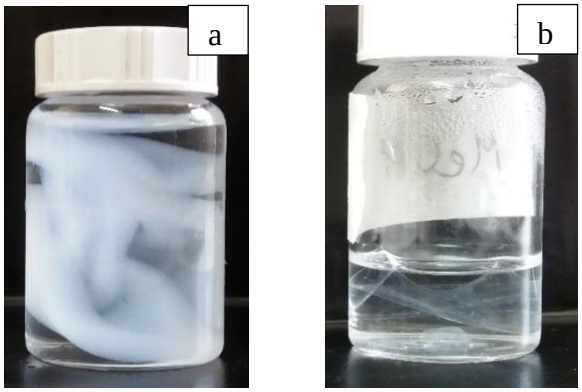

Figure 40-Organogels immersed in water using organic solvent. (a) Ethanol as solvent (b) Methanol as solvent.

3.10. Result of Synthesized Indium based Metal Organic gels (MIL-68)

All MIL-68 gels synthesized showed thixotropic properties which sheared and returned to its original shape when applied stress was removed over a period of time. The time for the gel to set back to its original shape, after the applied stress is removed is known as recovery time. Recovery time for the gels were measured by using a stop watch to determine how fast the gel could recover. Gels from EtOH solvent resets in 20 mins (Fig 41 a), while gels from MeOH and iPrOH takes 1 h to completely reset (Fig 41 b&c). The molar ratio of M-L was 1:1 Acetone solvent evaporated during synthesis producing yellow dried products, so it not known if it

would form a gel using solvent tight container. This makes conclusion indecisive for acetone (Fig 41 d). Factors influencing gelation recovery time are; temperature, metal-ligand ratio and concentration. Example was heating at higher temperature resets the gel more quickly than when left at room temperature.

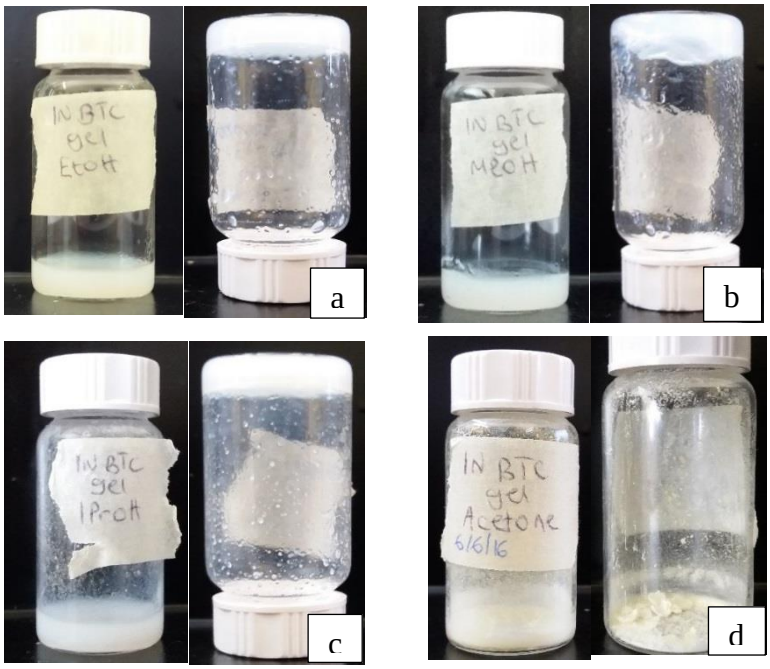

Figure 41-photograph of Indium metal organic gels with various solvents. (a) MIL-68 gel using ethanol as solvent (b) MIL-68 gel using methanol as solvent (c) MIL-68 gel using isopropanol as solvent (d) dried precipitates (no gel) using acetone as solvent

Discussion: Gelation of MIL-68 was confirmed by a test-tube inversion method as seen in Fig 41. Gelation was achieved by supramolecular self-assembly of coordination complexes through noncovalent interaction of hydrogen bonding between the carboxylic acid. This results to a three dimensional network created by weak interaction of van der Waals force between the branched alkyl chains. Acetone solvent failed to yield a gel probably because it belonged to a ketone family, lacking the functional OH group provided by alcohol for gelation process. This suggests that formation of MOGs are based on self-assembly of metal-solvent interactions of hydrogen bonding, π-π stacking and van der Waals forces. Thixotropy properties of the gels occurs as atoms starts to re-arrange themselves when at rest therefore returning to thier original shape after deformation. Also, thixotropic gel recovery time is a fundamental property which should observe $G' < G''$ after shearing and changing into $G' > G''$ after reforming. Where G' is the storage modulus and G'' is loss modulus.

3.11. Result of Synthesized MIL-68 MOGs using ethanol water mixture

Results of MIL-68 gels synthesized using ethanol water solvent ratio results in no gel produced. The presence of water in the solvent mixture disrupts the gelation process. It can be observed that as the water ratio decreases (from 50 % to 5 %) to that of ethanol, the appearance gets more gel-like as seen in Fig 42 and Table 5. From the results, the addition of water, no matter how little the ratio, disrupts gelation process of MIL-68 gels.

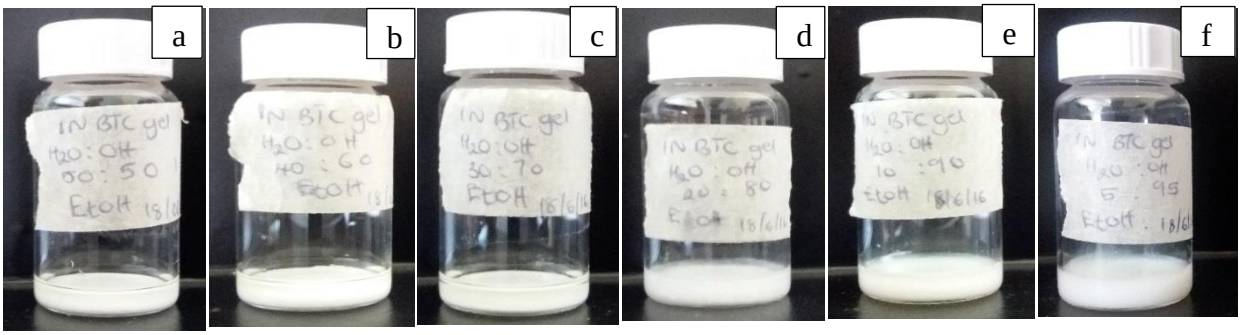

Figure 42- pictures showing water: ethanol ratio of INBTC gel (a) 50%:50% (b) 40%:60% (c) 30%:70% (d) 20%:80% (e) 10%:90% (f) 5%:95%

Discussion: Incorporating of water into solvent mixture was explored, as water is less expensive, easy to access and less toxic to the environment compared to organic solvents. Additionally, PEDGM monomer is very soluble and crosslinks way better for good photo-polymerization to organic solvent. Which could be employed for the crosslinking of MIL-68 gels.

Possible reasons why gelation failed from occurring could be; water contain (OH) as well ethanol containing hydroxyl group (-OH) attached to alkyl carbon. Upon solvothermal synthesis, the water (OH) dissolves with ethanol since both solvents are polar in nature. This lead to a hydrogen bond formed between the hydrogen of –OH group of ethanol and oxygen of water molecule. Which competes with the metal-ligand interactions of hydrogen bonding required for gelation. Another reason is the ligand carboxylic acid is polar and soluble in water. This might result in water competing to react with the carboxylic acid as it more polar to ethanol, thereby disrupting the gelation process of the system. It can be deduced from the results that water is not a good solvent for the gelation process of MIL-68.

3.12. Result of MIL-68 gels using alcohol solvents with increasing alkyl chain length

3.12.1. Using alcohol solvent 1-propanol

For MIL-68 MOGs using BTC ligands, thixotropic gels were attained with 1-propanol solvent at room temperature. The gel synthesis time was 3 mins at 0.4 mmol concentration, which was a highly viscous gel (Fig 43 a). To obtain a moderate viscous gel, the M-L concentration was reduced to 0.2 mmol (Fig 43 b). The set gel resets in 2 mins with a concentration of 0.4 mmol or 3-4 mins with 0.2 mmol. Using BDC ligand, no gel was produced after solvothermal synthesis at 80 °C for 24 h in an oven, as white metal and ligand compound precipitates out within the solvent (Fig 43 c). Note: the presence of the gel flowing on the walls of the inverted bottles was as a result of shaking effect that occurred when trying to capture a picture; as these gels are thixotropic gels which loses their viscosity when sheared.

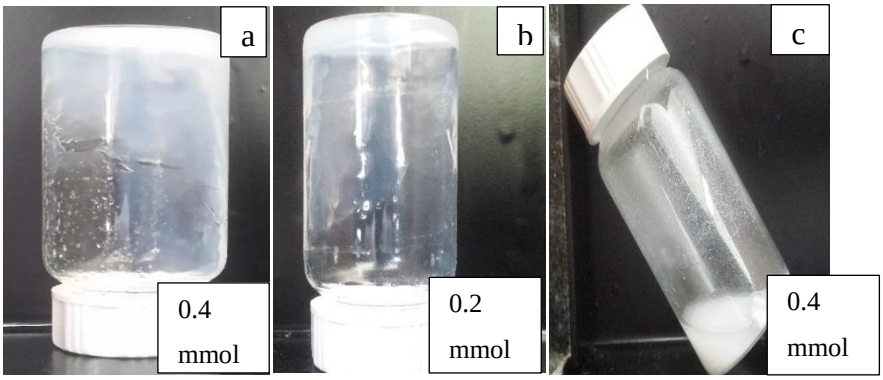

Figure 43- IN BTC GEL using solvent 1-propanol. a) Highly viscous gel with 0.4 mmol, b) good gel concentration with 0.2 mmol (c) no gelation process occurring with IN BDC using solvent 1-propanol

3.12.2. Using alcohol solvent 1-Butanol

A highly viscous and thixotropic gel was produced at room temperature in approx 2 mins. The gel resets in less than a minute when the tube is shaken vigorously (Fig 44).

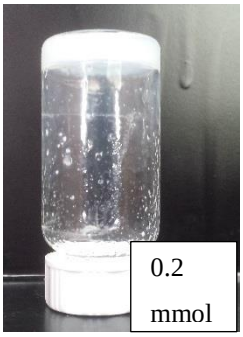

Figure 44-MIL-68 gel using solvent 1-butanol

3.12.3. Using alcohol solvent 2-Butanol

At 0.3 mmol a good thixotropic gel concentration was reached at room temperature in less than 5 mins. The gel resetted in 4 mins when the sample was shaken (Fig 45).

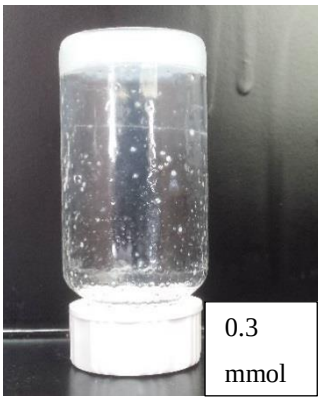

Figure 45- Good gel concentration of IN BTC using solvent 2-butanol.

3.12.4. Using alcohol solvent 1-pentanol

At 0.2 mmol, a weak thixotropic gel was produced at room temperature, resetting in approx. 10 mins (Fig 46 a). To achieve a good gel concentration, the M-L concentration was increased to 0.3 mmol and the gel obtained resets in 30 secs (Fig 46 b).

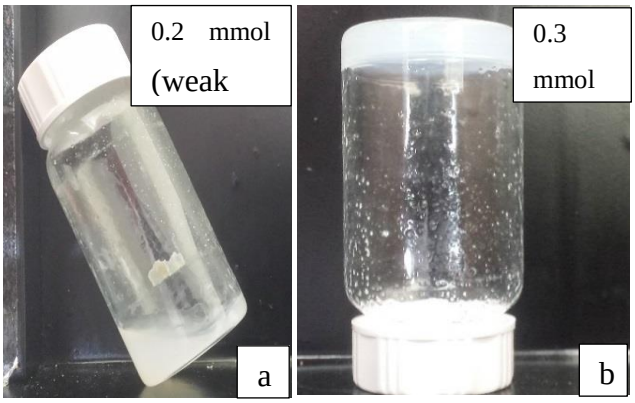

Figure 46- IN BTC gels produced using solvent 1-pentanol. a) Weak gel is produced at 0.2 mmol, b) good gel concentration attained at 0,3 mmol

3.12.5. Using alcohol solvent 2-heptanol

After the solvothermal synthetic procedure for 4 h, no gel was produced and instead white precipitates-sediments are seen at the base of the solvents (Fig 47). It was also noted that increasing the alkyl chain length resulted in the difficulty in dissolving both metal salts and ligands.

Figure 47-no gel produced with solvent 2-heptanol.

3.12.6. Summary and discussion on the effects of the different types of solvent on gelation

From the foregoing, the synthesis of thixotropic MIL-68 gel using alcohol solvent with increasing alkyl chain length resulted in difference in the parameters examined including; synthesis time and gel recovery time. Prominent factor includes; quick synthesis time of M-L coordination, self-initiation of reaction occurring at room temperature with less need of heat, increase in gel viscosity and fast recovery time. On the use of MeoH and EtOH, heating was required to induce the M-L reaction, while the gel recovery time took about 60 minutes and 20 minutes respectively whereas on the use of 1-propanol, 1-butanol and 1-pentanol were obtained at room temperature with a fast gel recovery time of 4 min, 2 min and < 1 min respectively. This shows that on increasing alkyl chain length, resulted in reduced gel recovery time, synthesis temperature and increase in gel viscosity. The use of 2-heptanol or other longer alkyl chain did not result in the formation of a gel.

3.13. Gallium Metal Organic Gels

3.13.1. Gallium Metal Organic Gels using H_3BTC

A translucent gel was synthesized with solvents (EtOH, 1-propanol and 2-propanol) at room temperature in 5 mins as seen in (Fig 48 a-c). Gels obtained were not thixotropic in nature, as when shaken, the gel was broken into smaller bits. Gallium gels shows similar physical properties to aluminium MOGs in terms of colour and non-thixtropy property.

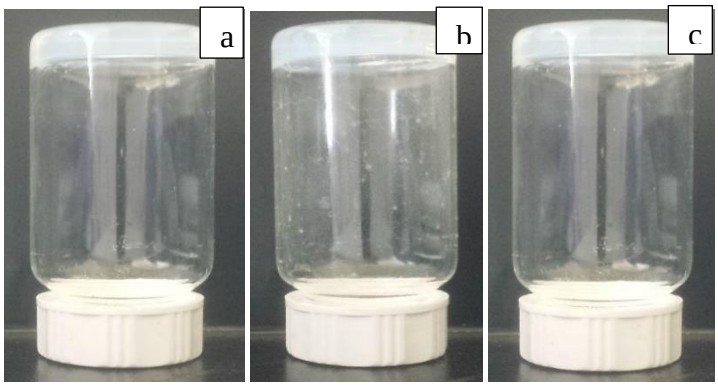

Figure 48-Ga BTC gel obtained using solvent a) EtOH b) 1-propanol c) 2-propanol.

3.13.2. Gallium Metal Organic Gels using H_2BDC

The synthesized gel produces a weak gel after 1 h which deteriorates and loses its gel properties to a fluid form when cooled to room temperature from an elevated temperature as seen in (Fig 49 a-b). The use of H_2 BDC ligand with gallium metal does not produce a viable gel.

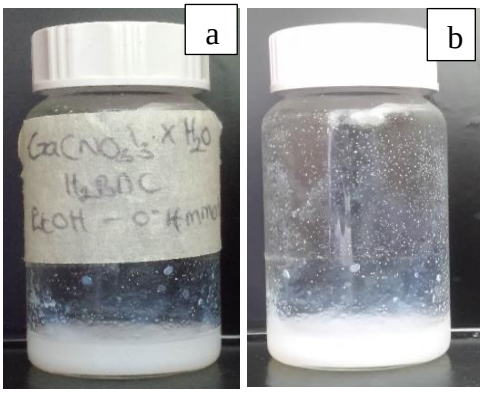

Figure 49-Ga BDC gel using solvents a) ethanol b) 1-propanol

3.14. Lanthanum Metal Organic Gels

Synthesis of lanthanum MOG using $La(NO_3)_3{\cdot}6H_2O$ with ligands (BTC or BDC) resulted to no gel produced as white precipitates settles out at the base of the solvents. It can be concluded that for the two ligands (BTC and BDC), lanthanum nitrate gel is not obtainable with reference to synthesis Table 20 (Fig 50 a-d).

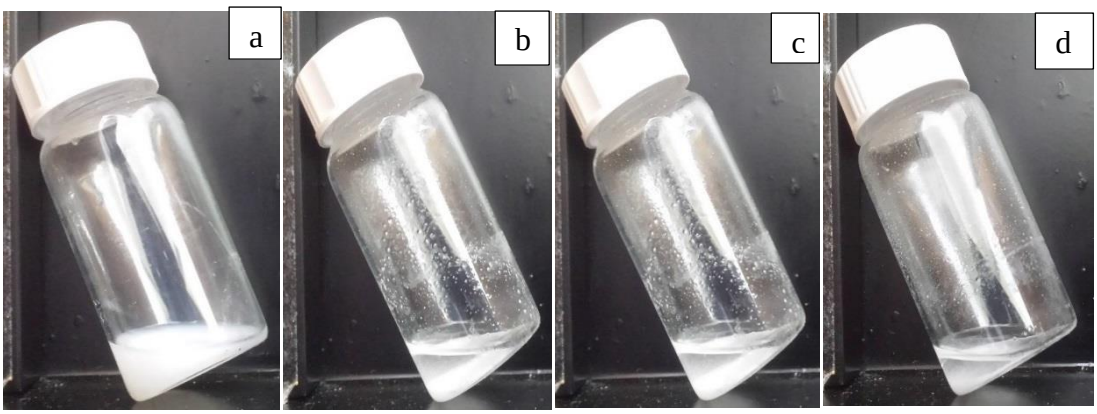

Figure 50-No gelation occurring with lanthanum metal salts and ligands (BTC/ BDC) using solvents a) BTC ligand with EtOH b) BTC ligand with 1-propanol c) BDC ligand with EtOH d)) BDC ligand with 1-propanol.

Result of Part C Experiments

3.15. Photo-crosslinking of Metal Organic gels with various solvents

Gels were obtained with solvents ethanol or methanol in the presence of a monomer (PEGDM) using Al^{3+} (BTC), Fe^{3+} and Cr^{3+} MOGs afters solvothermal synthesis. A simple inversion test tube method was used to test for gelation (Fig 51). All metal salts with BTC ligand used formed a gel with non-thixotropy properties except for Al^{3+} with BDC, which failed to yield a gel (Fig 51 d). The introduction of the PEDGM monomer helped provide an acrylate group needed for photo-polymerization of the gels. The gels were crosslinked by adding a photoinitiator (free radical initiator) to polymerize the system gel after UV-light dosage (365 nm 6W) for 3 h. crosslinking was confirmed by immersing the gels in water which resulted in the gel swelling. (Fig 52).

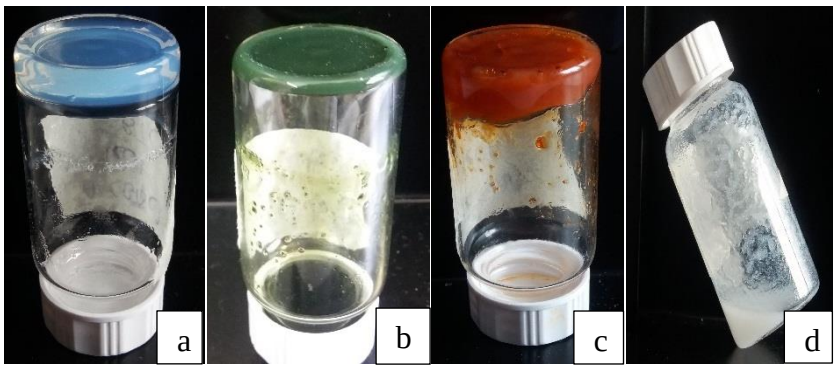

Figure 51- ethanol and methanol synthesized gels with PEGDM and photoinitiator incorporated within after solvothermal synthesis. (a) Al BTC gel (Al) (b) Cr BTC gel (C) Fe BTC gel (d) No gel produced with AL BDC.

MOGs solubility test

All gels were immersed in various organic solvent to test if they were insoluble to organic solvents. Solvents used include: chloroform, dichloromethane, acetone, methanol, ethanol, hexane and toluene. It was observed that immersion of Al (BTC) gel in acetone changes the gel back from white to a transparent gel as it was, before immersing in water after photoirradiation. When removed from acetone and re-immersed in water, the gel returns back to its whitish color. The solubility test in various organic solvent supports that crosslinking of the different gels polymer chains had occurred, resulting in the gels been insoluble. The disintegration of the MOGs into smaller bits especially MIL-101 (Cr) and MIL-100 (Fe) (Figs 52 a, b &c) was due to the weak gel synthesized or continuous shaking of the gels in organic solvent during the solubility test. However the gel remained insoluble and maintained their colour. Photocroslinking of MOGs gels was more feasible using methanol solvent as to ethanol, because methanol dissolves all reactant monomers easily producing a much homogeneous solution required for crossklinking. The experimental procedure shows crosslinking of MOGs is possible using a polymer conatining an acrylate group, which interacts with light in the prescence of a phtoinitiator to photopolymerize the gel by free radical polymerization.

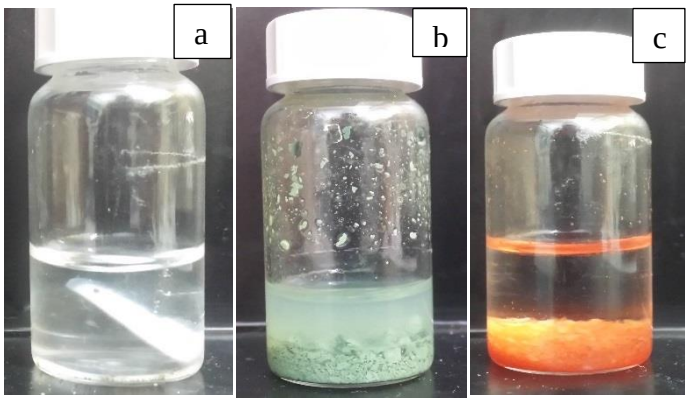

Figure 52-Results of MOGs disintegrating into smaller bits after being subjected to various organic solvent solubility test, but still remain insoluble in water. (a) Al BTC gel (b) Cr BTC gel (c) Fe BTC gel.

3.16. Synthesis and crosslinking of MIL-68 MOGs

Indium Metal Organic Gels was of primary focus of all gels, due to its great thixotropic properties which provides great flexibility when designing new compounds. Earlier experimental results showed ways of crosslinking MIL-68 based on different solvents such as EtOH, MeOH and IPrOH.

Photo-polymerization of indium based gels (MIL-68) was unsuccessful by adopting similar method of introducing a PEGDM monomer, used for crosslinking other MOG gels in previous experiments. The addition of PEGDM disrupted the gelation process of MIL-68, despite varying the gel synthetic conditions such as increase or decrease in mole ratio of PEGDM, solvent, metal ion and ligand concentration as seen in Table 19-21. The various conditions had no effect on improving the gelation process because of the presence of PEGDM. PEGDM method adopted in crosslinking Al BTC, Fe BTC and Cr BTC gels failed for IN BTC. The reason why PEGDM failed could be that it is a solid and requires much more force to dissolve compared to a liquid monomer with the same acrylate group. So a recommendation was to employ a liquid monomer such as acrylic acid or acryl amide for photo-polymerization of the gel.

3.17. Result for MIL-68 MOGs using a % ratio of monomer (allyl alcohol or acrylic acid) with alcohol solvent

Results of experimental procedure 2.3.16 shows allyl alcohol or acrylic acid {5 % (v/v) or 10 % (v/v)} when mixed with alcohol solvent such as 1-propanol, 1-butanol and ethanol and introducing the indium salt and BTC ligand afterwards, gives a thixotropic gel (Fig 53). 1-Propanol and 1- butanol solvents were chosen over ethanol because MIL-68 gels could be synthesized at room temperature over a short time frame. It was observed that solvent mixture of acrylic acid monomer would require heating slightly for 5 mins at 80 °C for gelation to occur, while allyl alcohol solvent mixture was still obtainable at room synthesis. Gels containing allyl alcohol with solvent 1-propanol and 1-butanol resets in 3-5 mins when at rest while gels containing acrylic acid resets between 2-4 mins when left at rest as seen in Table 22-22. Both gels rests fast when slightly heated in an oven for few seconds.

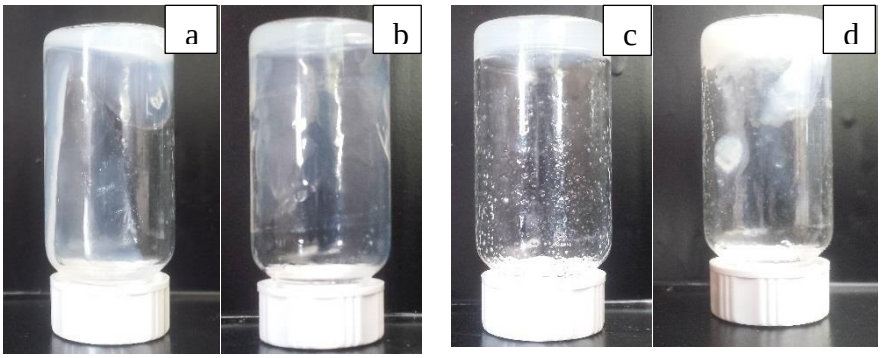

Figure 53-photograph of MIL-68 gel using a solvent mixture ratio of a) 1-propanol 95 % + allyl alcohol (5 %) b) 1-butanol 95 % + allyl alcohol (5 %) (c) 1-propanol (95 %, 90 %) + acrylic acid (5 %, 10 %) (d) 1-propanol (95 %, 90 %) + acrylic acid (5 %, 10 %)

Discussion: MIL-68 gels with acrylic acid or allyl alcohol still retained their gel structure, appearance and similar recovery time as to MIL-68 gel. The monomers acrylic acid and allyl alcohol possess vinyl bonds required for polymerization to occur. By incorporating this monomer with a photo-initiator, crosslinking of metal organic gels should be possible. For further experimental crosslinking of gels, acrylic acid was used over allyl alcohol as it is often difficult to polymerize allyl alcohol and also results in oligomers being produced in the presence of free-radical initiators.

3.18. Results for crosslinking MIL-68 (In) gel with UV-light

According to experimental procedure 2.3.18, the MIL-68 gel containing acrylic acid reagent was initiated for crosslinking by photoinititator I2959 with ethanol and 1-propanol solvent separtely. After UV-light exposure for 2 mins, the gel was partially and not fully crosslinked (Fig 54). To overcome this hurdle, the exposure time was increased sequentially, from 2 to 15 mins. The result remained the same as the 2 mins exposure time. It was also observed that the gel changes from white to a translucent liquid colour losing the gel properties after UV treatment but still having the partially crosslinked oligomer present in the liquid. The translucent liquid was placed in a vacuum first followed by oven heating at 40 °C with the aim to remove the solvent present within. Instead the liquid remained indicating it was not the solvent used during synthesis but could be excess acrylic acid used during synthesis.

Discussion: The partially crosslinked MIL-68 gel could be attributed to the acrylic acid reagent being insufficient in the network system to fully crosslink the gel. An increase in the acrylic acid monomer from 20 to 50 (% v/v) to enhance the gel photo-crosslinking, resulted in disrupting the gel structure. So finding a balance between the acrylic acid and the solvent ratio for the gel was unattainable to fully crosslink the gel. To solve this problem, using a thermal initiator such as ammonium persulfate with acrylamide and tetramethylethylenediamine (TEMED) could proffer possible option for crosslinking the gels, as heating might be required to induce the gelation process.

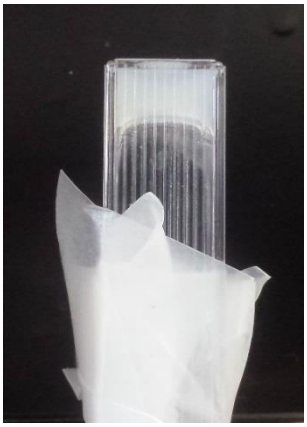

Figure 54-picture showing a partially crosslinked MIL-68 gel

Chapter 4. Conclusion and further research

4.1. Conclusion

In summary, this research project report demonstrates how functional MOFs or MOGs, which have inherent similar properties, can be processed or fabricated. The final products can then be used for commercial applications. The experimental process to achieving MOFs fabrication processability involved modifying coatings and lithographic techniques, which led to the successful patterning of MOFs of different types depending on the synthesis conditions. Also, the use of various approaches suitable for the synthesis and photo-crosslinking of MOGs without disrupting the gel mechanism were adopted.

Metal organic Frameworks

This research project demonstrates that the micro patterning of MOF crystals is possible using lithography techniques with further improvement required. In 2014, Paolo and co-workers[30] conducted an experiment demonstrating the importance of how advance materials can be developed by combining improved fabrication techniques with materials with unique properties. A key step to achieving this, was to confine functional materials to precise locations. In a similar study, Doherty and co-workers[4] presented a facile protocol that allowed the preparation of MOFs by simply combining UV-lithography. But unlike Doherty and co which focused on MOF film, this project employs Al^{3+} as the metal ion for coordination purposes, as well as the base substrate for MOF patterning. In addition, the type of resist and techniques used for coating are essential factors to consider when patterning MOFs, as these techniques could impede access to metal ion (Al^{3+}) in the alumina, required for M-L coordination. Photolithography proved as a useful coating technique for the patterning of NH_2-MIL-53 (Al) microcrystals on anodisc but failed for the patterning of microrods crystals growth when a modulator was added. The coating technique had limitations, as it did not prove as a viable technique for the patterning of different MOFs crystal growth. Suggestions for how to improve gold sputtering on alumina membrane were outlined in section 3.

Metal organic gels

Our preliminary results in this report have demonstrated that the use of metal ions with +3 charge alongside with ligands such as BDC and BTC results in the synthesis of metalorganic gels with various distinctive rheological, physical and chemical properties. Of all MOGs

synthesized using group 13 elements such as Al, In and Ga, Indium based gels exhibited affirmed thixotropic behaviour, where shaking the gels results in the formation of a free-flowing liquid which returns to its solid-phase gel upon resting. These gel-to-sol and sol-to-gel properties after cross-linking offer the gels as promising materials for various applications. It should be noted that the gel strength is concentration dependent.

An experiment conducted by Jose and David in 2015[85] where MOFs were transformed into polymer gels and vice versa via covalent crosslinking with a suitable bifunctional electrophile. Also, in 2013, Takumi and co-workers[86] reported a similar work, where MOF were transformed into polymer gels by simply crosslinking the organic linkers preorganized in the MOF. Unlike the work presented by Takumi and co-workers which involved the removal of the coordinated metal ions, this project allowed the metal ions, owing to the importance of the metal ion in further applications such as metalorganogel. Results obtained from the crosslinking of MOGs in this project support findings, that by possibly incorporating a monomer or polymer with an acrylate functional group and photo-crosslinking it with an initiator under UV–light source, a crosslinked MOG is attained. Examples of photo-crosslinked gels acquired in this project were Al BTC, Cr NH_2BDC, and Fe BTC MOGs by using a PEGDM monomer. Indium gel was an exception as it required the use of an acrylic acid monomer with an initiator to crosslink due to its delicate system, which could easily be disrupted.

In conclusion, metal-organic frameworks and metal-organic gels were ideal for use in this project as they could be processed for the development of 3-D cross-linkable materials or resins, due to the dynamic and reversible nature of metal-ligand bonds. In addition, it is possible to control crystal growth by patterning techniques, in order to provide an extensive variety of materials for diverse applications. Although all of the aims of this research project were not met, headways in the advancement of coatings and lithography techniques for the precise control of MOFs, as well as approaches suitable for crosslinking thixotropic gels, have been made that can aid further processability of the metal-containing polymers.

4.2. Future work

Our work on Metal Organic Frameworks and Metal Organic Gels is still early for various applications, such 3D printing as its still been looked into for potential processing of the gels into different shapes and sizes. However, for future studies there are a few areas to consider;

- The discovery of more effective micro and patterning techniques for the precise control of MOFs' functional properties for tailored applications. Photolithography using different coatings used for spatial control could be looked into.
- Due to limited time we could not carry out further characterizations such as rheological analysis Field emission scanning electron microscope (FE-SEM) and TEM on the various gels. Further research is required to understand the mechanism of gel formations as it is very difficult to produce thixotropic gels.
- Research was not carried out on fully crosslinking MIL-68 gels using a thermal initiator due to limited time.

References

1 B. Angélique, PhD Thesis, Ruhr University Bochum, 2011.

2 H.Mohideen and I. Mohamed, PhD Thesis, University of St Andrews, 2011.

3 Y. Lee, J. Kim and W. Ahn, *Korean J. Chem. Eng.,* 2013, **30 (9)**, 1667-1680.

4 C. M. Doherty, G. Grenci, R. Riccò, J. I. Mardel, J. Reboul, S. Furukawa, S. Kitagawa, A. J. Hill and P. Falcaro, *Adv Mater.,* 2013, **25**, 4701-4705.

5 B. K. Keitz, C. J. Yu, J. R. Long and R. Ameloot, *Angew. Chem. Int. Ed.,* 2014, **53(22)**, -5561- 5565.

6 J. M. 'Chin, E. Y. - Chen, A. G. - Menon, H. Y. - Tan, A. T. S. - Hor, M. K. - Schreyer and J. - Xu, *CrystEngComm,* 2013, **15(4)**, 654-657.

7 N. A. Ramsahye, G. Maurin, S. Bourrelly, P. L. Llewellyn, T. Loiseau, C. - Serre and G. - Ferey, *Chem. Commun.,* 2007, **31**, 3261-3263.

8 Chao Chen, Jun Kim, Wha-Seung Ahn, *Korean J. Chem. Eng.,* 2014, **31(11)**, 1919-1934.

9 S. L. Campello, G. Gentil, S. A. Junior and W. M. de Azevedo, *Mater Lett,* 2015, **148**, 200-203.

10 P. Falcaro, D. Buso, A. J. Hill and C. M. Doherty, *Adv Mater,* 2012, **24**, 3153-3168.

11 H. Furukawa, K. E. Cordova, M. O'Keeffe and O. M. Yaghi, *Science,* 2013, **341(6149)**, 1230444.

12 T. T. Y. Tan, M. R. Reithofer, E. Y. Chen, A. G. Menon, T. S. A. Hor, J. Xu and J. M. Chin, *J. Am. Chem. Soc.,* 2013, **135**, 16272-16275.

13 L. Keenan, (PHD), PhD Thesis, University of Bath, 2014.

14 L. Liu, PhD Thesis, Stockholm University, 2014.

15 S. Kitagawa, R. Kitaura and S. Noro, *Angew. Chem. Int Ed.,* 2004, **43**, 2334-2375.

16 M. Mingyan, PhD Thesis, Ruhr University Bochum, 2011.

17 C. Janiak, *Dalton Trans.,* 2003, **14**, 2781-2804.

18 S. L. James, *Chem. Soc. Rev.,* 2003, **32**, 276-288.

19 J. L. C. Rowsell and O. M. Yaghi, *Micropor Mesopor Mat.,* 2004, **73(1)**, 3-14.

20 C. Dey, T. Kundu, B. P. Biswal, A. Mallick and R. Banerjee, *Acta Crystallogr., Sect. B: Struct. Sci.,* 2013, **70**, 3-10.

21 R. K. Vakiti, M.Sc Chemistry, Western Kentucky University, 2012.

22 D. Peters, *J. Mater. Chem.,* 1996, **6 (10)**, 1605-1618.

23 H. Xu, B. W. Zeiger and K. S. Suslick, *Chem. Soc. Rev.,* 2013, **42 (7)**, 2555-2567.

24 T. R. C. Van Assche, G. Desmet, R. Ameloot, D. E. De Vos, H. Terryn and J. F. M. Denayer, *Microporous Mesoporous Mater.*, 2012, **158**, 209- 213.

25 A. Martinez Joaristi, J. Juan-Alcañiz, P. Serra-Crespo, F. Kapteijn and J. Gascon, *Cryst. Growth Des.*, 2012, **12**, 3489-3498.

26 M. Klimakow, P. Klobes, K. Rademann and F. Emmerling, *Microporous Mesoporous Mater.*, 2012, **154**, - 113-118.

27 F. A. Almeida Paz and J. Klinowski, *J. Solid State Chem.*, 2004, **177**, 3423-3432.

28 Y. Xia and G. Whitesides, *Angew. Chem.*, 1998, **37**, 550-575.

29 T. Betancourt and L. and Brannon-Peppas, *Int. J. Nanomedicine*, 2006, **1(4)**, 483.

30 P. Falcaro, R. Ricco, C. M. Doherty, K. Liang, A. J. Hill and M. J. Styles, *Chem. Soc. Rev.*, 2014, **43(16)**, 5513-5560.

31 J. Zhang and X. Chen, in *Metal-Organic Frameworks for Photonics Applications*, ed. nonymous, Springer, 2013, p. 1-26.

32 O. Dalstein, D. R. Ceratti, C. Boissière, D. Grosso, A. Cattoni and M. Faustini, *Adv. Funct. Mater.*, 2016, **26**, 81-90.

33 J. C. Hulteen, D. A. Treichel, M. T. Smith, M. L. Duval, T. R. Jensen and R. P. Van Duyne, *J. Phys. Chem. B*, 1999, **103**, 3854-3863.

34 K. Sakakibara, J. P. Hill and K. Ariga, *Small*, 2011, **7(10)**, - 1288-1308.

35 J. Behari, *Indian J. Exp. Biol.*, 2010, **48**, 1008-1019.

36 L. Chi, *Nanotechnology: Nanostructured Surfaces*, John Wiley & Sons, 2010, vol. 8

37 D. Lipomi, R. Martinez, L. Cademartiri and G. Whitesides, *Polym. Sci. Compr.*, 2012, - 211-231.

38 G. Rius Suñé, J. Bausells Roige and F. Pérez Murano, PhD Thesis. Universitat Autònoma de Barcelona, 2008.

39 S. Y. Chou, P. R. Krauss and P. J. Renstrom, *Appl. Phys. Lett.*, 1995, **67 (21)**, 3114-3116.

40 S. Y. Chou, P. R. Krauss and P. J. Renstrom, *J. Vac. Sci. Technol., B*, 1996, **14 (6)**, 4129-4133.

41 L. Filipponi, D. Sutherland and I.N. Center, *NANOYOU Teachers Kit in Nanoscinece and Nanotechnologies*, ed. nonymous, Aarhus University, Denmark, 2010, p. 3-21.

42 B. Ziaie, A. Baldi and M. Z. Atashbar, in *Springer Handbook of Nanotechnology*, ed. nonymous, Springer, 2004, p. 147-184.

43 Andrew G. Zanzal, and S. Rizvi, in *Handbook of Photomask Manufacturing Technology*, ed. Syed Rizvi, Taylor & Francis Group, California, U.S.A., 2005, p. 19-20.

44 S. Franssila, in *Introduction to Microfabrication*, ed. nonymous, John Wiley & Sons, Ltd, 2010, p. 1-13.

45 O. Shekhah, J. - Liu, R. A. Fischer and C. Woll, *Chem. Soc. Rev.*, 2011, **40(2)**, 1081-1106.

46 D. Zacher, O. Shekhah, C. Wöll and R. A. Fischer, *Chem. Soc. Rev.*, 2009, **38**, 1418-1429.

47 B. Liu and R. A. Fischer, *Organometallics and Materials Chemistry*, 2011, **54(12)**, 1851-1866.

48 A. Bétard and R. A. Fischer, *Chem. Rev.*, 2011, **112**, 1055-1083.

49 A. Summerfield, I. Cebula, M. Schrö der and P. Beton H, *J. Phys. Chem. C*, 2015, **119(41)**, 23544-23551.

50 M. N. Shah, PhD Thesis, Texas A&M University, 2012.

51 A. Bétard and R. A. Fischer, *Chem. Rev.*, 2011, **112(2)**, 1055-1083.

52 A. M. Grillet, L. M. Gloe and N. B. Wyatt, *Polymer gel rheology and adhesion*, INTECH Open Access Publisher, USA, 2012.

53 P. Parveen, S. S. Sulthana, K. Mahathi, M. S. Rekha and A. S. Devi, *Am. J. Phytomed Clin. Therap.*, 2014, **2**, 1299-1309.

54 S. K. Gulrez, G. O. Phillips and S. Al-Assaf, *Hydrogels: methods of preparation, characterisation and applications*, INTECH Open Access Publisher, 2011.

55 Y. Tanaka, *Viscoelastic Properties for Sol-Gel Transition*, INTECH Open Access Publisher, Japan, 2012.

56 H. H. Winter, *The critical gel: The universal material state between liquid and solid.*, Kluwer Academic Publishers, Dordrecht, Netherlands., 2002.

57 W. de Carvalho and M. Djabourov, *Rheol. Acta*, 1997, **36**, 591-609.

58 K. Hanabusa, D. Inoue, M. Suzuki, M. Kimura and H. Shirai, *Polym. J.*, 1999, **31**, 1159-1164.

59 C. H. Lee, V. Moturi and Y. Lee, *J. Control. Release*, 2009, **136**, 88-98.

60 P. Herh, J. Tkachuk, S. Wu, M. Bernzen and B. Rudolph, *Am. Lab.*, 1998, **30**, 12-14.

61 J. Mewis and N. J. Wagner, *Adv. Colloid Interface Sci.*, 2009, **147**, 214-227.

62 H. A. Barnes, *J. Non Newtonian Fluid Mech.*, 1997, **70**, 1-33.

63 R. Durairaj, N. Ekere and B. Salam, *J. Mater. Sci., Mater. Electron.*, 2004, **15**, 677-683.

64 X. Wang and R. McHale, *Macromol. Rapid Commun.*, 2010, **31**, 331-350.

65 X. Qian, B. Yadian, R. Wu, Y. Long, K. Zhou, B. Zhu and Y. Huang, *Int J. Hydrogen Energy*, 2013, **38**, 16710-16715.

66 H. Zhao, Q. Shi, H. Xiao and X. Li, *J. Porous. Mat.*, 2014, **21**, 691-697.

67 Y. Liu, L. He, J. Zhang, X. Wang and C. Su, *Chem. Mater.*, 2009, **21**, 557-563.

68 L. Zhang, B. Marzec, R. Clérac, Y. Chen, H. Zhang and W. Schmitt, *Chem. Commun.*, 2013, **49**, 66-68.

69 P. Sutar and T. K. Maji, *Chem. Commun.*, 2016, **52**, 8055-8074.

70 S. Li and F. Huo, *Nanoscale*, 2015, **7**, 7482-7501.

71 A. Angulo-Ibáñez, G. Beobide, O. Castillo, A. Luque, S. Pérez-Yáñez and D. Vallejo-Sánchez, *Polymer*, 2016, **8(1)**, 16.

72 Q. Wei and S. L. James, *Chem. Commun.*, 2005, **12**, 1555-1556.

73 A. Şahin, MSc Dissertation, İzmir Institute of Technology, 2004.

74 X. Qian, Z. Zhong, B. Yadian, J. Wu, K. Zhou, J. S. Teo, L. Chen, Y. Long and Y. Huang, *Int J. Hydrogen Energy*, 2014, **39**, 14496-14502.

75 Y. Pan, Y. Liu, G. Zeng, L. Zhao and Z. Lai, *Chem. Commun.*, 2011, **47(7)**, 2071-2073.

76 Sheng Lin-Gibson, Sidi Bencherif, James A. Cooper, Stephanie J. Wetzel, Joseph M. Antonucci, Brandon M. Vogel, Ferenc Horkay, and, and Newell R. Washburn., *Biomacromolecules*, 2004, **5 (4)**, 1280-1287.

77 M. Dai, M. Xiao, P. Xiao and J. Nie, *Polym. Adv. Technol.*, 2011, **22**, 738-742.

78 M. Alhamami, H. Doan and C. Cheng, *Materials*, 2014, **7**, 3198-3250.

79 J. Liu, X. - Zou, C. Liu, K. Cai, N. - Zhao, W. Zheng and G. Zhu, *CrystEngComm*, 2016, **18(4)**, 525-528.

80 K. Grigoras, V. Airaksinen and S. Franssila, *J. nanosci. nanotechnol*, 2009, **9(6)**, 3763-3770.

81 T. Hussain, A. T. Shah, K. Shehzad, A. Mujahid, Z. H. Farooqi, M. H. Raza, M. N. Ahmed and Z. U. Nisa, *Int. Nano Lett.*, 2015, **5**, 37-41.

82 Y. Pan, Y. Liu, G. Zeng, L. Zhao and Z. Lai, *Chem. Commun*, 2011, **47**, 2071-2073.

83 H. Lee, S. Lee, C. Xu, J. Xie, J. Lee, B. Wu, A. L. Koh, X. Wang, R. Sinclair and S. X. Wang, *Nanotechnology*, 2008, **19**, 165101.

84 C. Sun, C. Qin, X. Wang, G. Yang, K. Shao, Y. Lan, Z. Su, P. Huang, C. Wang and E. Wang, *Dalton Trans*, 2012, **41**, 6906-6909.

85 J. J. Marrero-Tellado and D. D. Díaz, *CrystEngComm*, 2015, **17**, 7978-7985.

86 T. Ishiwata, Y. Furukawa, K. Sugikawa, K. Kokado and K. Sada, *J. Am. Chem. Soc.*, 2013, **135**, 5427-5432.

Appendix 1

Determination of conjugation efficiency of PEGDM

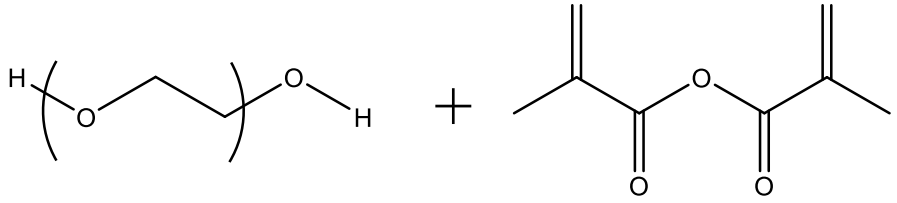

Polyethylene glycol methacrylic anhydride

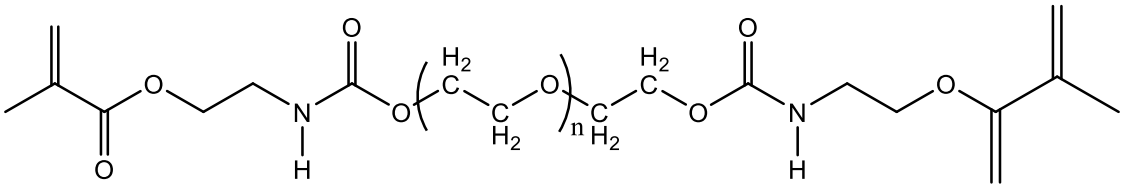

Polyethylene glycol Dimethacrylates

Observed integral values: integral of MA peak is 2; integral of PEDGM peak is about 2.17k

Average PEG molecular mass = 10,000

Average number of EG units = 44

Average no of EG units per PEG = (10,000/44) = 227

Each EG unit has 4 protons at $\delta \approx 3.64$

PEG unit x no of ^{1}H (227 x 4) = 908 protons per EG.

If each PEGDM has 2 MA units there are two protons at $\delta \approx 5.57$

If 100% addition of MA $\frac{\int \mathrm{MA}(5.57)}{\int PEG\ (3.64)} = \frac{2}{908}$

% Conjugation = $\frac{\frac{\int \mathrm{MA}}{\int PEG}}{2/908}\ x\ 100$

Using the observed integration values, $\int$ MA = 2, $\int$ EG = 2170

% Conjugation = $454\,\frac{\int \mathrm{MA}}{\int PEG} x\ 100 = 41.8\ \%$